博士論文（要約）

Doctorate Thesis (Abridged)

Understanding the functional role of selected bioactive compounds and altered genes on gastric carcinogenesis of the differentiated subtype using *A4gnt*-deficient mice model

（*A4gnt* 欠損マウスを用いた分化型胃がんに対する特定の生理活性物質と関連遺伝子の機能的役割の研究）

マーク ジョセフ　マラナン　デサメロ

Mark Joseph Maranan Desamero

Table of Contents

General Introduction

Overview

Gastric cancer (GC) is a broad encompassment of any forms of neoplasm occurring in the stomach whether it may be leiomyosarcomas, lymphomas, carcinoids, sarcomas, and adenocarcinomas (Ye et al., 2018). In most cases, however, it has been used exclusively to refer to the latter type, probably owing to the fact that it accounts to more than 95% of all diagnosed cases. Since 1975, where it was considered to be most common type of malignancy, a steep downhill trend has been progressively seen as a result of remarkable improvements in the multipronged aspects of this disease including detection, diagnosis, treatment, surveillance, as well as in the knowledge of various risk factors. According to the latest GLOBOCAN series by the International Agency for Research on Cancer (IARC), which compiles the global cancer incidence and mortality, GC was downgraded to only fifth most frequently reported cancer for both sexes combined in 2018 (~1000 new cases) (Bray et al., 2018), a notch lower than its previous placement in the 2008 estimates (Ferlay et al., 2010). In reference to mortality, it figured in third place with 8.2%, equivalent to about 783, 000 cases next to lung (18.4%) and colorectal (9.2%) cancers. Male patients are still at higher risk posing no less than 2-fold increase relative to the opposite sex, which could be more staggering in Western Asian countries i.e. Iran, Turkmenistan, Kyrgyzstan since it has been the leading cause of cancer-related loss among male patients (Bray et al., 2018). Countries belonging to Eastern Asia, Eastern Europe, and South America continue to be a regional hotspot of heightened incidence while Southern Asia, Africa, New Zealand, Australia, and North America prevail under the category of low-risk regions (Sitarz et al., 2018). As the disease has a predominantly older preponderance (>45 years old), the burden of GC is expected to perpetuate in the years to come because more countries especially those in developing/emerging economies are transitioning into an aging society in auxiliary to a rapidly inflating population growth (Jemal et al., 2010).

GC is essentially a net outcome of the vicious interaction between environmental insults (extrinsic or acquired factors) and genetic aberrations (intrinsic factors) that have accumulated over time (Tan and Yeoh, 2015; Sitarz et al., 2018; Ye et al., 2018; Avital et al., 2019) (Figure 1). Acquired factors include: nutritional (high salt, red and cured meat, and nitrate consumption; low dietary vitamin A and C; iron deficiency; poor water quality), occupational (foundry, mining, coal, steel, rubber, oil refinery, diesel exhaust, and cement industries), cigarette smoking, sedentary lifestyle, alcohol abuse, ionizing radiation, partial gastrectomy or prior gastric surgery, Eipstein-Barr virus (EBV), and *Helicobacter pylori* infection (Carneiro and Lauwers, 2013). Of these components, *H. pylori* is the single most definitive entity that is strongly linked with the development of GC (up to 60-90% of GC cases) especially those occurring in areas other than the gastric cardia. The magnitude of the relative risk it carries may be as high as six fold (Helicobacter and cancer collaborative group, 2001), and this can be further bloated up to around 20 fold when coupled with CagA antibody status (Malfertheiner et al., 2005). In this regard, the IARC designated this bacterium as a class I carcinogen of GC (IARC Working Group, 1994), though technically with a very low penetrance rate of only <1% in affected individuals (Menaker et al., 2004; Wroblewski et al., 2010; Lordick and Janjigian, 2016; Ye et al., 2018; Avital et al., 2019).

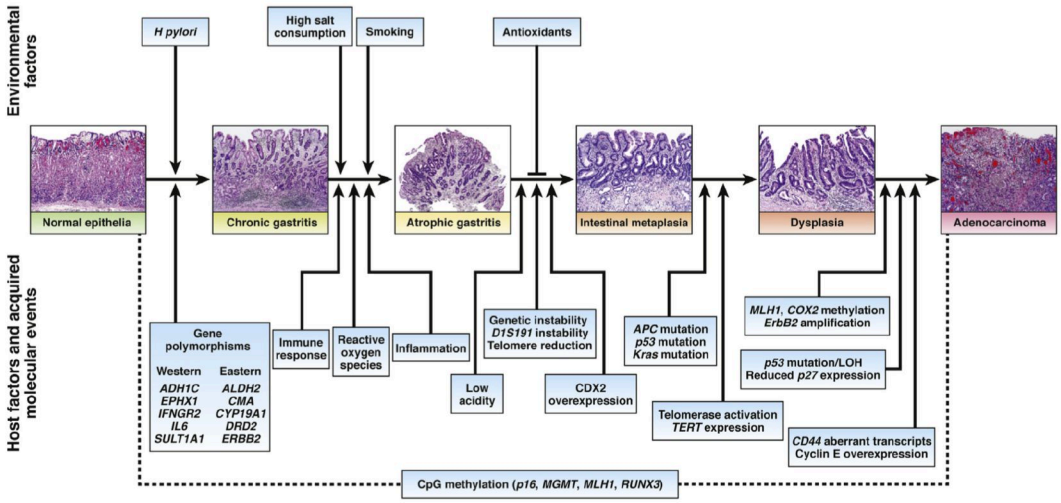

Figure 1. Schematic diagram of the intrinsic (host-related) and extrinsic factors (environmental) influencing the pathogenesis of GC especially the intestinal subtype. (Taken from Tan and Yeoh, 2015)

Genetic predisposing factors, on the other hand, consist of blood type A, ethnicity (Asians/Pacific Islanders, Hispanics, African Americans), obesity, pernicious anemia, familial clustering, hereditary cancer syndromes (~3% of GC cases: hereditary diffuse gastric cancer, HDGC; familial diffuse gastric cancer, FDGC; familial intestinal gastric cancer, FIGC; familial gastric cancer, FGC; gastric adenocarcinoma and proximal polyposis of stomach, GAPPS; and hereditary nonpolyposis colon cancer, HNPCC), *BRCA1* and *BRCA2* mutations, co-morbidities (familial adenomatous polyposis, Li-Fraumeni syndrome, Peutz-Jeghers syndrome, and Menetrier disease), and other driver alterations such as gene mutations, epigenetic changes, gene fusions, alternative splicing, somatic copy number alterations, and transcriptional changes involving microRNA (Mclean and El-Omar, 2014; Avital et al., 2019) (Figure 2).

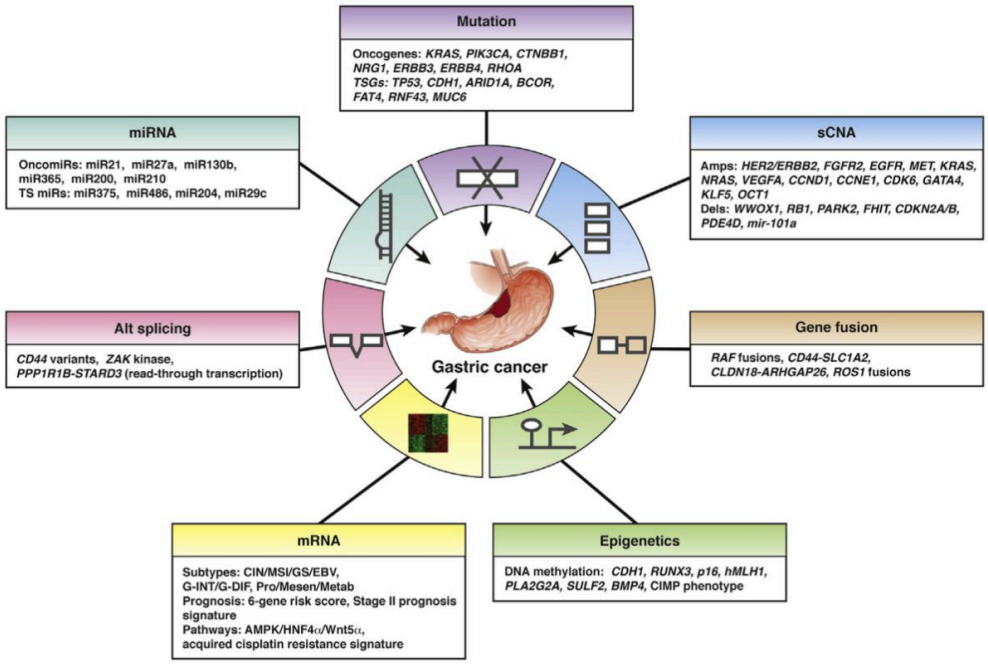

Figure 2. Common genomic driver alterations reported in GC. (Taken from Tan and Yeoh, 2015)

The marked degree of heterogeneity exemplified by GC is apparently mirrored in light of the available stratification systems. Unsurprisingly, none has fully encapsulated all the intricacies of this disease in one superior classification scheme. Basically, GC

classification can be operationally clustered into four groups on the basis of the following: depth of invasion, macroscopic/gross, histopathological, and genetic/molecular features (Summarized in Tables 1 and 2). Depending on the first category, GC is typically dichotomized either as early gastric cancer (EGC) or advanced gastric cancer (AGC). The former shows a highly confined lesion at the level of the gastric mucosa and/or submucosa whereas the latter displays lesions that are already permeating beyond the muscularis propia. Macroscopically, AGC lesions can be categorized using the Borrmann Classification System (1925) into: Type I (polypoid tumor), Type II (Ulcerated tumor with sharply demarcated margin), Type III (Ulcerating tumor without demarcated border; infiltrating), and Type IV (diffuse infiltrating tumor). An updated version of the Japanese classification system (2011) that caters both EGC (Type 0) and AGC (Type I-V) classify GC grossly as follows: Type 0 (0-I -protruding growth, 0-IIa - superficial elevated, 0-IIb -superficial flat, 0-IIc -superficial depressed, 0-III -excavated), Type I (mass), Type II (ulcerative), Type III (infiltrative ulcerative), Type IV (diffuse infiltrative), and Type V (unclassifiable) (Japanese Gastric Cancer Association, 2011). Meanwhile, much of the efforts on GC classification have been devoted on categorizing the disease with respect to their histopathological presentation. Perhaps, the simplest, oldest, yet most relevant stratification scheme even up to this present time is the one formulated by Lauren in 1965. In these criteria, GC lesions fall under two groups namely, intestinal and diffuse types. Intestinal-type GC consists of tumor cells thrown into tubular or glandular-like structures and displays well-demarcated progression of precursor lesions (chronic atrophic gastritis, intestinal metaplasia, dysplasia) while diffuse-type GC presents poorly cohesive cancer cells occurring singly or in clumps with relatively unknown or less identifiable precancerous stages (Lauren, 1965). A third group called indeterminate type was later coined to include lesions with mixed presentation. Several proposed schemes then followed including those from Mulligan (1975), Ming (1977), Goseki

(1992) and Carneiro (1995). The Ming's classification relies heavily on the pattern of tumor growth and invasion, which set it apart from the Goseki's classification that puts premium emphasis on tubular differentiation and mucin production. Nevertheless, amalgation of these systems would place the expanding type of Ming and the well-differentiated tubular/mucus scanty and well-differentiated tubular/mucus rich of Goseki under the intestinal type of the Lauren's criteria. Same parallels exist for the diffuse type wherein the infiltrating type of Ming and the poorly differentiated/mucus poor and poorly differentiated/mucus rich of Goseki would fall under this category. In 2010, a revisited WHO classification was released (Lauwers et al., 2010), which is virtually a co-existing list of the dominant and infrequent variants of tumors occurring in the stomach (Hu et al., 2012). The later subtyping system devised by the Japanese Gastric Cancer Association (2011) had drawn great inspiration from the WHO classification only with few resolutions made on subtle differences noted on tubular adenocarcinoma (well differentiated vs. moderately differentiated).

The molecular approach occupies a fairly new realm in the classification of GC. Due to the controversial utility of most histological-based classification systems in the prognostication and prediction of treatment responses or outcomes, many research groups have resorted to employ molecular pathology to address this crucial limitation. In addition, these configurations offer invaluable insights on the modifying influence of gastric microbiome, immune population, and tumor milieu in gastric carcinogenesis (Bijlsma et al., 2017; Park et al., 2019). One of the first attempts to molecular subtyping was reported by the groups of Boussioutas et al. (2003) and Chen et al. (2003). Using DNA microarray technology on paired tumor samples and adjacent normal mucosa, both works unveiled a high-resolution partitioning of gene expression signatures among intestinal, diffuse, and mixed type GC with accompanying identification of prognostically useful genes (i.e. *IGF2, PLA2G2A*). Likewise, Tay and colleagues (2003) exploited the same analytical platform and

detected three molecular GC subtypes as follows: tumorigenic, reactive, and gastric-like. They have also defined a minimal predictor gene set consisting of 12-17 genes that can potentially aid in accurate subtype prediction. Subsequent gene expression studies by Tan and co-workers (2011) identified two intrinsic subtypes of GC namely, Genomic-Intestinal (G-INT) and Genomic-Diffuse (G-DIF), based on the unsupervised analysis of 37 different human GC cell lines. As opposed to the G-DIF subtype, G-INT type correlated with increased survival time and favorable response with 5-FU and oxaliplatin. Whereas, of the three major groups (proliferative, metabolic, and mesenchymal) determined by Lei and colleagues (2013), metabolic type was found to be the least resistant to 5-FU while mesenchymal type exhibited the highest sensitivity to inhibitors of the phosphatidylinositol 3 kinase-AKT- mTOR pathway. By far, the two most sophisticated and comprehensive molecular profiling investigations on GC were those performed by The Cancer Genome Atlas (TCGA) and the Asian Cancer Research Group (ACRG). Following a careful integration of six different molecular platforms (somatic copy number analysis, whole-exome genome sequencing, DNA methylation profiling, messenger RNA sequencing, micro RNA sequencing, and sequencing and reverse-phase protein array), GC was assigned by the TCGA (Cancer Genome Atlas Research Network, 2014) into four broad classifications: Eipstein-Barr virus (EBV), Microsatellite instability (MSI), Genomically stable (GS), and Chromosomal instability (CIN). On the other hand, ACRG (Cristescu et al., 2015) developed a unique molecular subtyping system that incorporates both TP53 activation status and epithelial to mesenchymal transition (EMT) pattern therefore bolstering its prognostic value. This is reflected in the four molecular subtypes they proposed namely, MSI, Microsomal stable (MSS)/EMT, MSS/TP53^{+}, MSS/TP53^{-}.

A giant stride in our current understanding of the convoluted process of gastric carcinogenesis has been greatly aided by the utility of different *in vivo* mouse models in spite

of a number of existing limitations such as anatomical difference, strain resistance, underwhelming pathologies, prolonged latency period, varying standards of care and sanitation, and host related factors like gender, genetic background, and microbiome (Yu et al., 2014; Jiang and Yu, 2017). These models, whose availability has dynamically grown in years, can be fundamentally stratified into three categories: chemical-induced, infection-induced, and gene modified (Summarized in Table 3). Oral supplementation of N-methyl-N-nitrosourea (MNU) best represented the first group (Yamamoto et al., 2002). Analysis of MNU-treated mice has not only reinforced the notion of the predisposing risk imposed by nitrosamine compounds but also clarified the significance of few signaling networks i.e. Cox-2, NF-κB, p53, E-cadherin, in GC pathogenesis (Yamamoto et al., 2000; Takasu et al., 2008; Hayakawa et al., 2013). On another hand, *Helicobacter* (SS1 *pylori* strain and *H.* felis) infection studies have cemented the pivotal role of the bacterium on GC and shed some important information on the epidemiological impact of early treatment intervention, eradication regimens, and control of co-factors (Fox et al., 2000; Cai et al., 2005; Hayakawa et al., 2013). During the last couple of decades, bulk of the scientific works on GC has been largely gravitated towards the generation and functional utilization of gene modified animals. The genetic alteration in mice, which either obviate (KO) or insert (transgenic) a gene/s of interest, has led to a massive number of useful models that convincingly recapitulated the stepwise progression of human GC and resolved the obscure roles of acid secretion (INS-GAS, Gastrin$^{-/-}$, ACT-GAS, NH2$^{-/-}$, NH4$^{-/-}$), transcription factors (Cdx1 and Cdx2 transgenic, Klf4 conditional$^{-/-}$), inflammatory cytokines (IL1β transgenic), tumor suppressors (TFF1$^{-/-}$, MTH1$^{-/-}$), proto-oncogenes (K19/K-ras), signal transduction receptor (gp 130$^{757F/F}$), cell cycle components (p27Kip1$^{-/-}$), pH (CA IX$^{-/-}$), and signaling pathways and regulators (Runx3$^{-/-}$, NF-κB2$^{-/-}$, Smad4$^{+/-}$, TGF β1$^{-/-}$) on gastric tumorigenesis, among others (Tsukamoto et al., 2007; Yu et al., 2014; Poh et al., 2016).

α1, 4-*N*-acetylglucosaminyltransferase (*α4Gnt*) is a glycosyl transferase responsible for the biosynthesis of the *O*-glycan terminal- α1, 4-linked *N*-acetylglucosamine residues (αGlcNAc), which is uniquely contained in the secreted mucin by gland mucous cells such as cardiac gland cells, mucous neck cells, and pyloric gland cells (Nakayama et al., 1999; Yamanoi and Nakayama, 2018). Earlier reports have hinted a natural antibiotic function of αGlcNAc against *H. pylori* bacteria, which is primarily mediated via inhibition of the cell wall component, cholesteryl-α-D- glucopyranoside (Kawakubo et al., 2004). Also, loss of αGlcNAc has been typically encountered in cases of human differentiated-type gastric adenocarcinoma showing a strong association with depth of invasion, staging, and venous invasion (Shiratsu et al., 2014). More recently, it has been linked as a potential biomarker of malignant transformation of preneoplastic lesions including Barrett's esophagus (Iwaya et al., 2014), pancreatic intraepithelial neoplasia, intraductal papillary mucinous neoplasms (Ohya et al., 2017), and pyloric gland adenoma (Yamanoi et al., 2015); and as a useful diagnostic and prognostic marker of uterine cervical tumor of the gastric subtype (Ida et al., 2019). In *A4gnt* KO mice, deficiency in this particular enzyme congruently resulted to the complete absence of αGlcNAc expression thereby inducing a spontaneous development of gastric cancer through hyperplasia-dysplasia-adenocarcinoma continuum (Karasawa et al., 2012). These mutant animals demonstrate an age-dependent profile of heightened angiogenesis, inflammatory cell infiltration, and S-phase cell proliferation. Moreover, a differentially regulated expression of inflammation associated chemokine ligands, proinflammatory cytokines, and growth factors usually accompanied these aforementioned phenotypes (Karasawa et al., 2012). In the present thesis dissertation, I preferentially utilized this multistage, progressive mice model and established its potential suitability in facilitating both bioactivity testing and gene function studies. Specifically, in chapter 1, I ascertained the potential merit of oral administration of brown seaweed-derived β-glucan (Laminaran) on

gastric preneoplastic lesion in 12-week old *A4gnt* KO mice and described whether it could effectively restrain the progression of gastric dysplasia. For the second chapter, I characterized the antitumor activity of the crude ethanolic extract of propolis from the Philippine stingless bees (*Tetragonula biroi*, Friese) using 50-week old *A4gnt* KO mice showing a fully developed differentiated-type gastric adenocarcinoma, and dissected some of the plausible mechanisms whereby a tumor-suppressive response could be elicited. Finally in chapter 3, I explored the functional contribution of the tandem repeat-type galectin 4 (*Lgals4)* in *A4gnt* KO-induced gastric carcinogenesis through generation of a new animal model, *A4gnt* x *Lgals4* DKO mice and characterized the stage-specific (10-, 30-, 50-weeks old) phenotype and genetic traits including the possible processes that underlie these observed changes.

Table 1. Summary of the macroscopic (gross) and histopathological classifications of GC

Depth of Invasion	Macroscopic		Histopathological						
	Borrmann (1925)	*Japanese (2011-Updated)*	*Lauren (1965)*	*Mulligan (1972)*	*Ming (1977)*	*Goseki (1992)*	*Carneiro (1995)*	*WHO (2010-updated)*	*Japanese (2011)*
Early gastric cancer (EGC)		Type 0 (0-I - protruding growth 0-IIa - superficial elevated 0-IIb - superficial flat 0-IIc -superficial depressed 0-III- excavated)	Intestinal type	Intestinal cell type	Expanding type	Tubular- well differentiated Mucus-scanty Tubular- well differentiated Mucus-rich	Glandular type	Papillary adenocarcinoma Tubular adenocarcinoma	Papillary adenocarcinoma Tubular-well differentiated Tubular-moderately differentiated
Advanced gastric cancer (AGC)	Type I- polypoid tumor	Type I - mass						Mucinous adenocarcinoma	Mucinous adenocarcinoma
	Type II - ulcerated tumor with sharp demarcated margin	Type II - ulcerative	Diffuse type	Mucous cell type Pyloro-cardiac gland cell type	Infiltrating type	Tubular- poorly differentiated Mucus-scanty Tubular- poorly differentiated Mucus-rich	Isolated type	Poorly cohesive carcinoma incl. signet ring cell carcinoma	Poorly differentiated-solid type Poorly differentiated-non-solid type Signet ring cell carcinoma
	Type III - ulcerated tumor w/0 demarcated margin; infiltrating	Type III - infiltrative ulcerative						Mixed carcinoma	Carcinoid tumor
	Type IV - diffuse infiltrating tumor	Type IV - diffuse infiltrative					Solid variety	Adenosquamous carcinoma Hepatoid carcinoma Carcinoma with lymphoid stroma Undifferentiated carcinoma Hereditary diffuse carcinoma Parietal cell carcinoma Malignant rhabdoid tumor Mucoepidermoid carcinoma Paneth cell carcinoma	Adenosquamous carcinoma Hepatoid carcinoma Carcinoma with lymphoid stroma Undifferentiated carcinoma Endocrine carcinoma Squamous cell carcinoma Miscellaneous carcinoma
		Type V - unclassified	Indeterminate type				Mixed typed	Mixed adeno-neuroendocrine carcinoma Endodermal sinus tumor Embryonal carcinoma Pure gastric yolk sac tumor Oncocytic adenocarcinoma	

Table 2. Summary of the molecular/genetic classification of GC

Genetic/Molecular				
Tan et al. (2011)	Lei et al. (2013)	The Cancer Genome Atlas (TCGA, 2014)	Asian Cancer Research Group (ACRG, 2015)	Bijlsma et al. (2017)
Genomic Intestinal (G-INT)	Proliferative	Eipstein Barr Virus	MSI High	Epithelial
Genomic Diffuse (G-DIF)	Mesenchymal	Microsattelite Instable (MSI)	Microsatellite Stable (MSS)/EMT	Immunogenic
	Metabolic	Genomically Stable (GS)	MSS/TP53 Intact	Metabolic
		Chromosomal Instability (CIN)	MSS/TP53 Loss	Mesenchymal
				Organ-specific

Table 3. Genetically modified models and their observed lesions

Model	Age of Onset	Metaplasia	Hyperplasia	Dysplasia	Carcinoma	Invasion	Metastasis
TFF$^{-/-}$	12 months	ND	Y	Y	Y	Y	N
gp130$^{757F/F}$	3 months	Y	Y	Y	Y	Y	N
Cdx2 transgenic	12 weeks	Y	Y	N	Y	N	N
INS-GAS	20 months	Y	ND	Y	Y	Y	N
ACT-GAS	20 months	ND	Y	ND	Y	N	N
Gastrin$^{-/-}$	12 months	Y	Y	Y	Y	N	N
Atp4a$^{-/-}$	12 months	Y	Y	N	N	N	N
NHE2$^{-/-}$	3 months	ND	Y	N	N	N	N
NHE4$^{-/-}$	9 weeks	N	N	N	N	N	N
Kvlqt1$^{-/-}$	3 months	ND	Y	N	N	N	N
H2R$^{-/-}$	16 weeks	N	Y	N	N	N	N
HDC$^{-/-}$	12 months	Y	Y	N	N	N	N
IQGAP1$^{-/-}$	15 months	ND	Y	Y	N	N	N
TGFβ1$^{-/-}$	20 days	Y	Y	N	N	N	N
Smad4$^{-/-}$	9 months	ND	Y	Y	Y	Y	N
Runx3$^{-/-}$	8 months	ND	Y	Y	N	N	N
Apc$^{-/-}$	20 weeks	ND	Y	Y	Y	Y	N
MTH1$^{-/-}$	18 months	ND	Y	Y	Y	N	N
K19-C2mE transgenic	45 weeks	Y	Y	Y	Y	N	N
Tsp$^{-/-}$	3 weeks	Y	Y	N	N	N	N
Tgfα transgenic	6 weeks	ND	Y	Y	N	N	N
AhR transgenic	3 months	Y	Y	Y	Y	Y	N
Klf4$^{-/-}$	35 weeks	ND	Y	Y	Y	N	N
p27$^{-/-}$	60 weeks	Y	Y	Y	Y	N	N
Car9$^{-/-}$	4 weeks	ND	Y	N	N	N	N
CEA SV40 transgenic	37 days	ND	ND	Y	Y	Y	N
H^+/K^+-ATPase β subunit SV40 transgenic	12 months	N	N	Y	Y	N	N
H^+/K^+-ATPase β subunit	20 months	ND	ND	Y	Y	Y	N
Shh$^{-/-}$	18.5d embryo	Y	Y	N	N	N	N
Occludin$^{-/-}$	10 months	N	N	Y	N	N	N
ClC2$^{-/-}$	9 weeks	N	N	Y	N	N	N
Cdh1$^{-/-}$p53$^{-/-}$	6 months	Y	Y	Y	Y	Y	Y

*Y-Yes, N-No, ND-Not Detectable (Taken from Jiang and Yu, 2017)

General Methodology

Animal Care and Preparation

Animals were strictly maintained under a specific pathogen free environment following a lighting regimen of 12 hr. light: dark cycle and caged in appropriate density using standard polycarbonate cages. Commercial rodent pellets (CRF, Oriental Yeast Co., Ltd., Japan) and water were provided in ad libitum basis.

Histopathology

Intraperitoneal (IP) injection of Bromodeoxyuridine solution (5-bromo-2-deoxyuridine, BrdU) (10mg/kg), which permits visualization of cells at the proliferative S-phase of the cell cycle, was instituted one hour before commencing sacrifice. Mice were euthanized via cervical dislocation and stomach along with a small portion of the duodenum was resected and cut open by making a midline incision along the greater curvature. Samples were washed with 1x PBS to remove food debris, dabbed onto a clean paper towel, and divided into half for the following analyses: For histopathological/immunohistochemical examination, half of the specimen was flattened onto a filter paper, sandwiched in a cassette with a biopsy sponge pads, fixed in buffered formalin (10%) for at least 48 hours, and processed using the standard paraffin protocol. Samples were subsequently cut into four-micrometer thickness and then subjected to routine H&E. On the other hand, the remaining half of the stomach samples were placed into a 1.5 ml microcentrifuge tube containing RNA*later*™ solution (Invitrogen, Carlsbad, CA, USA) and stored at -80°C refrigerator until further analysis.

Assessment of the gross pyloric mucosal lesion

Upon opening the resected stomach samples, gross lesions that are confined at the level of the pyloric antrum was evaluated and graded semi-quantitatively using a defined scoring system enumerated as follows: 0 – healthy mucosa/none, 1 – mildly, 2 – moderately, 3 – markedly elevated.

Microscopic evaluation of the pyloric mucosal thickness and PMNLs infiltration

Estimation of the thickness of the pyloric mucosa (μm) was accomplished using the prepared H&E sections by measuring a properly oriented pyloric mucosa starting from the base up to the highest point of the epithelium and then averaging the quantifications obtained from at least three different areas. Meanwhile, examination of the number of infiltrating PMNLs was determined using a predefined 100 μm area having the highest cell density and the mean of triplicate count was similarly obtained.

CD3 and BrdU immunohistochemistry

Previously prepared stomach tissue sections were deparaffinized with four changes of xylene followed with rehydration by dipping in decreasing concentrations of alcohol (100%, 95%, 90%, 80%, 70%) and washing with three changes of Tris-buffered saline (TBS, 0.1M, pH 7.4) solution. Tissue sections were next subjected to varying antigen retrieval procedures depending on what is deemed optimal for each given marker. For CD3, slides were incubated in 0.1 M sodium citrate solution (pH 6) for 10 minutes at 121°C whereas samples were initially digested in 4N HCl at room temperature for 30 minutes followed by incubation in 0.5% trypsin (Gibco®, Life Technologies Corp., USA) at 37°C atmosphere for 30 minutes for BrdU. Tissue sections were subsequently treated with 10% H_2O_2-methanol solution for 15 minutes at room temperature to block endogenous peroxidase activity. Reduction of non-specific background staining was achieved by immersing slides in 8% skimmed milk for 1 hour at 37ºC for CD3 or by applying blocking reagent A (vial 1) using the Histofine Mousestain Kit (Nicherei Biosciences, Tokyo, Japan) protocol for BrdU. After which, tissue samples were incubated with primary antibodies, anti-CD3 (DakoCytomation, Glostrup, Denmark; rabbit; polyclonal; ready-to-use) and anti-BrdU (DakoCytomation, Glostrup, Denmark; mouse; clone Bu20a; 1:50), and set aside in a humidified atmosphere at 4ºC for at least 12 hours (overnight). This was followed by washing with three changes of TBS solution

and then identification of primary antibody binding sites by immunolabeling for 1 hour at room temperature using ready-to-use HRP-conjugated rabbit secondary antibody (DakoCytomation, Glostrup, Denmark) for CD3. In the case of BrdU, additional blocking with blocking reagent B was performed and then labeling with a universal immuno-peroxidase polymer (Simple Stain Mouse Max PO) for 10 minutes at room temperature. Presence of any immunoreactivity was visualized through incubation with 3,3'-diaminobenzidine tetrahydrochloride (DAB)- H_2O_2 solution. Finally, tissue sections were counterstained with Mayer's haematoxylin, dehydrated in increasing grades of alcohol, cleared with xylene, and mounted using a permanent mounting medium (Multi Mount 480, Matsunami Glass Industry, Ltd., Osaka, Japan).

Determination of CD3 and BrdU immunostaining was achieved by counting the total number of positive cells in a defined 100 μm area with the highest cell density and getting the average count of triplicate measurements.

Quantitative Real Time PCR (qRT-PCR)

Stomach tissue samples kept in RNA*later*™ solution were transferred into a tube containing lysis buffer and homogenized using a Shake Master Auto BMS-A20TPver.2.0 (BMS, Tokyo, Japan). RNA extraction was performed by closely adhering to instructions provided in the Nucleospin® RNA isolation kit (Macherel-Nagel, Düren, Germany) and RNA concentration per sample was determined using a BioSpec-nano spectrophotometer (Shimadzu, Kyoto, Japan). First strand cDNA was subsequently synthesized following the PrimeScript™ RT reagent kit (Perfect Real Time) (Takara Bio, Shiga, Japan) protocol. Briefly, ten microliter reaction volume containing 0.6 μg RNA, 2 μl 5x Primescript buffer, 0.5 μl oligo-dT primer, 0.5 μl random 6mers, and 0.5 μl Primescript enzyme mix was prepared and run in a C1000™ Thermal cycler (Bio-Rad Laboratories Co., Ltd., California,

USA) using the succeeding settings as follows: stage 1 – 37°C for 15 minutes, stage 2 - 85°C for 5 seconds, and stage 3 - 4°C hold.

Gene transcription levels of selected cytokines (interleukins, chemokines, growth factors) were measured using the TB Green™ *Premix Ex Taq*™ II (TIi RNaseH Plus) (Takara Bio, Shiga, Japan) kit and StepOnePlus™ Real-Time PCR (Applied Biosystems, California, USA). In a 96 well PCR plate, each well was added with a total reaction volume of 20 µl consisting of 5 µl cDNA, 10 µl TB Green, 0.4 µl ROX dye and 10 µM primer mix. Plate was heated at 98°C for 1 minute and then underwent 40 thermal cycles of 95°C for 30 s, 95°C for 5 s, and 60°C for 34 s. The reaction was terminated after one cycle of melting curve at 95°C for 15 s, 60°C for 1 m, and 95°C for 15 s. Determination of mRNA expression was performed using the comparative CT method by setting *Actb* as internal control gene and C57BL/6J as reference animal with its mean mRNA expression level set at 1.0. All analysis was done in duplicates.

Statistical Analyses

For comparison of only two groups, Independent sample T-test or the non-parametric Mann-Whitney U test were utilized. In the event of comparing more than three groups, One Way Analysis of Variance (ANOVA) with Tukey HSD posttest was used for normally distributed data as confirmed by Levene's Test. Otherwise, robust test for equality of variances with Games-Howell posttest or the non-parametric Kruskal Wallis Test was selected. All analyses were performed using SPSS v.24 (Chicago, IL, USA) and values with $P<0.05$ were considered statistically significant while those with $P<0.01$ were deemed highly significant. Data were shown as mean ± SE.

Chapter 1

Gastroprotective efficacy of brown seaweed-derived β-glucan on gastric dysplasia development in *A4gnt* KO mice model of gastric adenocarcinoma

Introduction

Due to the limited therapeutic value of most currently available treatment options and control measures against highly debilitating diseases such as cancer, the paradigm of disease management has greatly shifted to early disease detection and prevention. This has resulted in extensive studies exploring the possible contribution of food and nutrition thus, giving rise to the concept of "functional foods", which generally refers to any food components possessing health-enhancing properties in supplementary with their apparent nutritional benefits (ILSI, 1999). At present, a growing list of examples has been increasingly reported including probiotics, lycopene, phytochemicals, docosahexanoic acid (DHA), eicosapentanoic acid (EPA) and β-glucans, etc. (Hasler et al., 2002).

β-glucans belong to the broadly diverse group of non-toxic polysaccharides defined by the presence of β-(1,3)-D-glucopyranosyl backbone with variable length β-(1,4)- or β-(1,6)-linked side chains (Samuelsen et al., 2014). They commonly serve a structural and storage functions and typically obtained from a wide variety of sources such as edible mushrooms (*Pleurotus ostreatus*, *Lentinus edodes*, *Schizophyllum commune*, *Grifola frondosa*, *Sparassis crispa*, *Sclerotium rolfsii*), plants, oats, yeast (*Saccharomyces cerevisiae*), microalgae (*Euglena gracilis*), and seaweeds (*Laminaria digitata*, *Saccharina longicruris*, *Durvilaea Antarctica* (Barsanti et al., 2011). Since humans and vertebrate animals are naturally incapable of synthesizing this compound intrinsically, they are oftentimes considered as biological response modifiers (BRMs) that can trigger a non-specific immune response (Novak et al., 2008). In addition, they are known to elicit a myriad of health-promoting activities like prebiotic, anti-infective, anti-inflammatory, anti-cancer, antioxidant, immunomodulatory, and glucose- and cholesterol-lowering efficacies, among others (Driscoll et al., 2009; Masuda et al., 2009; Ruthes et al., 2013).

Over the last couple of decades, knowledge on β-glucans has tremendously escalated especially those from marine-derived sources. This great deal of research attention is no longer surprising as these marine organisms are now being progressively incorporated in the normal diet of people. In Japan, for instance, seaweed consumption was projected at 20% of the daily food intake, which essentially translates to an average of about 1.6 kg of dry seaweeds per person per year (Collins et al., 2016). Among the major types of macro algae or seaweeds, brown seaweeds (Phaeophyceae) comprise the ultimate source of marine β-glucans, which are popularly regarded as "Laminarin" or "Laminaran". Although comparable with the more common β-glucans from mushrooms i.e. Grifolan from Maitake and Lentinan from Shiitake in terms of solubility being both soluble, Laminaran granule has a relatively smaller molecular size (~4kDa vs 30kDa for Grifolan and 500kDa for Lentinan) (Nakashima et al., 2018). Unlike others also, much of what has been known about Laminaran practically delved on isolation, structure elucidation, and *in vitro* efficacy (Hazama et al., 2009; Baranoski et al., 2015). Here in this current paper, I tested the hypothesis that purified β-glucan from the brown algae, *Eisenia bicyclis*, could substantially restrict the progression of gastric dysplasia as uniquely displayed by 12-15 week-old *A4gnt* KO mice. The findings that this study will generate may provide a strong indication for the consumption of brown seaweed-derived β-glucans as an effective control strategy for gastric preneoplastic lesion development.

Results

Laminaran improved gross lesion showing reduced gastric mucosal elevation

Consistent with previous publication (Karasawa et al., 2012), *A4gnt* –deficient mice at around 15 weeks of age were confirmed to exhibit spontaneous tumor growth that is strictly confined at the area of the gastric antrum. To initially characterize the efficacy of oral supplementation of Laminaran for 3 consecutive weeks (21 days), stomach tissue samples collected from all treatment groups were scrutinized for possible changes in the formation of the gross lesion. As illustrated in Fig.1, *A4gnt* KO + Laminaran group revealed a significant indication of gross improvement as shown by the relatively lower mean score of 1.19 ± 0.40 as compared to that of the untreated counterpart, which obtained a mean score of 1.87 ± 0.35. This implies the tendency for Laminaran to downscale the gross elevation of the gastric mucosa.

Laminaran decreased the gastric mucosal thickness

Prepared stomach tissue sections were next evaluated microscopically for gastric mucosal thickness. As expected, the substantial improvement in the rate of gross tumor growth observed in the *A4gnt* KO + Laminaran group efficiently translated to a marked reduction in the thickness of the pyloric mucosa as compared to those of the *A4gnt* KO + dH_2O group (453.82 ± 20.96 vs. 530.29 ± 54.65) (see Fig. 2).

Laminaran induced differential sequestration of inflammatory cells

Due to the pivotal role of inflammatory cell infiltrates in the initiation and progression of gastric tumor in *A4gnt* KO mice model, the number of polymorphonuclear leukocytes (PMNLs) and CD3- labeled lymphocytes was accounted. An apparent disaccord in the infiltration pattern of these immune cells was discovered upon comparison of the studied treatment groups. Whereas a considerable decrement in the number of PMNLs was unveiled in *A4gnt* KO + Laminaran group in converse with the untreated KO group (18.96 ± 4.50 vs

31.64 ± 7.97 cells) (Fig.), the opposite was true when considering the mean count of sequestered CD3-positive T-lymphocytes (12.75 ± 3.09 vs 6.39 ± 3.94) (Fig).

Laminaran influenced the proliferative and angiogenic processes

Control of proliferation and angiogenesis are two other mechanisms deemed crucial for *A4gnt* KO-induced gastric carcinogenesis. In view of this perspective, it was compelling to examine the consequence of Laminaran administration on these processes. As clearly shown in Fig. 4A, *A4gnt* KO + Laminaran group registered an average number of BrdU-positive cells of around 166.54 ± 23.54 cells, signifying a 26% deduction in the count of these highly proliferating cells relative to those of *A4gnt* KO + dH_2O group that figured about 226.09 ± 26.63 cells. When it comes to the distribution of angiogenic cells, a remarkable diminution in the number of CD-31-positive was noted on *A4gnt* KO + Laminaran group tallying around 4.64 ± 1.40 cells in contrary to about 7.28 ± 2.87 cells exemplified by the *A4gnt* KO + dH_2O group.

Laminaran modified the transcriptional profile of selected cytokines

The capacity of Laminaran to bring about changes at the transcriptional level was next investigated using selected genes whose expression profiles were previously established to be differentially altered between wildtype control and *A4gnt* KO animals (Karasawa et al., 2012). As revealed by the quantitative real time PCR data, a sharp decline in *Il11* gene expression was disclosed by the *A4gnt* KO + Laminaran group attaining a statistical significance in contrast to those of untreated control group (7.02 ± 9.72 vs 24.73 ± 13.60). Surprisingly, with respect to *Il10* expression, the *A4gnt* KO + dH_2O control group registered a mean expression level of only 0.50 ± 0.32 as opposed to that of the *A4gnt* KO + Laminaran group, which appeared to restore the transcription level of this gene after registering a mean value of 1.09 ± 0.51. Although there were some possibilities for a Laminaran-mediated

transcriptional regulation, the gene expression profile of the remaining genes was found to be statistically comparable between the two KO treatment groups.

Laminaran increased IL-10 protein expression

IL-10 immunohistochemistry was additionally performed to validate the real time PCR finding of significant preservation of its gene expression. Unlike the untreated control group, pyloric epithelium of *A4gnt* KO + Laminaran group exhibited a relatively higher IL-10 expression showing a cytoplasmic staining pattern with weak to moderate intensity. Coincidentally, these Laminaran-treated KO mice also manifested an increased number of parietal glands along the gastric corpus having a moderate to strong IL-10 expression as compared to those untreated counterpart.

Discussion

As exciting developments in β-glucan research have stirred the attention of many scientific groups globally, more and more investigations have been aggressively undertaken to acquire an in-depth understanding of the role of this bioactive molecule. Previously, our group along with others has already laid down evidence on the tissue-preserving action of β-glucan from various sources including the function of their signaling receptors (Sandvik et al., 2007; Gulmen et al., 2010; Yan et al., 2011; Masuda et al., 2013; Tang et al., 2015). However, a fairly limited number of studies have been dedicated to clarify the potential benefit of β-glucan supplementation in addressing the early stages of the preneoplastic cascade. Bobek and Galvaby (2011) earlier reported that Pleuran administration caused substantial alleviation of the aberrant crypt foci (ACF) lesions following dimethylhydrazine (DMH) induction. On the other hand, in a more recent paper by Shen and colleagues (2016), both soluble and insoluble oat-derived β-glucans effectively reversed the effects of DMH-induced early colon carcinogenesis through enhancement of short-chain fatty acids (SCFA), reduction of fecal bile acid levels, and promotion of tumor cell apoptosis. Yet, one major drawback of these above-mentioned these studies is the relatively variable induction of preneoplastic lesion as some animals already manifested way more advanced stages of cancer. Therefore, in light of this apparent limitation, I hereby employed a unique mice model of differentiated-type gastric adenocarcinoma, *A4gnt* KO mice, which present a well-demarcated development of low-grade gastric dysplasia at 15-18 week of age.

Chronic inflammation signifies a critical event in the carcinogenic process, especially in the differentiated or intestinal subtype (Correa et al., 2012), as it triggers the requisite stimuli to initiate the vicious cycle of inflammation-metaplasia-dysplasia-invasive carcinoma succession (Lu et al., 2006; Grivennikov et al., 2010). It promotes disruption of the cellular homeostatic balance through uncontrolled regulation of several inflammatory signals

emanating from various mediators and effectors such as immune cells, enzymes, soluble signals, growth factors, and activated downstream signaling molecules (Coussens et al., 2002; Bartsch et al., 2006; Karin et al., 2006). In this current work, Laminaran supplementation induced substantial improvement of the gross mucosal lesion as evidenced by the profound depression of gastric mucosal elevation. Microscopically, this gross finding correlated with a marked inhibition of gastric mucosal thickness together with a notable decrement in PMNLs influx, which is concordant with previous publications (Staton et al., 2007; Smiderle et al., 2008; Tanaka et al., 2011). This indicates that resolution of the ensuing inflammation comprise one of the protective actions of Laminaran.

Dysplastic morphologic transformation typically develops whenever there is a deregulation in the tight control of the cellular proliferative process (Cooper et al., 2012). This particular response is also recapitulated by *A4gnt*-deficient animals starting at 10 weeks of age due to a heightened epithelial mucosal cell proliferation instead of retarded apoptotic pathway. In connection to this, BrdU labeling, which permits identification of actively dividing cells in the S-phase of the cell cycle (Zacchetti et al., 2003), was subsequently evaluated. A considerable diminution in BrdU-labeled cells was clearly demonstrated in Laminaran-treated KO group relative to those of the untreated control counterpart. In concurrence with this data, the group of Jafaar et al. (2014) similarly observed a significantly depressed proliferation of BrdU incorporated LCC9- and LY2 endocrine resistant breast cancer cells but not MDA-MB-231 triple negative cells. Contrarily, β-glucan stimulated a profound cell growth following anterior cruciate ligament transection and partial medial meniscectomy-induced osteoarthritis in rats (Kim etal., 2001). This marked inconsistency may be explained in part by the notion that β-glucan dictates control of cell proliferation depending on the nature of the offending stimulus eventually leading to restoration of the normal cellular state and function.

I subsequently examine the influence of Laminaran on angiogenesis owing to the widely recognized contribution of this process on assisting in the multistage transition to neoplastic transformation (Xu et al., 2016). Using CD31 marker, an increased density of both nascent and developed endothelial cells was documented in *A4gnt* KO control mice group. In compatible with this observation, CD-31 immunoreaction was also significantly augmented in reported cases of human colorectal adenoma-carcinoma sequence (ACS) specifically during the initial stages of colorectal dysplasia (Staton et al., 2007). Interestingly, oral administration of Laminaran notably deduced the number of CD31-positive endothelial cells thus denoting a prominent inhibitory response on angiogenesis. Other experimental investigations also highlighted the anti-angiogenic property of β-glucan as proven by various *in vivo* as well as *ex vivo* assays (Hoffman et al., 1996; Yamamoto et al., 2009), which are in consonance with this present study. However, note that the apparent consensus regarding this property of β-glucan has been made not on the basis of premalignant lesion but on the findings taken from already established tumors. Nevertheless, irrespective of the stage, these results collectively imply that Laminaran may effectively restrain the angiogenic process to efficiently reverse the progressive development of dysplastic lesion into full-blown carcinoma.

It is worth mentioning in the current paper the unusual detection of a remarkable increment in the magnitude of CD3 immunoexpression, which indirectly provides useful information on the number of infiltrating T cell populations. I initially tested the hypothesis that these cells are presumably IL-10-producing T cells in due consideration of the significant escalated levels of *Il10* gene as revealed by qRT-PCR findings. Unexpectedly, only a trace number of immunopositive cells was determined after performing both immunohistochemical and immunofluorescence examinations (data not shown). In normal intestinal mucosa, Tsukada and colleagues (2003) found that β-glucan treatment provoked a substantial

augmentation of γδ- and αβ-expressing CD8 T lymphocytes, which are commonly involved in cytotoxic reaction. As the present data are rather insufficient in form to prove this conjecture, additional experiments are definitely warranted to confirm whether the aforementioned T cell populations were actually expanded following oral application of Laminaran.

Since *A4gnt* KO induction has been intricately associated with a prominent transcriptional regulation of several inflammation-associated genes, the potential modulatory influence of Laminaran on these genes was also carefully scrutinized. Of these, the appreciable overexpression in the gene levels of *Il10* along with a notable decreased in *Il11* was of particular interest, entailing a higher likelihood for polarity towards an anti-inflammatory function. Moreover, a significant restoration of IL-10 was validated at the protein level, concurring significantly with those of the transcriptional data. *Il10* is the gene encoding for the IL10 protein, a bifunctional cytokine exhibiting either a pro-inflammatory or anti-inflammatory activity (Mannino et al., 2015). Deficiency of this gene in mice (IL-$10^{-/-}$ mice) has been shown to invoke a parallel phenotype as that of *A4gnt* KO mice such as an elevated inflammatory cell infiltration of the mucosal epithelium, increased density of angiogenic cells, escalated release of proinflammatory cytokines and excessive influx of infiltrates of immune cells (Berg et al., 1998; Tanikawa et al., 2012). It acts mainly on receptors found on dendritic cells and macrophages including their co-stimulatory molecules, the interaction of which led to a cascade of inhibitory signals affecting various inflammation cytokines (IL-1, 6, and 12) and chemokines (CC- and CXC-type) (Mosser et al., 2008). Coincidentally, aside from the light to moderate grade of IL-10 staining of the pyloric epithelium, Laminaran treated mice also characteristically manifested a relatively greater number of IL-10 reactive parietal cells showing a moderately intense staining pattern in converse to the corresponding mucosal glands noted in the untreated KO mice. However, the

extent of immunostaining in this treated animals was comparably lower when contrast with those of the wildtype C57BL/6J group. On the basis of this particular observation, it seems likely that the magnitude of IL-10 immunostaining by parietal cells dictate in part the degree of the preservation of the gastric function. Indeed, this was validated by the Lee and colleague (2017), whose recent work underscores a strong direct relationship between IL-10 expression by parietal cells and initiation of preneoplastic lesions as explicitly shown in tamoxifen-induced spasmolytic polypeptide-expressing metaplasia (SPEM) mice model. In the attempt to reliably explain the potential involvement of *Il11* in the marked improvement of gastric phenotype following Laminaran supplementation, our group generated an *A4gnt/Il11* double deficient (DKO). The detailed discussion for this newly generated model is reserved in the last chapter of this present dissertation. Briefly, a highly significant regression of preneoplastic lesion was dramatically displayed by *A4gnt/Il11* DKO mice showing almost comparable phenotype as those of the wildtype control animals. This suggests that a significantly delayed development and progression of lesion was elicited in these animals therefore, firmly underscoring the significant role of IL-11 in *A4gnt* KO- induced carcinogenesis.

To date, the specific molecular details by which β-glucan exerts protective function still remains a subject of continuous discourse. This is further complicated by the high divergence documented with respect to their origin, branching pattern, charge, tertiary conformation, and solubility (Novak et al., 2008). For low molecular weight or soluble-type β-glucans like Laminaran, these molecules are believed to be actively phagocytized by intestinal macrophages after oral ingestion and this action is mediated mainly through interaction with dectin-1 receptors found on these cells (and in various immune cells such as dendritic cells, lymphocytes and myeloid cells) (Brown et al., 2001). Laminaran are then carried to various lymphatic organs such as lymph nodes, spleen, and bone marrow before

reaching the systemic circulation and induce a biological response (Hong et al., 2004). The group of Rice *et al.* (2005) earlier purported that Laminaran supplementation can effectively elevate dectin-1 expression in the gut-associated lymphoid tissues (GALT) found in the Payer's patches. In this connection, I additionally examined the expression of *Clec7a* (gene encoding for Dectin-1) in the harvested pyloric tissues but unfortunately failed to observe a statistically significant difference between KO treatment groups. Corroborating this finding, it was confirmed by Goodridge and colleagues (2011) the inherent incapability of soluble-type β-glucans to facilitate biological response via dectin-1 signaling because of its apparent inability to eliminate the participation of the inhibitory membrane tyrosine phosphatase from the "phagocytic synapse", thereby substantiating in part its utilization as a functional dectin-1 antagonist (Brown et al., 2001; Tang et al., 2015). Further validating these results, it was observed in irradiated *A4gnt* KO mice, which have undergone bone marrow transplantation with dectin-1 deletion, the trifling contribution of dectin-1 signaling in the development and progression of gastric lesion (Masaya et al., unpublished data). The relative increase in Dectin-1 expression may be ascribed to the established tendency of soluble β-glucans to promote receptor recycling (Herre et al., 2004). Alternatively, Laminaran may also act upon mucosal epithelial cells in a dectin-1-independent manner (Rice et al., 2005). This mechanism appear to be of significant value in *A4gnt* KO mice model, although the present data cannot sufficiently support this conjecture. In a recent investigation on C. *albicans*-mediated immunity, the protective property of both soluble (Laminaran) and particulate β-glucans was ascribed to a novel PRR receptor found on oral epithelial cells and identified as Ephrin type A-receptor 2 (EphA2) (Swidergall et al., 2018). This receptor is member of the erythropoietin-producing hepatocellular (Eph) receptor kinase family that is largely involved in a number of physiological actions including epithelial cell survival, proliferation, and migration (Pitulescu et al., 2010). I next detected the expression level of this particular gene

among the various treatment groups using real time PCR. Interestingly, a significant but modest amplification of the *Epha2* gene was exhibited by the *A4gnt* KO + Laminaran group in contrast to wildtype control group. However, statistical difference was only established in Laminaran-treated KO group versus untreated KO control group after restricted inclusion of data from all female animals (0.89±0.07 vs 1.23±0.26, p=0.037; n=5). More experiments are definitely warranted to clarify the promising contributory role of EphA2 and its signaling pathway in this specialized mice model.

Additional Methodology

Chemical and dosage

Laminaran, a purified low molecular weight soluble-type β-glucan from *Eisenia bicyclis*, was obtained from Tokyo Chemical Industries Co., Ltd. (Tokyo, Japan). It is mainly composed of linear glucose polymers with β- (1-3) linkage and contained few interspersing β- (1-6)-associated branches (Ermakova et al., 2013). The degree of polymerization (DP) is estimated to be around 20-25 while the distribution of β-D-1, 3 and β-D-1, 6 glycosidic bonds has a ratio of about 1.5:1 (Men'shova et al., 2013). Consistent with previous publications, a dosage of 100 mg/kg body weight was similarly tested in this present work (Hong et al., 2014; Shen et al., 2016).

Animals

Twelve week-old *A4gnt* KO mice of both sexes were specifically selected for this experiment. As stipulated in the General introduction section, at this age, these animals characteristically display a low-grade dysplasia showing slight alterations of normal gland morphology such as papillary enfolding and crypt serrations (Karasawa et al., 2012). Age-matched C57BL/6J mice, which were procured from Nihon SLC, served as useful wildtype control.

The experimental procedures hereby performed were in strict compliance with the guidelines set by the Institutional Animal Care and Use Committee, Graduate School of Agriculture and Life Sciences, The University of Tokyo with Approval No. P17-005H02.

Treatment group

C57BL/6J and *A4gnt* KO animals were randomly designated into three treatment groups as shown below:

Group 1: wildtype + distilled water (normal control, n=8)

Group 2: *A4gnt* KO + distilled water (non-treated control, n=12)

Group 3: *A4gnt* KO + Laminaran (treated, n=12)

All treatments were intragastrically administered on a daily basis for a total duration of 21 days.

Immunohistochemistry

In addition to CD3 and BrdU markers, immunohistochemical detection of CD31 and IL-10 proteins was also conducted. As detailed in the General Methodology section, both markers were subjected to the exact same procedures as that of CD3. The following are the complete information for the primary antibody used: CD31 (Neomarkers, CA, USA; rabbit; polyclonal; ready-to-use) and IL-10 (BD Biosciences, CA, USA; mouse; clone JES-2A5; 1:10).

CD31-positive staining was also quantified by tallying the total number of positive cells contained in a 100 μm area and the mean of at least three measurements was computed. For IL-10, immunoreaction was adjudged semi-quantitatively based on the percentage distribution of positive cells showing cytoplasmic labeling as reflected in the following scoring system: 1- 0-10%, 2- 11-25%, 3- 26-50%, 4- >50%. Quantifications were made by evaluating at least three different microscopic fields using x200 magnification.

Quantitative Real Time PCR (qRT-PCR)

As mentioned in the general methodology section, qRT-PCR was employed to measure the gene expression level of selected inflammation associated cytokines. The details of forward and reverse primers were summarized in Table.

Figure Legends

Fig. 1-1. Laminaran administration resulted in a substantial amelioration of the gross mucosal elevation showing a milder phenotype. Data are shown as mean±SD. Means with different letters are significant at $P<0.01$ using Students T-test.

Fig. 1-2. Laminaran treatment considerably reduced the mean thickness of the pyloric mucosa. Scale: 500μm. Data are shown as mean±SD. Means with different letters are significant at $P<0.01$ using One-way ANOVA with Games-Howell posttest.

Fig. 1-3. Laminaran invariably affected the infiltration of inflammatory cells. (A) The mean number of infiltrating PMNLs per 100μm area. (B) The mean count of CD3-positive T cells per 100μm area. Data are shown as mean±SD. Means with different letters are significant at $P<0.05$ using One-way ANOVA with Tukey HSD posttest.

Fig. 1-4. Laminaran treatment negatively influenced the proliferative and angiogenic processes in gastric dysplasia. (A) Representative photomicrographs of BrdU labeling among the different treatment groups. Scale bars: 50μm. (B) Photomicrographs showing the density of the distribution of CD31-positive angiogenic cell in different treatment groups. Scale: 100μm. Data are shown as mean±SD. Means with different letters are significant at $P<0.05$ using One-way ANOVA with Games-Howell or Tukey HSD posttest.

Fig. 1-5. Oral supplementation with Laminaran differentially regulated the mean expression levels of selected cytokines (interleukins, chemokines, and growth factors) whose gene expressions were substantially altered following *A4gnt* KO-induced gastric carcinogenesis. Real Time PCR data are shown as mean±SD. Means with different letters are significant at $P<0.05$ or * $P<0.01$ using One-way ANOVA with Games-Howell or Tukey HSD posttest.

Fig. 1-6. Administration of Laminaran substantially increased IL-10 expression. (A) Epithelial cells in the pyloric mucosa exhibit weak to moderately granular cytoplasmic IL-10 immunostaining between Laminaran-treated and untreated group. (B) IL-10 is detected in

parietal cells of the gastric fundic mucosa demonstrating weak to strong cytoplasmic staining between Laminaran-treated and untreated group. Scale: 100μm. Percentage distribution of IL-10 immunoreactive cells in at least three microscopic fields (X200) was semi-quantitatively scored as follows: 1- 0-10%, 2- 11-25%, 3- 26-50%, 4- >50%. Data are shown as mean±SD. *Significant at $P<0.05$ using Students T-test.

Figure 1-1

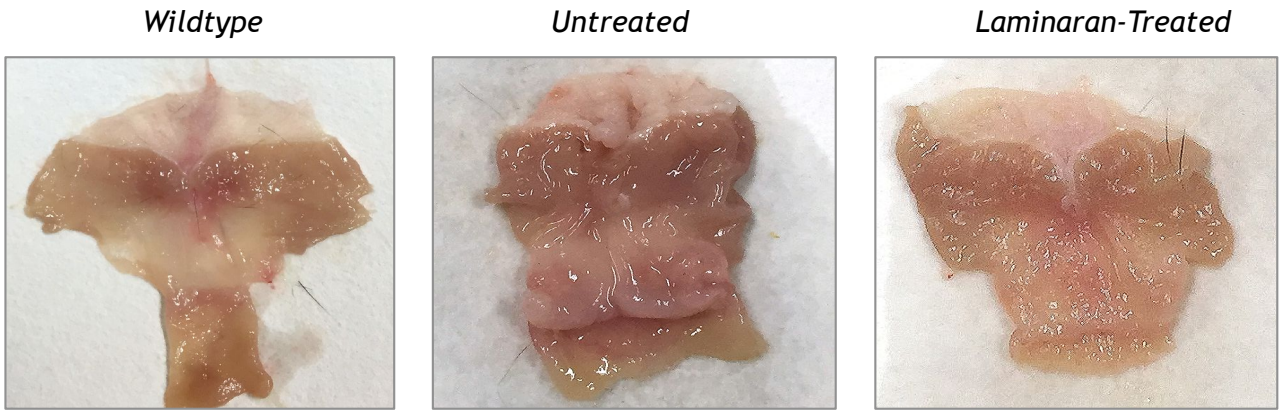

0	None
1	Mildly
2	Moderately
3	Markedly

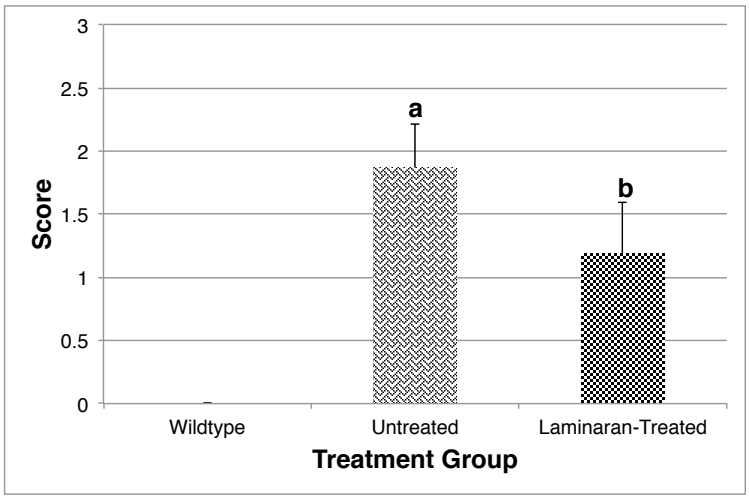

Figure 1-2

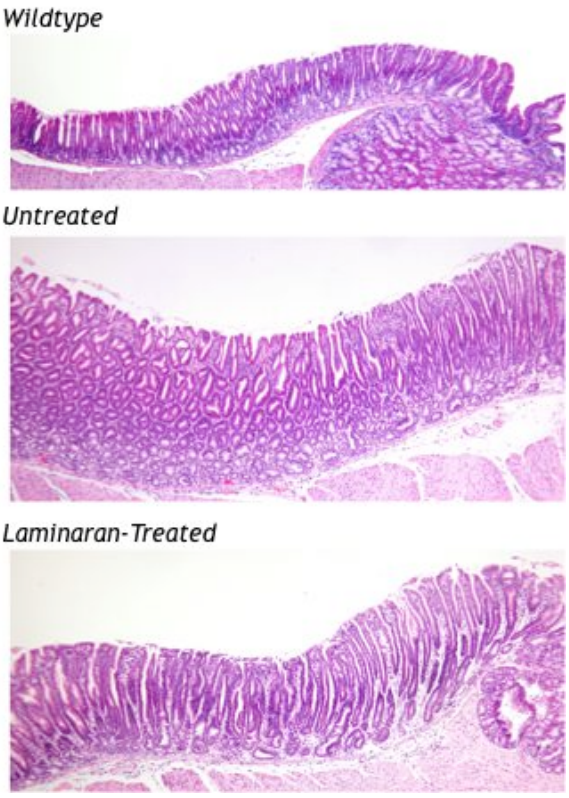
Wildtype
Untreated
Laminaran-Treated

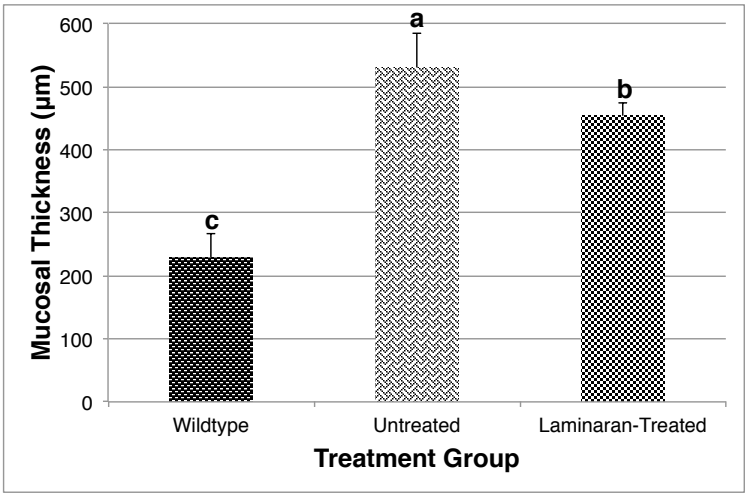
Mucosal Thickness (µm)
600
500
400
300
200
100
0
a
b
c
Wildtype
Untreated
Laminaran-Treated
Treatment Group

Figure 1-3

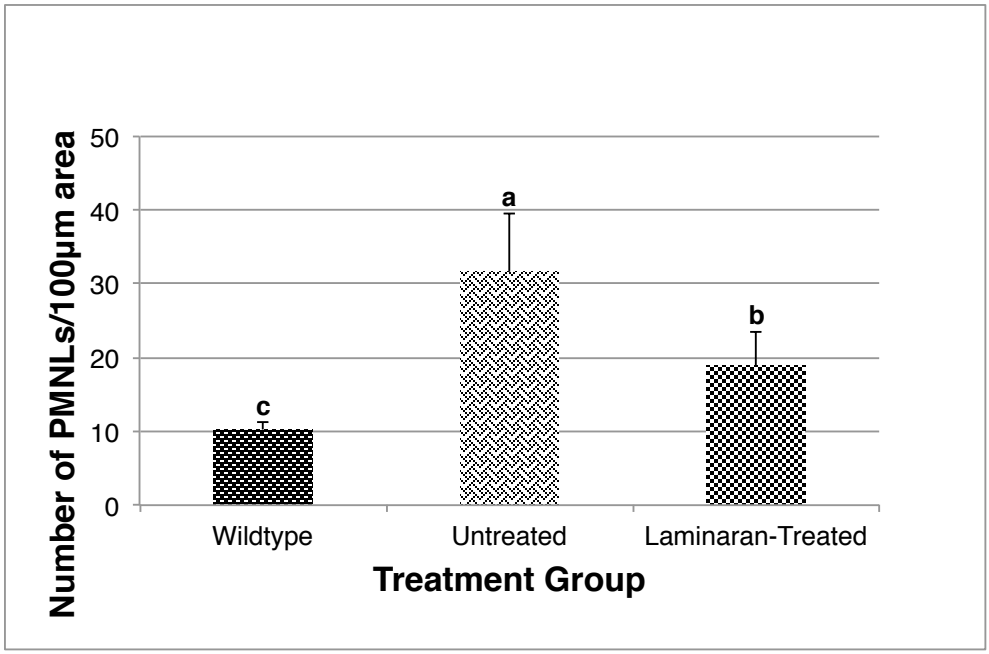
Number of PMNLs/100µm area
50
40
30
20
10
0
a
b
c
Wildtype
Untreated
Laminaran-Treated
Treatment Group

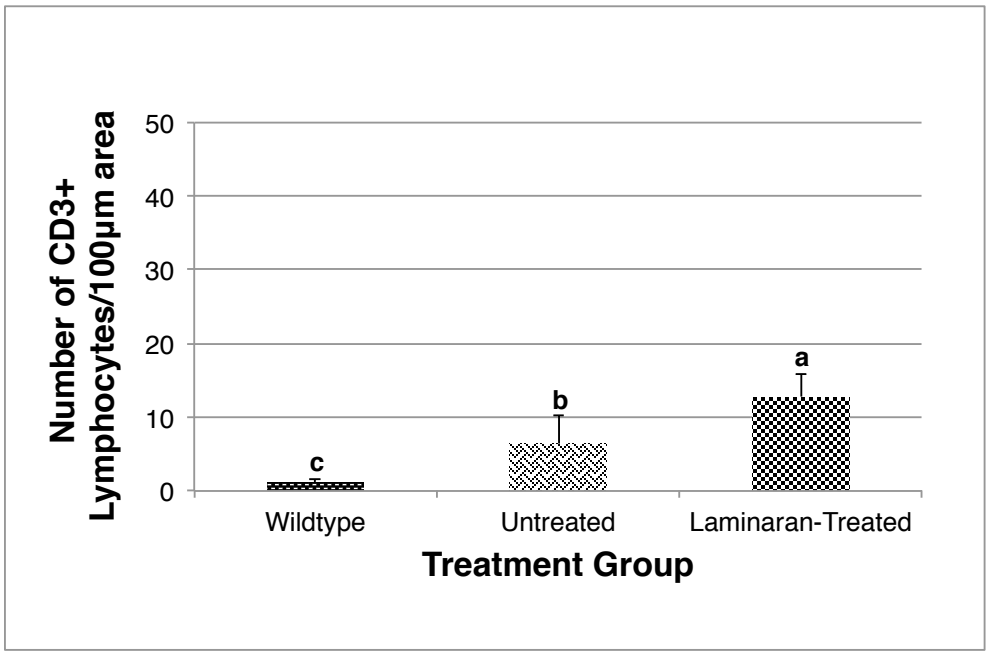
Number of CD3+ Lymphocytes/100µm area
50
40
30
20
10
0
a
b
c
Wildtype
Untreated
Laminaran-Treated
Treatment Group

Figure 1-4

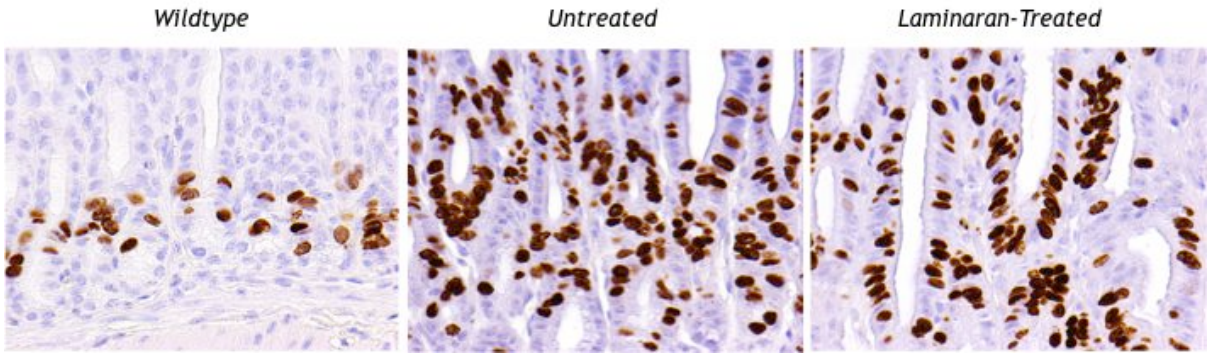
Wildtype
Untreated
Laminaran-Treated

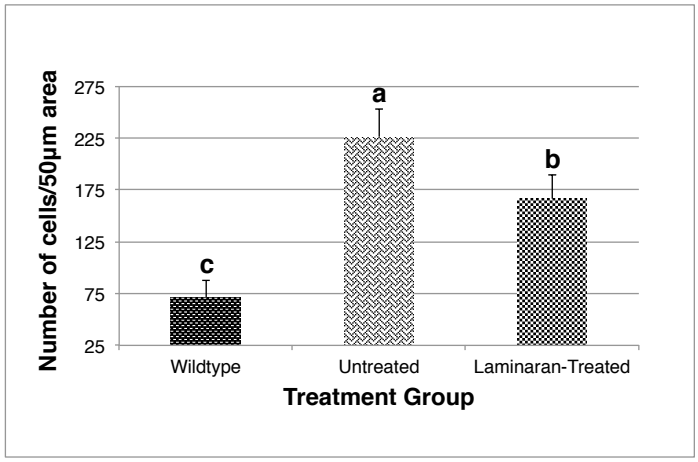
Number of cells/50µm area
275
225
175
125
75
25
a
b
c
Wildtype
Untreated
Laminaran-Treated
Treatment Group

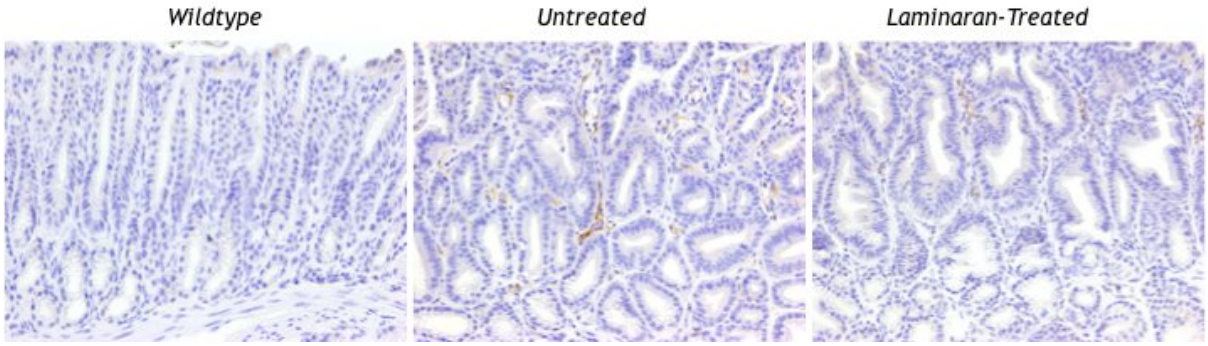
Wildtype
Untreated
Laminaran-Treated

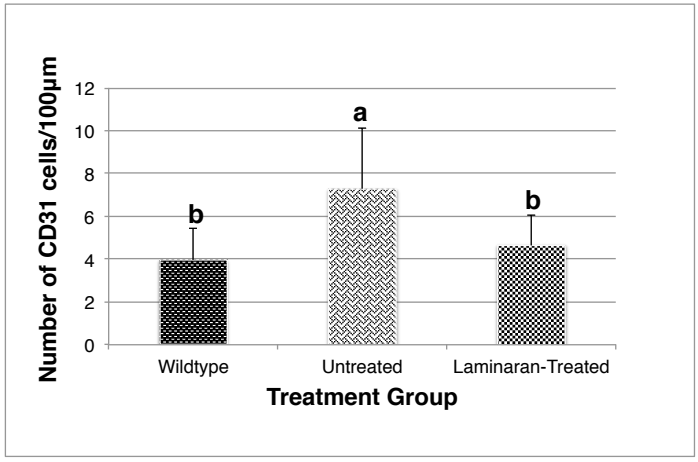
Number of CD31 cells/100µm
12
10
8
6
4
2
0
a
b
b
Wildtype
Untreated
Laminaran-Treated
Treatment Group

Figure 1-5

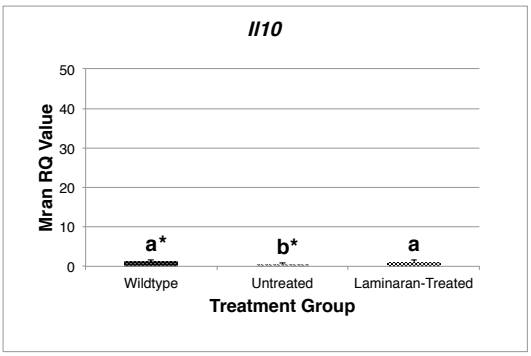
Il10
Mran RQ Value
50
40
30
20
10
0
a*
b*
a
Wildtype
Untreated
Laminaran-Treated
Treatment Group

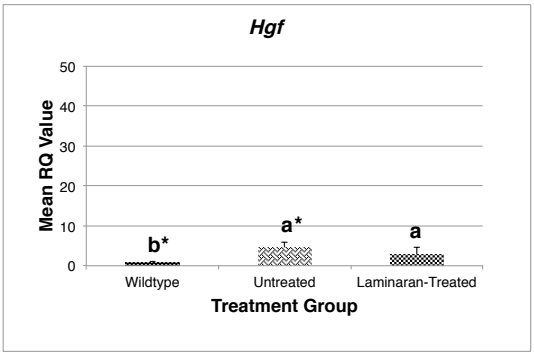
Hgf
Mean RQ Value
50
40
30
20
10
0
b*
a*
a
Wildtype
Untreated
Laminaran-Treated
Treatment Group

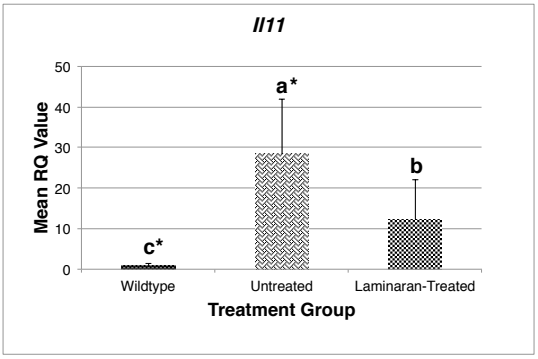
Il11
Mean RQ Value
50
40
30
20
10
0
c*
a*
b
Wildtype
Untreated
Laminaran-Treated
Treatment Group

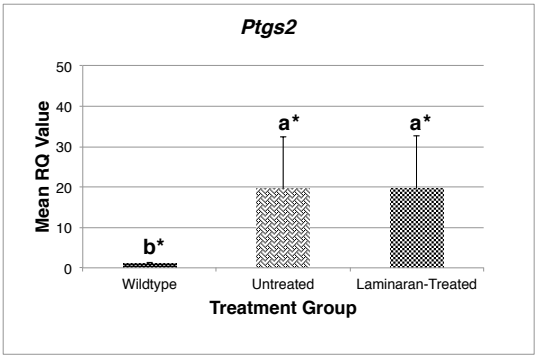
Ptgs2
Mean RQ Value
50
40
30
20
10
0
b*
a*
a*
Wildtype
Untreated
Laminaran-Treated
Treatment Group

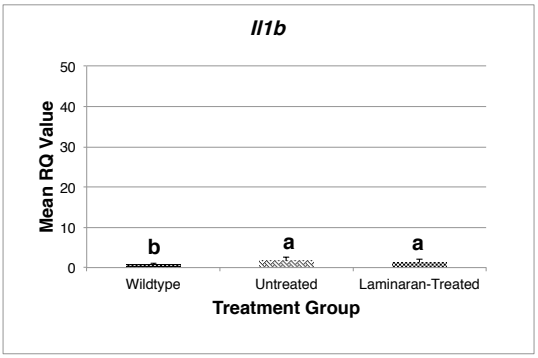
Il1b
Mean RQ Value
50
40
30
20
10
0
b
a
a
Wildtype
Untreated
Laminaran-Treated
Treatment Group

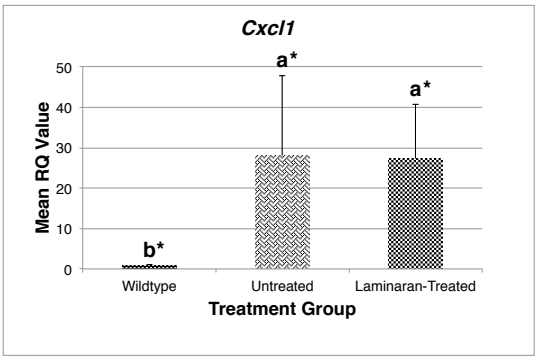
Cxcl1
Mean RQ Value
50
40
30
20
10
0
b*
a*
a*
Wildtype
Untreated
Laminaran-Treated
Treatment Group

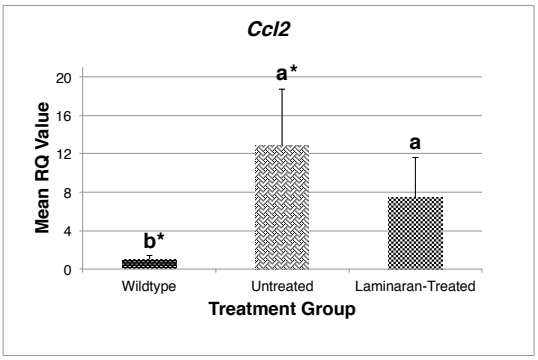
Ccl2
Mean RQ Value
20
16
12
8
4
0
b*
a*
a
Wildtype
Untreated
Laminaran-Treated
Treatment Group

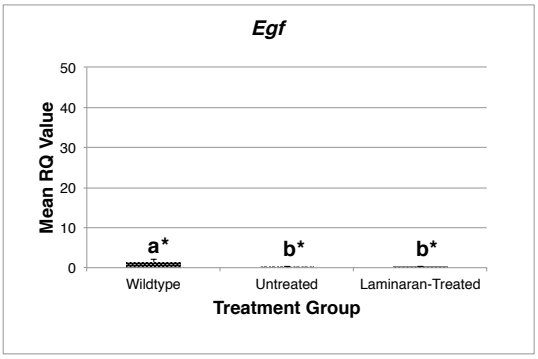
Egf
Mean RQ Value
50
40
30
20
10
0
a*
b*
b*
Wildtype
Untreated
Laminaran-Treated
Treatment Group

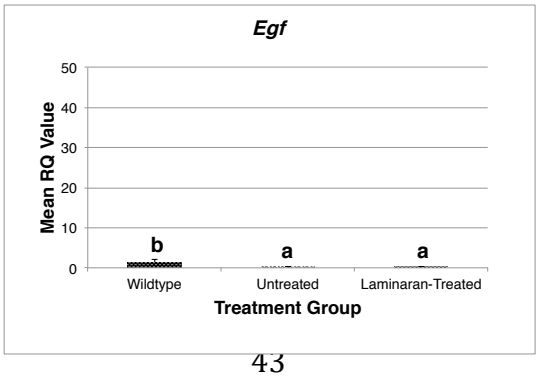
Egf
Mean RQ Value
50
40
30
20
10
0
b
a
a
Wildtype
Untreated
Laminaran-Treated
Treatment Group

Figure 1-6

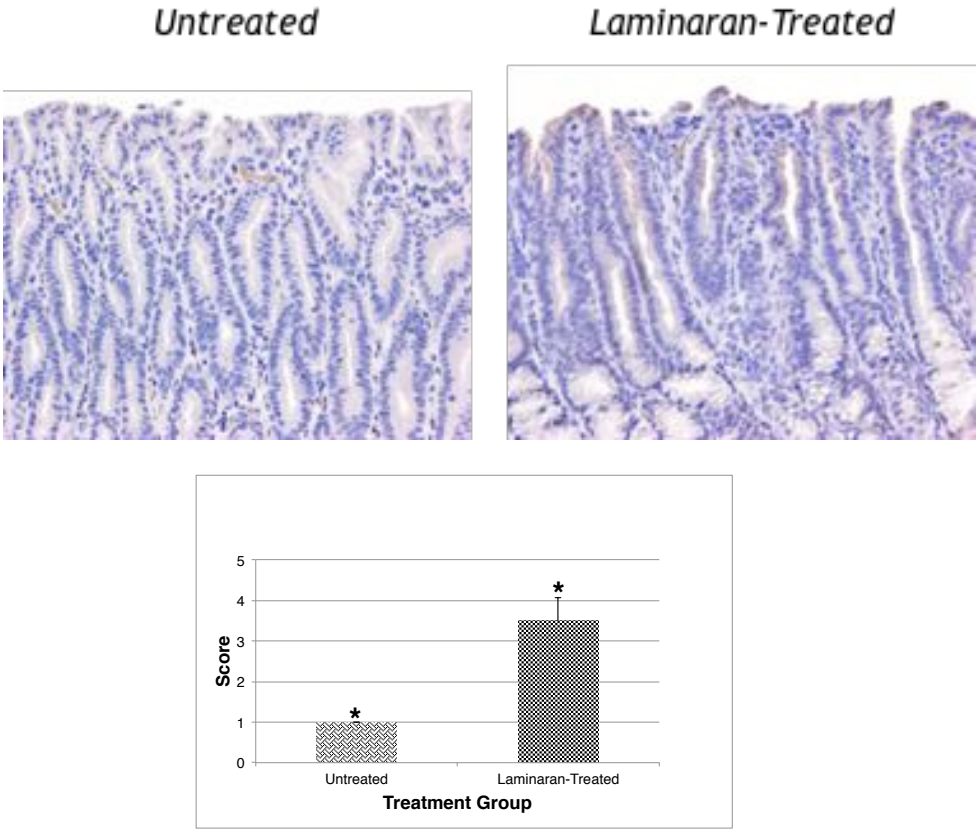
Untreated
Laminaran-Treated
Score
5
4
3
2
1
0
*
*
Untreated
Laminaran-Treated
Treatment Group

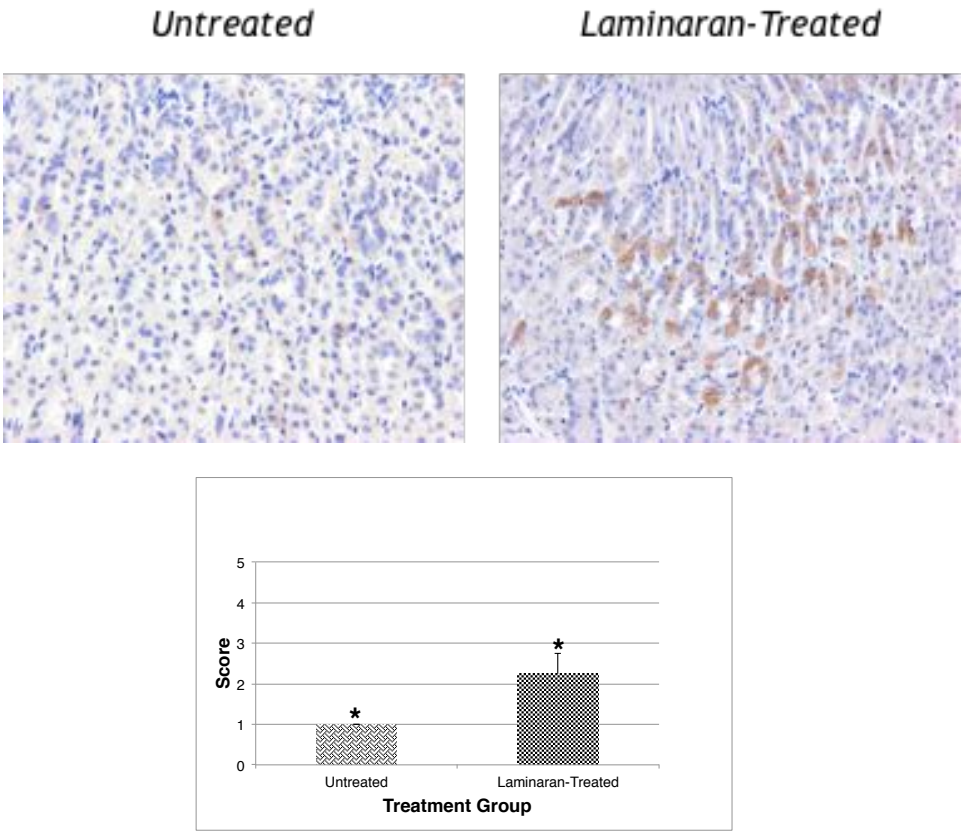
Untreated
Laminaran-Treated
Score
5
4
3
2
1
0
*
*
Untreated
Laminaran-Treated
Treatment Group

Figure 1-7

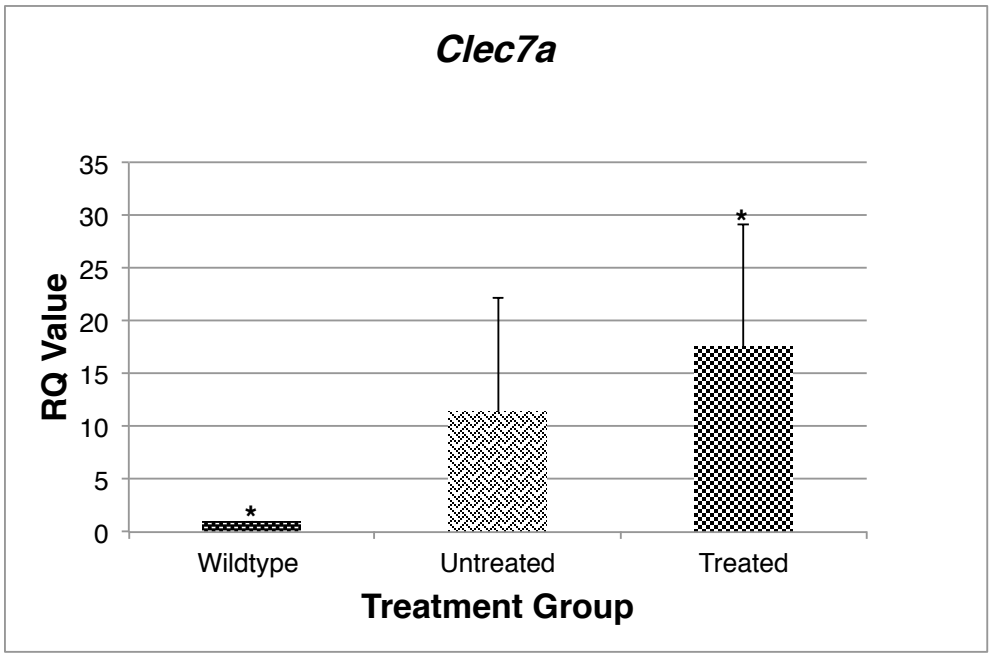
Clec7a
35
30
25
20
15
10
5
0
RQ Value
*
*
Wildtype
Untreated
Treated
Treatment Group

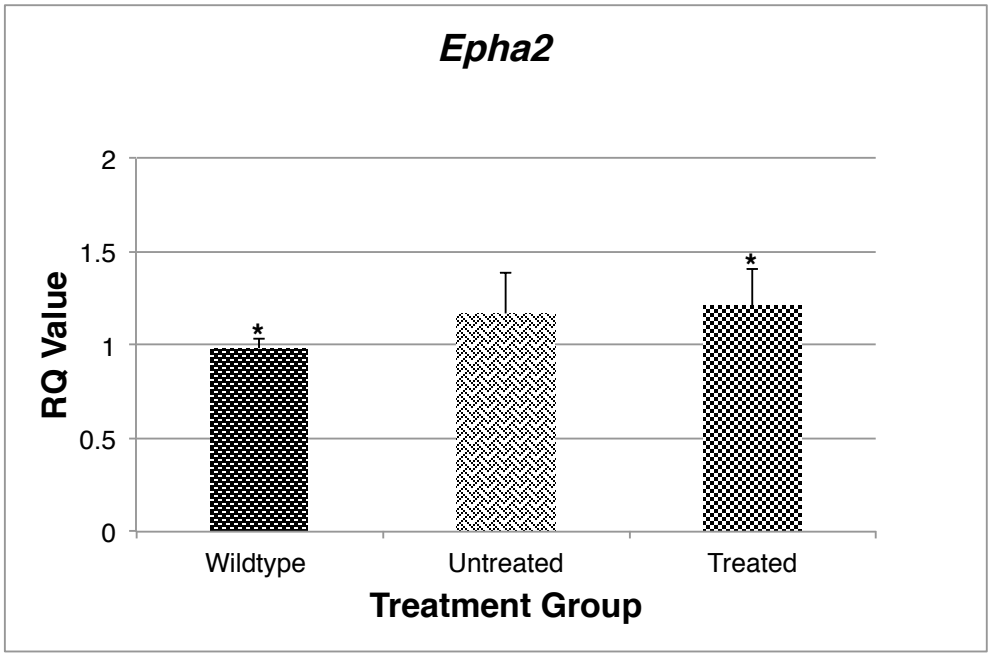
Epha2
2
1.5
1
0.5
0
RQ Value
*
*
Wildtype
Untreated
Treated
Treatment Group

Table 1-1.

List of real-time PCR primers

Genes	Forward	Reverse
Actb	AAGTGTGACGTTGACATCCG	GATCCACATCTGCTGGAAGG
Il1b	GCAACTGTTCCTGAACTCAACT	ATCTTTTGGGGTCCGTCAACT
Il10	GCTCTTACTGACTGGCATGAG	CGCAGCTCTAGGAGCATGTG
Il11	TGTTCTCCTAACCCGATCCCT	CAGGAAGCTGCAAAGATCCCA
Cxcl1	CTGGGATTCACCTCAAGAACATC	CAGGGTCAAGGCAAGCCTC
Ccl2	TTAAAAACCTGGATCGGAACCAA	GCATTAGCTTCAGATTTACGGGT
Hgf	ATGTGGGGGACCAAACTTCTG	GGATGGCGACATGAAGCAG
Egf	AGCATCTCTCGGATTGACCCA	CCTGTCCCGTTAAGGAAAACTCT
Fgf7	CTCTACAGGTCATGCTTCCACC	ACAGAACAGTCTTCTCACCCT
Ptgs2	TTCAACACACTCTATCACTGGC	AGAAGCGTTTGCGGTACTCAT

Chapter 2

Tumor inhibitory potential of stingless bee propolis in various experimental models of differentiated-type gastric adenocarcinoma

Introduction

Tremendous advances in early disease diagnosis have revolutionized the mortality landscape of gastric cancer (GC) as seen in the last decades. However, according to the latest GLOBOCAN 2018 estimates, it continues to be a major disease burden affecting approximately 783,000 individuals whose gravity has been widely observed in East Asian countries like Japan, Mongolia, and Korea[1]. To date, surgical resection remains the cornerstone of GC therapy with curative intent but still around 40-65% of localized GC patients are refractory showing relapse in the tumor bed, anastomosis or regional lymph nodes (McDonald et al., 2001; Thrumurthy et al., 2015). To address this gap, multimodal approaches and targeted therapies have previously emerged, thus providing considerable support to surgery alone (McDonald et al., 2010; Cunningham et al., 2006; Sakuramoto et al., 2007; Bang et al., 2010). Unfortunately, all these regimens have been plagued with serious adverse events of toxicity, which significantly influence patient's compliance eventually leading to untimely treatment withdrawal. Therefore, in view of this apparent drawback, any alternative or auxiliary treatment modalities where GC patients could profit in terms of fewer complications and better quality of life are greatly warranted.

In recent years, renewed interests in natural products have taken the spotlight of drug discovery and cancer research (Harvey et al., 2015; Lee et al., 2018). Propolis, a bee-derived substance consisting of bees' own salivary secretion together with collected resins, exudates, and oils, is a natural healing agent that has been highly regarded owing to its low toxicity, relative safety, and pronounced biological functionality (Silva-Carvalho et al., 2015). It contains a broad diversity of chemical composition that is not only remarkably influenced by season, geographical location, bee species, extraction method, and existing vegetation but also is attributable to its putative bioactivities (Sforcin et al., 2010; Sanches et al., 2017). In particular reference to its anti-cancer property, propolis samples from Brazil, Netherlands,

Portugal, New Zealand, Korea, Taiwan, China, and Algeria have been shown to inhibit a wide spectrum of *in vitro* human cancer cell lines of lung, stomach, cervical, esophageal, brain, laryngeal, skin, and breast carcinoma (Chen et a., 2007; Ishihara et al., 2009; Calhelha et al., 2014; Catchpole et al., 2015; Wang et al., 2016; Brihoum et al., 2018). This response was purported to mechanistically involve the induction of proline dehydrogenase/proline hydrogenase- and DNA fragmentation-initiated apoptosis; regulation of glutathione and glutathione S-transferase; inhibition of NF-κB and JNK signaling pathways; upregulation of p53, Bax, cleaved-caspase-3 and 9, and MAPK-associated proteins; and modulation of the components of the cell cycle (El-Khawaga et al., 2003, Watabe et al., 2004; Motomura et al., 2008; Xuan et al., 2014; Celinska-Janowicz et al., 2018). However, in spite of these great deal of evidences and convincing role in carcinogenesis, the anti-tumor potential of propolis from the native species of Philippine stingless bees (*Tetragonula biroi* Friese) is largely unknown and sparingly investigated. Previously, our group was the first to describe that crude EEP from this indigenous bee species could exert potent neuroprotective activity through abrogation of the neurologic deficit and neuronal damage in a rat model of ischemic stroke (Desamero et al., 2018). In this current report, I attempted to explore whether possible anti-cancer efficacy might also be included in its repertoire of bioactivities; hence I carried out a pharmacognostic evaluation of EEP from Philippine stingless bees with specific emphasis on its tumor-suppressing potential in *in vitro* and *in vivo* models of differentiated-type gastric adenocarcinoma.

Results

EEP specifically retarded the growth of human GC cells belonging to the differentiated subtype.

The tumor-suppressing efficacy of the present EEP sample was preliminarily evaluated *in vitro* using four human GC cell lines. These cells were first stratified into respective subtype on the basis of their differential transcriptional expression of adhesion molecule markers, LGALS4 (encoding for Galectin-4) and CDH17 (encoding for Li-cadherin). In keeping with this proposed classification scheme for human GC by Tan *et al*. (2011), AGS, MKN-45, and NUGC4 were classified under differentiated-type whereas MKN-74 was categorized into diffuse-type. Cancer cells were subsequently subjected to cell viability experiment by exposing cells into increasing EEP concentrations (1-1000 μg/ml) over three determined time points (24 h, 48 h, and 72 h) (Fig. 1). As shown in Fig. 2 and Table 1, a concentration- and time-course-dependent proliferative restriction was characteristically unveiled by all GC cell lines belonging to the differentiated subtype. Specifically, NUGC4 cells exemplified the lowest IC_{50} value at 24 hours, which registered only 580 μg/ml followed by AGS and MKN45 with values of 650 μg/ml and 1156 μg/ml, respectively. Noteworthily, at 48 hours, AGS cells recorded an astounding inhibition rate of ~71% (IC_{50} 188 μg/ml) and this was further reduced to ~94% by 72 hours (IC_{50} μg/ml). On the other hand, a slightly dissimilar IC_{50} value at 72 hours was observed between NUGC-4 and MKN-45 cells (315 μg/ml VS 318. μg/ml). Meanwhile, the diffuse-type MKN-74 cells were less sensitized to EEP-induced inhibition requiring a fairly higher EEP concentration (≥ 500 μg/ml), thus resulting to >900 μg/ml IC_{50} even after 72-hour incubation period.

EEP acts in vitro through modulation of the cell cycle and apoptotic machineries.

The encouraging data of the proliferation experiment evoked further inquiries into the possible mechanisms that underpinned this perceived activity. Since the contribution of the

cell cycle and apoptosis are immensely recognized in cancer (Evan et al., 2001) and that these could be regulated by propolis as already pointed out by numerous studies (El-Khawaga et al., 2003; Sulaiman et al., 2012; Kustiawan et al., 2015), the potential involvement of the present EEP sample on these processes was promptly investigated. Real time PCR analysis was performed on GC cells treated with culture medium alone (control) or EEP (IC_{50} at 48 h) to detect changes in the transcription level of selected genes implicated in cell cycle progression and apoptosis. Among these genes, a striking upregulation was characteristically disclosed by *CDKN1A* attaining a statistically significant result for AGS (p <0.001) and NUGC-4 (p <0.050) and a propensity for increased expression for MKN-45 (Fig. 2A, Supplementary Table 3). Noteworthily, this distinct overexpression was only established in all differentiated-type GC cell lines but not diffuse-type (MKN-74), possibly suggesting subtype-specific proclivity. In stark contrast, gene expression levels of *CDK1* and *CCND1* were significantly demoted. Also, whereas marked elevation of *CDKN1A* was accompanied by a profound increment in the levels of *CDKN1B* (p <0.001) and *TP53* (p <0.005) in AGS cells, *CDK2* expression levels in NUGC-4 and MKN-45 cells were concomitantly down regulated (Fig. 2A, Supplementary Table 3). On the other hand, no clear-cut pattern seemed discernible concerning the expression profile of several apoptosis-associated genes. Nevertheless, it could not be discounted that in some cancer cell lines a response suggestive of an apoptotic phenomenon was undeniably expressed such as the significant induction of *BAX* (p <0.001) and *BAD* (p <0.003) in AGS as well as the considerable down-expression of *BCL2L1* in MKN-45 (p <0.050), and *BCL2* in NUGC4 (p <0.001). In the case of MKN-74 cells, the resulting gene transcription findings firmly asserted the lack of positive response to EEP treatment (Fig. 2A, Supplementary Table 3 Moreover, cell cycle analysis and TUNEL assay were subsequently undertaken to elaborate the ability of EEP to trigger cell cycle arrest and apoptosis. As shown in Fig. 1B, EEP-treated AGS cells were significantly arrested at the

G0/G1 phase showing a prominently sharpened peak, which accounts for around 66% of total cells counted as compared to only about 55% documented in the corresponding untreated cells. Additionally, this perceptible increment in G0/G1 phase following EEP treatment was accompanied by a significant augmentation in the number of S-phase cells together with a marked depletion of cells at the G2/M and multi-nuclear phases relative to those of the untreated control counterpart. No evident difference, however, was noted on sub-G1 phase cells. Meanwhile, as depicted in Figs. 1C and 1D, DNA fragmentation was only modestly promoted in AGS and NUGC-4 cells after EEP treatment but dramatically enhanced in MKN-45 cells wherein more than 35% of cancer cells were accounted to have undergone apoptosis.

EEP supplementation induces promising anti-tumor response in mice model of differentiated-type gastric adenocarcinoma.

To provide a proof of concept that such *in vitro* response could be replicated in the context of a more complicated system, I considered utilizing a unique animal model that can aptly recapitulate the intricacies of differentiated-type GC. *A4gnt* KO mice deficient in the gene encoding for α1, 4-*N*-acetylglucosaminyltransferase notably develop gastric cancer in a spontaneous manner of hyperplasia-dysplasia-adenocarcinoma sequence (Karasawa et al., 2012). In the present study, 60 week-old *A4gnt* KO mice exhibiting full-blown gastric adenocarcinoma, and matched wildtype C57BL/6J animals were intragastrically administered with distilled water or EEP for a treatment duration of 30 days. Upon sacrifice, careful scrutiny of the harvested mouse stomach tissues revealed a significant regression of the gross mucosal elevation in the *A4gnt* KO + EEP treatment group in comparison to the untreated control group (Fig. 3A, Supplementary Fig. 2) as essentially affirmed by semi-quantitative scoring analysis (Fig. 3D). Microscopically, this coincided with a sizeable reduction of the mean pyloric thickness in the EEP-treated *A4gnt* KO group with ~30% decrement as opposed

to that of the corresponding control group given only distilled water (529.93 ± 45.08 μm vs 792.99 ± 105.90 μm) (Fig. 3B, Fig 3E). In addition, subsequent examination of the CD3-positive T-lymphocytic cell infiltration in the *A4gnt* KO + EEP treatment group likewise depicted a marked decline in the mean cell count tallying only 20.59 ± 4.08 cells as compared to around 40.68 ± 12.94 cells obtained in the untreated control counterpart (Fig. 3C, Fig 3F). Another thing worth mentioning also was the observation that no glaring difference could be deciphered between the distilled water and EEP-treated wildtype C57BL/6J animals with respect to their gross morphology (Fig. 3A), gastric mucosal thickness (Fig. 3B), and T-lymphocyte sequestration (Fig. 3C). Therefore, on the basis of all these findings, it can be deduced that EEP may exert promising *in vivo* anti-tumor efficacy against differentiated-type gastric adenocarcinoma.

EEP consistently affects cell cycle process in vivo to confer efficient anti-tumor action.

I next endeavored to search for specific mechanisms to which I could ascribe the pronounced *in vivo* anti-tumor action of our present EEP sample. In this connection, real time PCR technique was initially employed to inspect several inflammation-associated genes that are deemed crucial in *A4gnt* KO-induced carcinogenesis (Karasawa et al., 2012). Upon gene expression analysis however, no overt changes were determined between the mRNA expression profiles of these genes in both *A4gnt* KO treatment groups except for a tendency for higher *Il10* transcription (Supplementary Fig. 3, Supplementary Table 4). Therefore, in light of this obvious indication for alternative mechanistic pathway, and in conjunction with the present *in vitro* data, we examined thereafter those genes associated with cell cycle progression and apoptosis. As illustrated in Fig. 4A and Supplementary Table 5, a specific and profound modulation was visibly observed in a number of cell cycle protein-encoding genes following EEP administration. In particular, *Cdkn1a* was considerably overexpressed (p <0.001) in *A4gnt* KO + EEP treatment group and this prominent increment as validated at

the protein level (Fig. 4B and 4C) was documented to occur in a statistically different manner in relation to those of the untreated wildtype and *A4gnt* KO control animals. Similarly, this significant gene level augmentation was also found in the wildtype + EEP treatment group in contrast to the untreated wildtype counterpart thereby strongly supporting the gene-specific regulatory influence of EEP. In addition, *A4gnt* KO mice treated with EEP also exemplified a substantial increase in *Cdkn1b* (p <0.008) and a decrease in *Cdk1* (p <0.045) expressions in converse with the *A4gnt* KO + dH_2O group. On a different note, assessment of the apoptosis-related genes between *A4gnt* KO treatment groups unveiled a perplexing interplay of several contrasting genes (*Bl2l1*, *Bcl2*, and *Bad*) (Fig. 4A, Supplementary Table 5), possibly insinuating the trivial relevance of this process in the perceived *in vivo* response.

To further contend that cell cycle participation constitutes a distinctive anti-cancer feature of our EEP sample, I then performed *in vivo* BrdU labeling. Interestingly, EEP supplementation in *A4gnt* KO mice elicited a remarkable diminution in the number of actively dividing BrdU-positive S-phase cells approximating only ~65% of the mean cell count registered in those of the corresponding KO control animals (220.45 ± 26.87 vs. 334.57 ± 59.08) (Figs. 4D and 4E). Meanwhile, BrdU labeling between wildtype treatment groups did not seem to solicit any statistical significance. Lastly, we aimed to validate the role of apoptosis by analyzing DNA fragmentation through TUNEL Assay. As demonstrated in Figs. 4F and 4G, the marginal increase in the number of cells undergoing apoptosis in the *A4gnt* KO + EEP treatment group as distinguished from its untreated counterpart, somehow reinforced the notion that this mechanism might only be accountable to a lesser extent in the *in vivo* anti-tumor action of the present EEP sample.

Chemical composition of crude EEP.

Preliminary phytochemical screening of the crude EEP from Philippine stingless bee yielded more than 500 chemical constituents encompassing widely diverse groups, which

include carbohydrates, steroids, alkaloids, anthraquinones, phenols, terpenoids, etc. Of these, about 15 chemical compounds were identified as promising candidates with anti-cancer activity as supported by structure analysis and review of prior literature reports (Supplementary Table 6).

Discussion

The bulk of the so-called "Pacific-type propolis" found in countries in the Far East region like Japan, Indonesia, Thailand, Taiwan, and Philippines is primarily produced by a distinct species of bees known as stingless bees. This propolis, as discriminated from those of the Brazilian green-type and Poplar-type, is exceptionally enriched in geranyl flavanone constituents instead of the commonly documented artepillin C or caffeic acid phenethyl ester (CAPE) (Bankova et al., 2005). Nevertheless, irrespective of the type, they are virtually comparable vis-à-vis the extent of their biofunctional activities such as anticancer, antimicrobial, anti-inflammatory, antioxidant, and wound healing properties (Sanches et al., 2017; Sawaya et al., 2009; Massaro et al., 2011, Ribeiro-Junior et al., 2015). In the Philippines, *Tetragonula biroi* Friese (syn *Trigona biroi*), locally recognized as "Kiwot", comprise an important indigenous population of stingless bees. They are greatly valued as an effective pollinator and are mostly preferred for propolis production due to higher cost efficiency and increased resistance to parasitic infestation (Cervancia et al., 2016). Expectedly, this has raised consciousness to strengthen studies on the multifaceted aspects of this bee propolis (Desamero et al., 2017; Lamberte et al., 2011; Alvarez et al., 2013; Ragasa et al., 2015), albeit, scientific inquiries relating to their biofunctional properties especially anti-tumor efficacy are lagging behind and remain nearly unstudied. Therefore, the present paper was designed to cater the apparent paucity of knowledge on the tumor-suppressing potential of Philippine stingless bee propolis. Here, we described that the EEP-induced reduction in gastric cancer cell proliferation *in vitro* and tumor growth regression *in vivo* were intimately associated with the specific and profound modulation of the components of the cell cycle machinery and in part, the apoptotic process.

Resistance against cancer growth and proliferation does no longer represent an unprecedented role for honeybee- and stingless bee-derived propolis. Accumulating lines of

compelling evidence in literature have explicitly illuminated the causal relationship between propolis exposure and proliferative restriction in a broad range of human and murine *in vitro* cancer cell lines. For instance, propolis samples from the Thai stingless bees, *Trigona laeviceps*, and Indonesian stingless bees, *Trigona incisa, Timia apicalis, Trigona fusco-balteata,* and *Trigona fuscibasis* have exhibited marked cytotoxicity and anti-proliferative activity toward SW620 colon carcinoma, BT474 breast carcinoma, HepG2 hepatocellular carcinoma, and ChaGo-I lung carcinoma (Umthong et al., 2011; Kustiawan et al., 2014) whereas Brazilian geopropolis from *Melipona scutellaris* stingless bees has been effective against U251 glioma, UACC-62 melanoma, MCF-7 breast adenocarcinoma, NCI-ADR/RES multi-drug resistant ovarian carcinoma, 786-0 renal carcinoma, NCI-H460 lung non-small cell carcinoma, PC-3 prostate carcinoma, and OVCAR-03 ovarian carcinoma (da Cunha et al., 2013). In GC, strong evidence supporting this role comes from investigations using AGS, Kato III, NCI-N87, NUGC-4, MKN-1, and MKN-28 cells (Umthong et al., 2011; Akao et al., 2003; Teerasripreecha et al., 2012; Amini-Sarteshnizi et al., 2015). In the present paper, we further extended this growing list of tested GC cell lines by including MKN-45 and MKN-74 in addition to AGS and NUGC-4. These cells were preliminary classified into differentiated and diffuse subtype following the two-marker system of genomic GC classification by Tan and colleagues (2011) (Tan et al., 2011). Based on the differential gene expression of adhesion molecules, *LGALS4* and *CDH17,* AGS, NUGC-4, and MKN-45 cells were categorized into the former while MKN-74 was designated into the latter. As demonstrated in this report, all the studied GC cell lines, except MKN-74, disclosed a concentration- and time course-dependent sensitivity to EEP exposure, although the generated IC_{50} value at 72 hours was relatively higher than those of earlier reported studies (Akao et al., 2003; Amini-Sarteshnizi et al., 2015). Nonetheless, we were able to document in this work that EEP from the Philippine stingless bees also possess promising anti-proliferative activity. More

importantly, we have herein established the first account that EEP treatment may display GC subtype specificity showing prominent suppressive efficacy against the differentiated-type. However, one caveat of this finding was that the enhanced anti-proliferative activity might be due to cell line growth capacity (Ishihara et al., 2009).

To provide a more meaningful assertion that EEP treatment could foster an increased differentiated GC subtype susceptibility, I utilized a spontaneous disease animal model of GC (*A4gnt* KO mice) that uniquely recapitulates a well-developed differentiated-type gastric adenocarcinoma at around 60-weeks of age. Upon oral supplementation of distilled water or EEP for 30 consecutive days, stomach tissue samples of EEP-treated *A4gnt* KO mice exemplified a remarkable regression of gross mucosal elevation, which corresponded histologically to substantial reduction of pyloric mucosal thickness and T-lymphocyte infiltration. These results strongly suggest that EEP treatment presumably mediates a significant tumor-demoting action against differentiated GC subtype. Congruent with these findings, oral administration of Iranian propolis significantly retarded the growth of gastric tumor lesions in Wistar rats following MNNG-initiated gastric carcinogenesis (Alizadeh et al., 2015). In another study using xenograft model of mammary carcinoma, water-soluble derivative of Croatian propolis successfully elicited an appreciably delayed tumor formation (Orsolic et al., 2005). Meanwhile, hydroalcoholic extract of Brazilian green propolis evidently dampened the tumor growth induction in DMBA-induced mice model of dermal carcinogenesis although failed to impinge on inflammatory lymphocyte sequestration (Pereira-Filho et al., 2014). However, propolis treatment in all these above-mentioned studies, in converse to our study, has been carried out either prophylactically or concurrently with tumor induction. Therefore, the deliberate application of EEP under the circumstance of already existing tumor as in the case of *A4gnt* KO mice in this present work proffered an indisputable justification for its pronounced therapeutic anti-cancer property.

Cell cycle progression is a well-orchestrated process requiring tight coordination of the homeostatic balance between cyclin/cyclin-dependent kinase protein (CDK) complexes and their inhibitor proteins (CKI) (Hunter et al., 1994). Any perturbations involving its regulation have afforded cancers with unconstrained development (Akama et al., 1996; Franklin et al., 2000). Conceivably, targeted control of this mechanism has been inexorably exploited by most bioactive compounds and chemotherapeutic drug preparations. In this paper, we demonstrated the regulatory potential of our EEP sample on this process unveiling the exclusive and profound modulation of several cell cycle related gene transcripts in all differentiated-type GC cell lines. Specifically, *CDKN1A*, which encodes for the p21 protein, was strikingly upregulated, and this was accompanied by marked down-regulated levels of *CCND1*, *CDK1,* and *CDK2* genes encoding for the Cyclin D1, Cdk1, and Cdk2 proteins, respectively. Reconcilably, EEP treatment in *A4gnt* KO mice also led to a significant increase in the gene and protein levels of *Cdkn1a* coupled with a propensity to restore *Ccnd1* and *Cdk1* gene expressions. Moreover, this notable transcriptional modulation coincided with the prominent cell cycle cessation at the G0/G1 phase in AGS cells along with a marked reduction in the number of *in vivo* BrdU-positive S-phase cells in the *A4gnt* KO + EEP treatment group in comparison to the untreated KO control group. In consonance with our data, exposure to propolis and its bioactive components has stimulated a significant increment in p21 mRNA and protein expressions resulting to cell cycle arrest at G0/G1 phase of various human cancer cell lines of colon and lung carcinoma (Shimizu et al., 2014; Weng et al., 2007; Tang et al., 2017). Intriguingly, this increase in G1 cells as validated using the bi-parametric BrdU/DNA cell cycle analysis in another study essentially correlated to a reduced S-phase cell population (Sulaiman et al., 2012). p21, also known as $p21^{WAF1, CIP1, SDI1, CAP20, MDA6}$, belongs to the Cip/Kip family of cyclin-CDK complex inhibitors that play diverse roles including cell cycle control, transcriptional regulation, senescence, cell differentiation,

cytoskeletal dynamics, and apoptosis (Abbas et al., 2009). It can mediate a p53-dependent G1 growth arrest through inhibition of cyclin D/Cdk4 and Cyclin E/Cdk2 complexes following DNA damage and oxidative stress (He et al., 2005; Besson et al., 2008). Alternatively, in a p53-independent manner, it may also serve as a master growth suppressing effector by blocking G1/S transition via disruption of Cyclin E/Cdk2 and Cyclin A/Cdk2 complexes thus promoting phosphorylation of retinoblastoma (RB) and sequestration of E2F1; as well as regulating G2/M checkpoint through repressive action on Cyclin B1/Cdk1 and Cyclin A/Cdk1 (Abbas et al., 2009). Therefore, drawing from these accounts, it seems reasonable to imply that p21-induced G0/G1 phase arrest mediates the significant tumor suppressing potential of our present EEP sample.

I cannot also exclude the probability of the apoptotic machinery assisting synergistically in the anti-tumor efficacy of our EEP sample. In the current work, although I did not find any distinct consensus regarding the gene transcriptional profile of selected apoptosis markers in differentiated-type GC cell lines after EEP treatment, these cells manifested a response indicative of such phenomenon including the significant overexpression of pro-apoptotic genes, *BAX* and *BAD* in AGS cells along with the down-regulation of the anti-apoptotic genes, *BCL2L1* in MKN-45 and *BCL2* in NUGC-4 cells. As verified through TUNEL assay, the disparate degrees of DNA fragmentation occurring in these cell lines may potentially explain this apparent disaccord in gene expression. Concordantly, propolis administration has similarly provoked the differential induction of apoptosis-associated markers in previous studies of various human cancer cell lines. While it has initiated DNA fragmentation via activation of *BAX* and inhibition of *BCL2* and *BCL-XL* (encoded by the *BCL2L1* gene) in laryngeal carcinoma Hep-2 cells and colon carcinoma HL-60 cells (Sulaiman et al., 2012; Frion-Herrera et al., 2018), a decrease in *BCL2* without alteration in *BAX* was reported in another study using U937 leukemic cells (Motomura et al.,

2008). At present, we could hardly offer any substantial rationalization to what seems to be a specific regulatory role of our propolis sample on the *in vivo* gene expressions of *Bad* and *Bcl2l1* in expending its apoptotic effect. Whether this simultaneous induction indicates a compensatory response remains to be elucidated. Nevertheless, the significant augmentation of both of these genes in *A4gnt* KO + EEP treatment group that was reminiscent of those of AGS cells, the absence of substantial sub-G1 phase accumulation in AGS cells, and the marginal *in vivo* induction of FITC-dUTP-positive apoptotic cells likely suggest the trifling involvement of this mechanism in the tumor-suppressing potential of our present EEP sample. Additionally, the formerly held perception that an active cell cycle was a requisite for apoptosis induction and that p21 stimulation conferred protection against apoptosis by cell cycle disruption (Abbas et al., 2009) further supplemented this contention.

Finally, I sought to tentatively identify some candidate compounds in our crude EEP sample that may possibly serve as useful chemical markers with anti-cancer efficacy. Since few chemical-profiling studies by LC-MS analysis have already been conducted on samples of Philippine stingless bee propolis including those obtained from the same colonies as in the present work (Alvarez et al., 2013; Ragasa et al., 2015), I decided to utilize a different analytical platform, hence employing GC-MS/MS analysis. Out of over 500 chemical components herein identified, 15 were preliminarily selected as potential candidate compounds mostly belonging to the terpenoid and phenolic acid groups. For example, β-eudesmol and guaiol are both classified under the sesquiterpene class of terpenoids. These compounds have been commonly reported as major constituents of propolis samples from Lebanon, Turkey, Croatia, Greece, China, and Brazil (Melliou et al., 2006; Kaskoniene et al., 2014; Yang et al., 2014; Jerkovic et al., 2016; Bayram et al., 2017; Noureddine et al., 2017). Interestingly, both have been well established to mediate anticancer activity either through G1 phase arrest and caspase-initiated apoptosis (Kotawong et al., 2018) or through mTOR

signaling pathway control (Yang et al., 2018). On the other hand, gallic acid, protocatechuic acid, and pterostilbene were some of the identified phenolic acids. The former two compounds have been previously detected in Chinese, Uruguayan, Brazilian, Greek, and Cypriot propolis (Bonvehi et al., 1994; Kalogeropoulos et al., 2009) whereas the latter has been found almost exclusively in samples of Australian propolis (Silva-Carvalho et al., 2015). Treatment with gallic acid and pterostilbene has been earlier shown to elicit significant growth restriction of MDA-MB-231 triple-negative breast adenocarcinoma and AGS gastric carcinoma (Pan et al., 2007; Lee et al., 2017). This marked inhibition necessitated in part the modification of the cell cycle process via p21- and p27- induced G1 phase blockage, which is compatible with our current findings.

Further testing of the these selected candidate compounds, whether alone or in combination, on different human cancer cell lines as well as in *in vivo* cancer models like *A4gnt* KO mice may provide a more meaningful validation of their applicability as a potential anticancer therapeutic agent with cytostatic or cytotoxic properties.

Additional Methodology

Cell lines

Four human gastric cancer cell lines namely, AGS, NUGC-4, MKN-45, and MKN-74 were generously provided by Dr. Jun Nakayama of Shinshu Medical University. The specific procurement details for each cell lines are as follows: AGS (American Type Culture Collection, Manassas, VA, USA), NUGC-4 and MKN-45 (Riken Bioresource Center Cell Bank, Tsukuba, Ibaraki, Japan), and MKN-74 (JRCB Cell Bank, Osaka, Japan). These cells were cultured in 10% heat-inactivated fetal bovine serum (FBS)-supplemented RPMI 1640 medium containing 1% Penicillin –Streptomycin (10,000 units/10,000 μg/ml) and grown until confluency in a humidified chamber with 5% CO_2 at 37°C.

Propolis sample extraction and preparation

Crude ethanolic extracts of Philippine propolis from Philippine stingless bees (*Tetragonula biroi*, Friese) were obtained from the UPLB Bee Program Meliponary, Institute of Biological Sciences, University of the Philippines Los Baños. The detailed extraction procedure was exhaustively discussed in our earlier publication (Desamero *et al.*, 2017). Briefly, fresh propolis sheets totaling 150 grams were dissolved in a flask with 500 ml of 70% analytical grade ethanol. The mixture was then agitated, decanted, filtered using #1 Whattman filter paper, kept in a dark bottle to protect from light, and finally stored at 4°C refrigerator. Crude extracts were verified to conform to set standards for Philippine stingless bees propolis, therefore ensuring product authenticity. The final concentration of crude propolis extract used in the study was 300 mg/ml.

Cell proliferation (MTT) assay

MTT (Nacalai Tesque Inc., Kyoto, Japan) assay was employed to examine the viability of all studied human gastric cancer cell lines following incubation with crude propolis extracts. Cells were aliquot in 200μl culture medium and grown into a 96- well

culture plate (Nunclon™ Delta Surface, Thermo Fisher Scientific, Suzhou, China) at a determined density optimal for each gastric cancer cell lines as follows: ($5X10^3$ for AGS, $7X10^3$ for MKN45; $1X10^4$ for NUG4; and $3x10^4$ for MKN74). Cells were then incubated for 24 hours at 37°C in a humidified atmosphere with 5% CO_2. After allowing cells to settle down, culture medium was aspirated and replenished with fresh culture medium containing increasing concentrations of EEP (blank, 0, 1, 10, 100, 250, 500, 1000 µg/ml) followed by incubation at three different times schedules of 24, 48, and 72 hours. Every after desired incubation period, 10µl MTT solution (Nacalai Tesque, Inc., Japan) was added into each well and set aside for 4 hours at 37°C. Formed precipitates were solubilized thereafter by applying 100µl of solubilization solution (Isopropanolol with 0.04mol/l HCl) and mixed thoroughly by pipetting. Absorbance readings were quantified with a 168-1130J1 iMark™ microplate reader (BioRad, Japan) set at 570 nm. Values taken from duplicates of two independent experiments were used in data acquisition and reporting. Cisplatin, a well-established cytotoxic drug, was tested in parallel with all treatments and used as a suitable positive control.

Percentage (%) viability of each human gastric cancer cells was determined using the following computations: [(A_{570} Treated cells-A_{570} Blank)/(A_{570} Control cells-A_{570} Blank)*100]. Half minimal inhibitory concentration (IC_{50}) was additionally calculated by graphing the obtained % viability against its EEP concentration and the plot that generated the best correlation was chosen.

Cell cycle analysis (Propidium Iodide Staining)

Influence of propolis treatment on the specific phase of the cell cycle was scrutinized by flow cytometric analysis (BD FACSVerse™ Flow Cytometer, BD Biosciences, San Jose, CA, USA). Briefly, AGS cells were incubated at an appropriate density into a 6-well/flat-bottom microplate for 24 hours at 37°C in a humidified atmosphere with 5% CO_2.

Synchronization at G0 phase was performed by incubating cells with culture medium without FBS (serum deprivation) for 24 hours prior to cell culture with either complete medium alone (control) or complete medium + EEP (treated, IC_{50} at 48 h) for the next 48 hours. AGS cells were then trypsinized, washed two times with 1x sterile PBS, ethanol-fixed for at least 30 minutes, and stained with propidium iodide solution (50µg/ml, Sigma-Aldrich, St. Louis, MO, USA) for 1 hour in a humidified chamber set at 37°C. Flow cytometry was then performed using BD FACSuite software with a total of 10,000 events. All analysis was run using triplicates of each treatment group and the data obtained from the average of two independent studies were utilized.

Apoptosis (TUNEL) assay

DNA fragmentation, an early indication of cell apoptosis, was subsequently carried out to validate the significance of this process in the growth inhibition documented both *in vitro* and *in vivo*. Following the MEBSTAIN apoptosis TUNEL kit direct technique (Medical and Biological Laboratories Co., Ltd., Woburn, MA, USA), human gastric cancer cells suspended in 200µl complete medium were initially cultured for 24 hours into an 8-well chamber slide (BioCoat™ Collagen Type I Cellware; Corning, Bedford, Miami, USA) at 37°C in a humidified atmosphere with 5% CO_2. After ensuring sufficient cell adherence following the incubation period, the culture medium was aspirated and replenished with 200µl fresh medium containing either culture medium alone (control) or culture medium + EEP at IC_{50} value at 48 hours (treated) and then allowed to incubate for another 48 hours. Cells were washed with PBS, fixed with 4% paraformaldehyde for 15 minutes at 4°C, and permeabilized following application of PBST solution containing 0.5% Tween-20 and 1% BSA for 15 minutes at RT. DNA nick-end labeling commenced afterwards by incubating cells with a prepared TdT solution comprising of TdT buffer II, FITC-dUTP, and TdT at a ratio of 18:1:1 in a 37°C incubator for 1 hour. Finally, cells were washed with PBS thrice,

mounted with permanent mounting medium containing DAPI (Vectashield®, Vector Laboratories, Inc., Burlingame, CA, USA), and analyzed with the aid of a confocal laser-scanning microscope (LSM510 Version 2.02; Carl Zeiss, Jena, Germany). Positive control cells were additionally incubated with DNase I in 50 mM Tris-HCl and 1 mg/ml BSA solution for 10 minutes at RT prior to TdT labeling whereas negative control cells were incubated in TdT solution devoid of TdT reagent (TdT buffer II and FITC-dUTP only). Estimation of the number of apoptotic human gastric cancer cells was accomplished by getting the total number of FITC-dUTP-labeled cells per 1000 cells counted and the average percentage of triplicate measurement was computed. On the other hand, analysis of *in vivo* experiment was done by initially incubating the prepared tissue sections for at least 30 minutes at 37°C incubator with proteinase K. After washing three times with distilled water, DNA nick end labeling immediately proceeded by initial pre-incubation with TdT buffer II for 10 minutes at RT and then incubation with TdT solution for 1 hour in a 37°C atmosphere. Tissue sections were eventually rinsed by immersing in TB solution for 15 minutes at RT followed by washing with distilled water and then mounted and visualized as described above. Assessment of the apoptotic signal was executed by counting the total apoptotic cells in a pre-defined 100μm and the average tally from at least six separate evaluations was used.

Animals

Sixty week-old *A4gnt* KO mice of both sexes were preferentially chosen for this study. As again stipulated in the General introduction section, these mutant animals present differentiate-type gastric adenocarcinoma depicting histological signs of cribriform gland formation and irregular tubular gland orientation.

The experimental procedures hereby performed were in faithful compliance with the guidelines for the ethical use of experimental animals set by the Institutional Animal Care

and Use Committee, Graduate School of Agriculture and Life Sciences, The University of Tokyo (Approval No. P17-005H03).

Treatment group

C57BL/6J and *A4gnt* KO animals were randomly assigned into four treatment groups as detailed below:

Group i: C57BL/6J + distilled water (n=7)

Group ii: C57BL/6J + EEP (100 mg/kg BW, n=7)

Group iii: *A4gnt* KO mice + distilled water (n=10)

Group iv: *A4gnt* KO mice + EEP (100 mg/kg BW, n=10)

Before administration, EEP was dissolved in sterilized distilled water thus effectively diluting the carrier ethanol contained in the crude extract of propolis. All treatments were supplemented intragastrically on a daily basis for 30 days period.

Immunohistochemistry

Alongside CD3 and BrdU markers, p21 protein detection was additionally performed using the described procedures for CD3. The details of the p21 primary antibody are as follows: anti-p21 (Abcam, Tokyo, Japan; rabbit; clone ab188224; 1:200 dilution). Quantification of p21 immunolabeling similarly followed those of CD3 marker.

Quantitative real-time PCR (qRT-PCR)

For *in vitro* experiment, 2 ml aliquots of human gastric cancer cells were cultured into a 6-well/flat-bottom microplate (Iwaki, AGC Techno Glass Co, Ltd., Shizuoka, Japan) at an appropriate density ($4X10^5$ for AGS, $6X10^5$ for MKN45; $7X10^5$ for NUG4; and $1x10^6$ for MKN74) and incubated at 37°C in a humidified chamber with 5% CO_2 for 24 hours. Following this incubation, the medium was removed and replaced with a new one containing culture medium alone (control) or culture medium + EEP whose concentration approximated the 48-hour IC_{50} value (treated) computed for each cell lines and further cultured for another

48 hours. Samples were trypsinized and transferred into a new 1.5 microcentrifuge tube then added with lysis buffer. Triplicate samples representing three independent experiments were used. For *in vivo* experiment, previously harvest stomach tissue samples were similarly processed according to the aforementioned protocol specified in the General methodology section.

Aside from the aforementioned genes in section 1, in this present study, several genes encoding selected apoptotic, cell cycle, and inflammatory proteins were also inspected as follows: (Human gastric cancer cell lines) *BAX*, *BAD, BCL2*, *BCL2L1*, *CDKN1A*, *CDKN1B*, *P53, CDK1, CDK2, CCND*; (Mice) *Ifng, Il6, Tnfa, Bax, Bad, Bcl2, Bcl2l1, Cdkn1a, Cdkn1b, p53, Cdk1, Cdk2, Ccnd1*. The details of forward and reverse primers were summarized in Table.

GC-MS/MS assay

GC-MS/MS analysis was performed using the trimethylsilyl (TMS) ether derivatives of EEP. Briefly, samples were freeze-dried, oxymated using methoxyamine hydrochloride in pyridine (20 mg/ml) for 90 minutes at 30°C, and silylated for 30 minutes at 30°C with MSTFA. The resulting derivatized EEP was injected into a GCMS-TQ8040 (Shimadzu, Kyoto, Japan) equipped with an Agilent J&W DB-5 (30 m × 0.25 mm ID, 1.00 μm film, Agilent Technologies Japan, Ltd., Tokyo, Japan) in a splitless mode. The carrier gas helium was set at a constant flow rate of 1.1 ml/min with a linear velocity of 39 cm/s. Meanwhile, the injection temperature, pressure, and total flow were programmed as follows: 280 °C, 83.7 kPa, and 17.1 ml/min. A starting oven temperature of 100°C was maintained for 4 minutes and then raise up until 320°C at a constant increment of 10°C /min followed by 11-minute hold. The ion source and interface were run at a setting of 200°C and 280°C, respectively. Recording of mass spectra fell within the range of 45-600 *m/z*. Finally, using GCMS solution

Ver.4.45 (Shimadzu, Kyoto, Japan) together with NIST 17 mass spectral library, detected compounds derived from both chromatograms and mass spectral findings were identified.

Figure Legends

Fig. 2-1. EEP selectively impedes proliferation of differentiated-type GC cell lines. Cell proliferation of four human gastric cancer cell lines (AGS, MKN-45, NUGC-4, MKN-74) following incubation with varying concentrations of EPP (1-1000 μg/ml) at different time points of 24 h, 48 h, and 72 h as determined by MTT assay.

Fig. 2-2. EEP acts *in vitro* through modulation of the cell cycle and apoptotic machineries. (**A**) Real time PCR profile of selected genes associated in cell cycle regulation and apoptosis in four human GC cell lines following 48 hour-incubation with either culture medium alone or EEP whose concentration approximated the determined IC_{50} value (@ 48 h) for each respective cell lines. Data shown as mean ± SD are representative of three independent experiments with each experiment run in duplicates. $^{\#}P < 0.05$ and $^{**}P < 0.01$ using Independent sample t-test, $^{\ddagger}P < 0.05$ using Mann-Whitney U test. (**B**) Cell cycle analysis of AGS cells using propidium iodide staining depicting the representative raw data of the untreated control and EEP-treated cells (IC_{50} value @ 48 h) (left) and graphical analysis of the cell cycle distribution in the sub-G1, G0/G1, S, G2/M, and multi-nuclear phases (right). Data are shown as mean ± SD taken from triplicates of two independent experiments. NS-not significant, * $P < 0.01$ using Independent sample t-test. **(C)** Validation of DNA fragmentation-initiated apoptosis using TUNEL assay in three sensitive human GC cell lines after application of either culture medium alone or EEP at respective IC_{50} concentration at 48 h (above). Positive control cells were subjected to DNase I treatment prior to TdT labeling while negative control cells were incubated in TdT solution in lieu of TdT reagent (below). Scale bar: 100μm (**D**) Comparison of the number of cells undergoing apoptosis expressed as % apoptotic cells between untreated and EEP-treated groups in three human GC cell lines. $^{*}P < 0.05$ using Independent sample t-test.

Fig. 2-3. EEP supplementation induces promising anti-tumor response in mice model of differentiated-type gastric adenocarcinoma. (**A**) Representative stomach tissues of 60-week old C57BL/6J and *A4gnt* KO mice reflecting the gross mucosal elevation of the pyloric antrum following oral administration of respective treatments for 30 consecutive days. (**B**) H&E sections of the mouse pyloric mucosa among the different treatment groups. Scale bar: 100μm (**C**) T-lymphocyte infiltration of the pyloric mucosa among the different treatment groups as depicted by CD3 immunostaining. Scale bar: 100μm (**D**) Comparison of the gross mucosal elevation score among the different treatment groups. 0 - none/healthy mucosa, 1 - mildly, 2 – moderately, 3 - markedly. $^{*}P < 0.05$ using Independent-sample t-test. (**E**) Comparison of the gastric mucosal thickness among the different treatment groups expressed as mean measurement (μm) taken from at least three different areas of the pyloric mucosa. Means with different letter are significant at $P < 0.05$ using ANOVA with Tukey-HSD posttest. (**F**) Comparison of the number of CD3-positive T-lymphocytes among the different treatment groups expressed as mean count per 100μm area taken from at least three different points with the highest cell density. Means with different letter are significant at $P < 0.05$ using ANOVA with Tukey-HSD posttest. i – Wildtype + dH_20, ii – Wildtype + EEP, iii – *A4gnt* KO + dH_20, iv - *A4gnt* KO + EEP.

Fig. 2-4. EEP consistently affects cell cycle process *in vivo* to confer efficient anti-tumor action. (**A**) mRNA expression levels of several genes related to cell cycle regulation and apoptosis among the different treatment groups using real time PCR. Data are shown as an average of two independent experiments with each analysis run in duplicates. Means with different letter are significant at $P < 0.05$ using ANOVA with Tukey-HSD posttest. $^{**}P < 0.05$ using Kruskal-Wallis test. (**B**) Representative sections of gastric pyloric mucosa depicting p21 immunoreaction between untreated and EEP-treated *A4gnt* KO mice. Scale bar: 100μm (**C**) Comparison of the number of p21-positive cells between untreated and EEP-

treated A4gnt KO animals expressed as mean counts per 100μm taken from at least three different areas with the highest cell density. $^{*}P < 0.05$ using Independent sample t-test. (**D**) Representative sections of gastric pyloric mucosa among the different treatment groups showing BrdU labeling of actively dividing cells in the synthesis (S) phase of the cell cycle. Scale bar: 100μm (**E**) Comparison of the number of BrdU-positive cells among the different treatment groups expressed as mean counts per 100μm area taken from at least three different points with the highest cell density. Means with different letter are significant at $P < 0.05$ using ANOVA with Tukey-HSD posttest. (**F**) Representative sections of pyloric mucosa demonstrating cells undergoing apoptosis between untreated and EEP-treated *A4gnt* KO mice as revealed by TUNEL assay. Scale bar: 100μm (**G**) Comparison of the number of FITC-dUTP-positive cells expressed as mean counts per 100μm area taken from at least three different points with the highest cell density. $P < 0.05$ using Independent sample t-test. . i – Wildtype + dH_20, ii – Wildtype + EEP, iii – *A4gnt* KO + dH_20, iv - *A4gnt* KO + EEP.

Figure 2-1

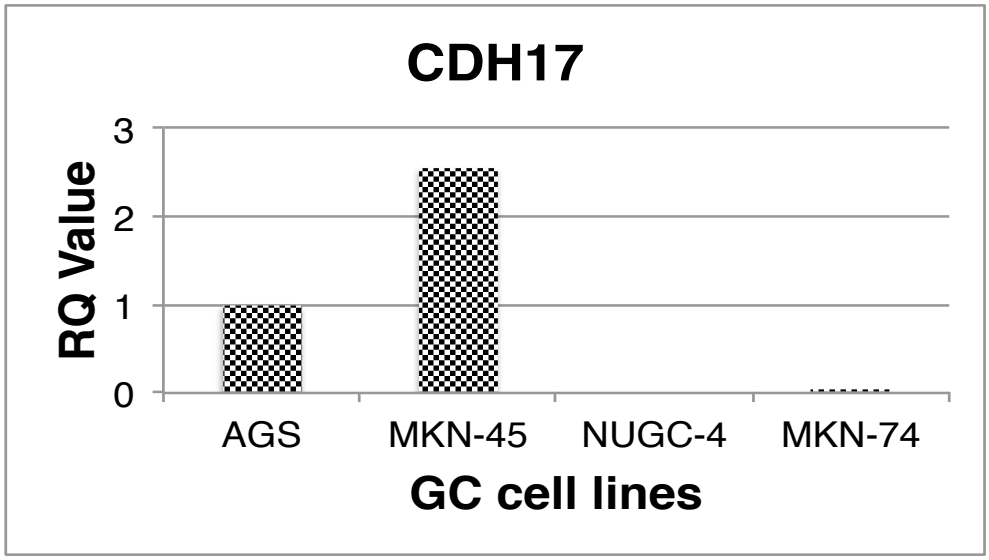
CDH17
RQ Value
3
2
1
0
AGS
MKN-45
NUGC-4
MKN-74
GC cell lines

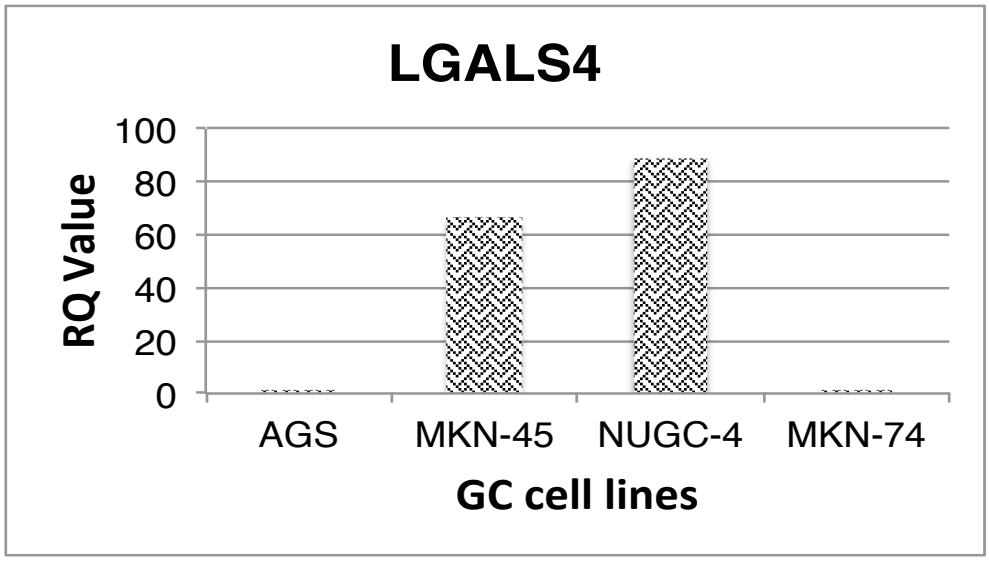
LGALS4
RQ Value
100
80
60
40
20
0
AGS
MKN-45
NUGC-4
MKN-74
GC cell lines

Figure 2-2

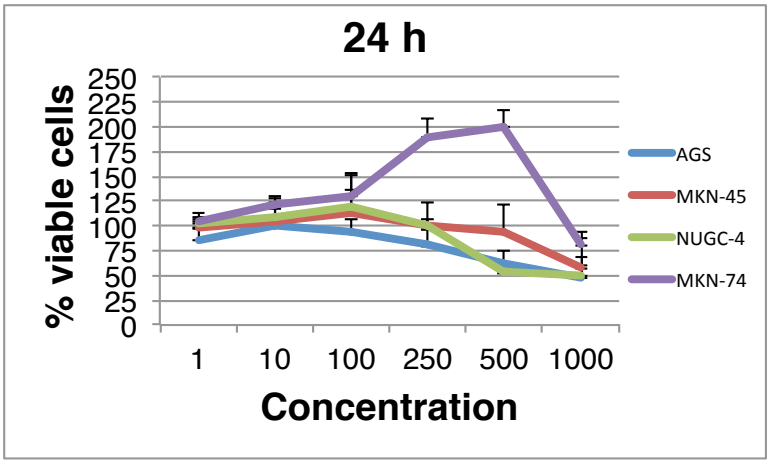
24 h
% viable cells
250
225
200
175
150
125
100
75
50
25
0
1
10
100
250
500
1000
Concentration
AGS
MKN-45
NUGC-4
MKN-74

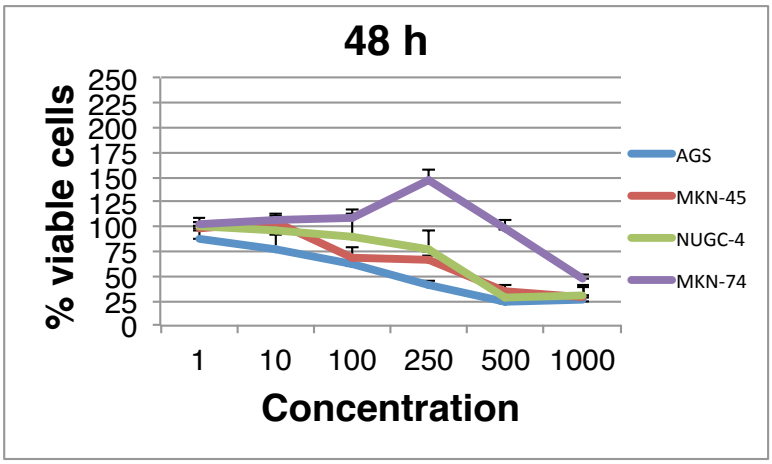
48 h
% viable cells
250
225
200
175
150
125
100
75
50
25
0
1
10
100
250
500
1000
Concentration
AGS
MKN-45
NUGC-4
MKN-74

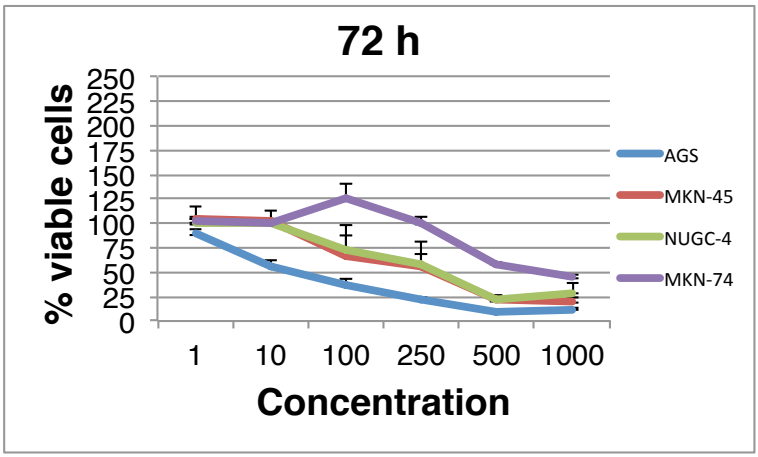
72 h
% viable cells
250
225
200
175
150
125
100
75
50
25
0
1
10
100
250
500
1000
Concentration
AGS
MKN-45
NUGC-4
MKN-74

Figure 2-3

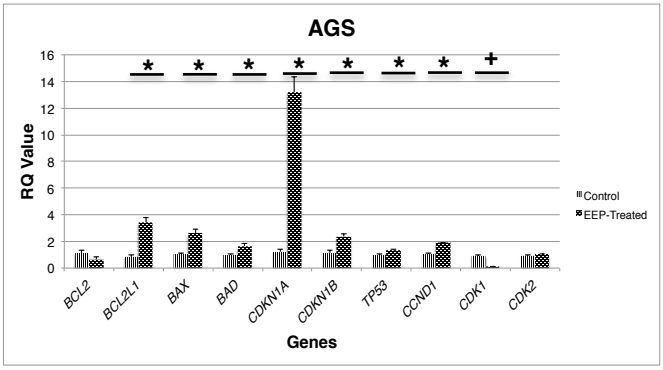
AGS
RQ Value
Genes
Control
EEP-Treated
BCL2
BCL2L1
BAX
BAD
CDKN1A
CDKN1B
TP53
CCND1
CDK1
CDK2

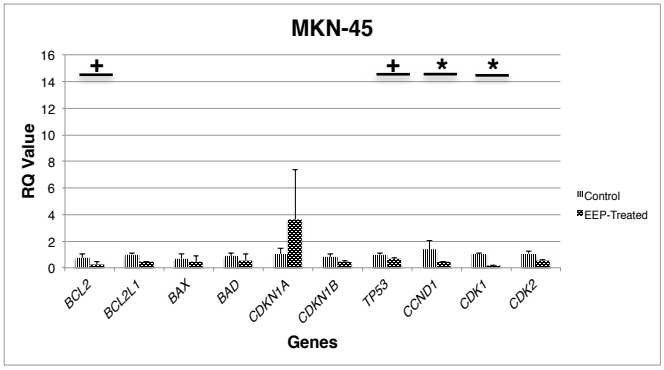
MKN-45
RQ Value
Genes
Control
EEP-Treated
BCL2
BCL2L1
BAX
BAD
CDKN1A
CDKN1B
TP53
CCND1
CDK1
CDK2

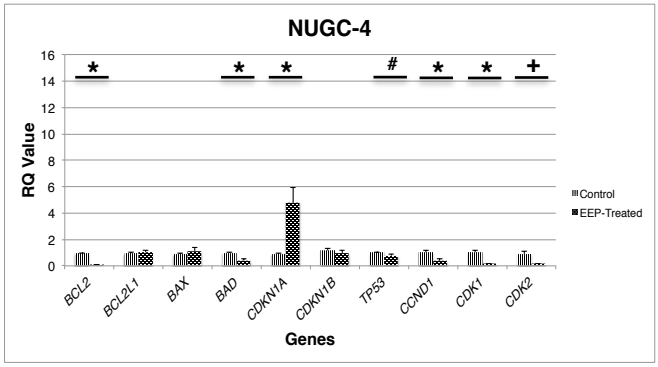
NUGC-4
RQ Value
Genes
Control
EEP-Treated
BCL2
BCL2L1
BAX
BAD
CDKN1A
CDKN1B
TP53
CCND1
CDK1
CDK2

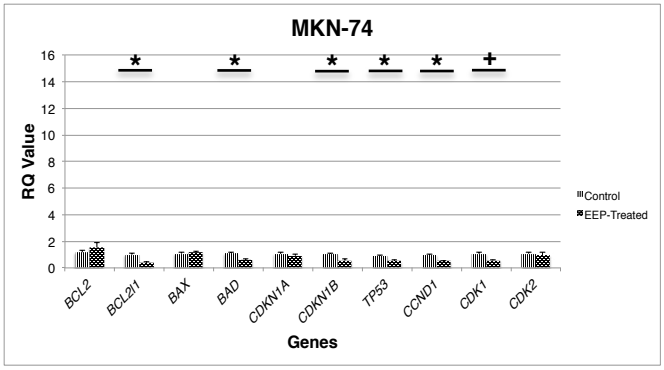
MKN-74
RQ Value
Genes
Control
EEP-Treated
BCL2
BCL2l1
BAX
BAD
CDKN1A
CDKN1B
TP53
CCND1
CDK1
CDK2

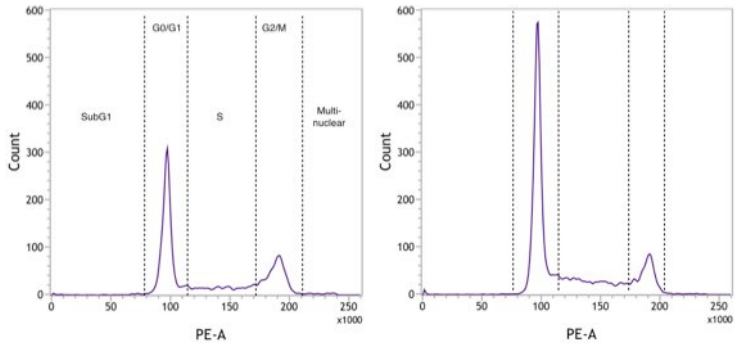
G0/G1
G2/M
SubG1
S
Multi-nuclear
Count
PE-A
x1000

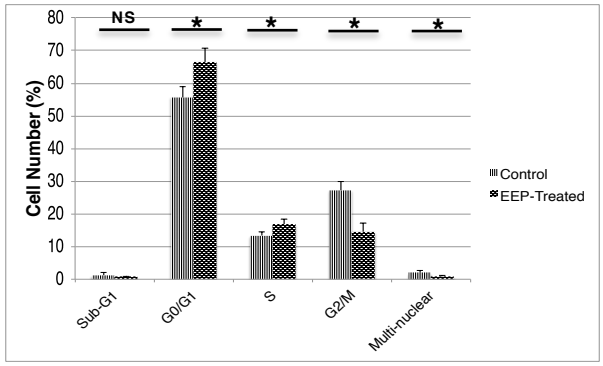
NS
Cell Number (%)
Control
EEP-Treated
Sub-G1
G0/G1
S
G2/M
Multi-nuclear

Figure 2-4

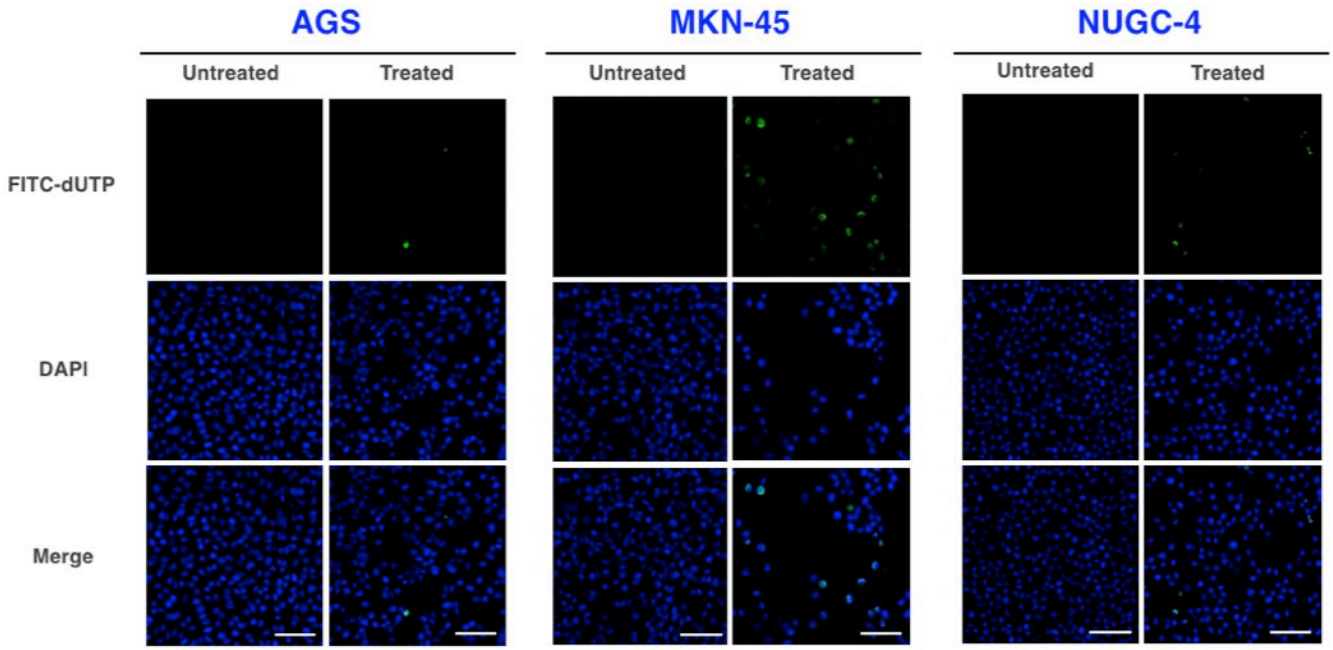
AGS
MKN-45
NUGC-4
Untreated
Treated
FITC-dUTP
DAPI
Merge

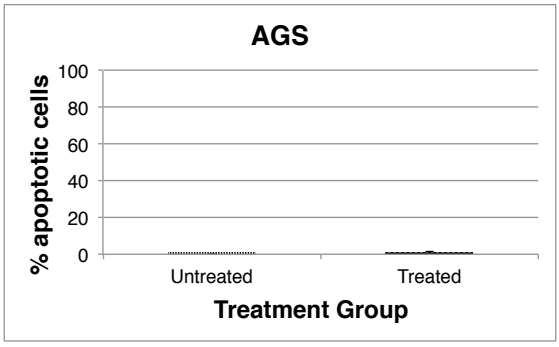
AGS
% apoptotic cells
100
80
60
40
20
0
Untreated
Treated
Treatment Group

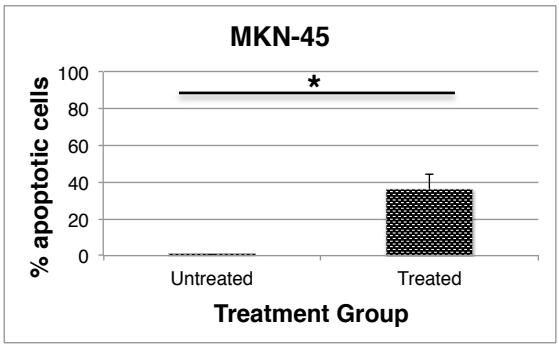
MKN-45
% apoptotic cells
*
Untreated
Treated
Treatment Group

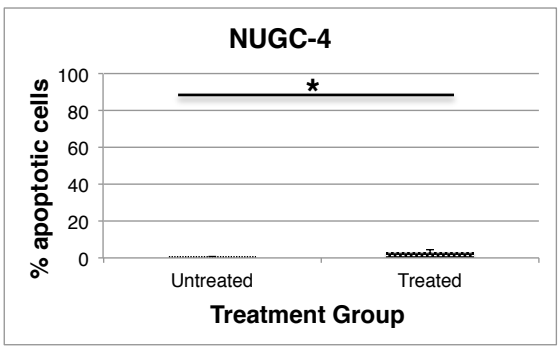
NUGC-4
% apoptotic cells
*
Untreated
Treated
Treatment Group

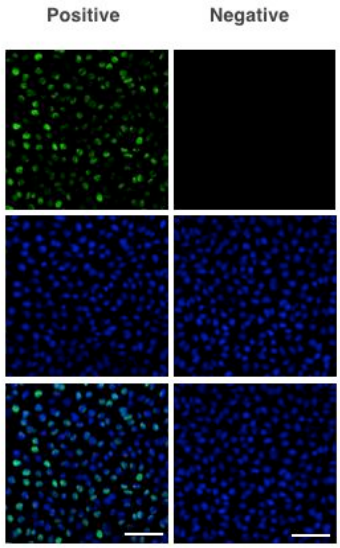
Positive
Negative

Figure 2-5

i – Wildtype + dH_2O

ii – Wildtype + EEP

iii – A4gnt KO + dH_2O

iv – A4gnt KO + EEP

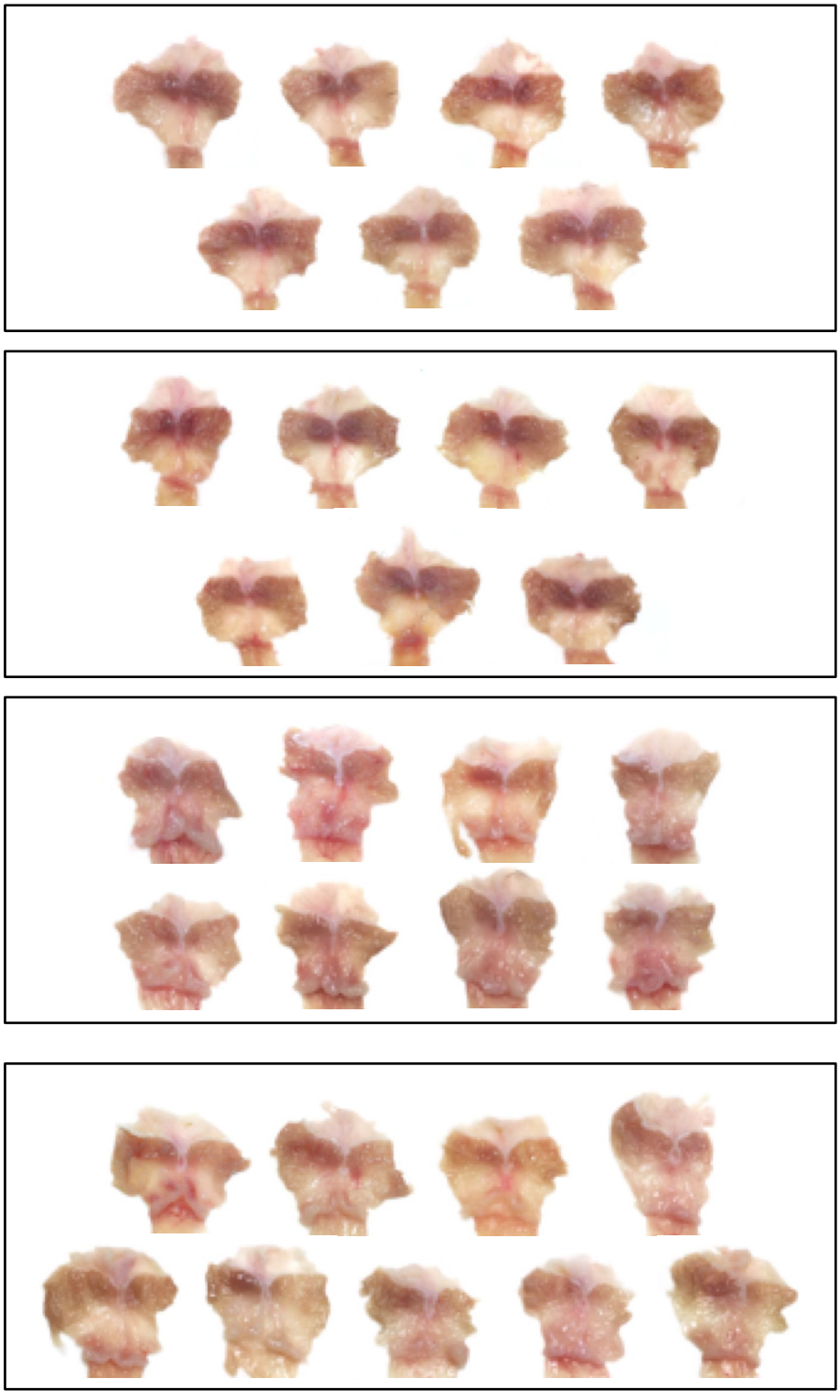

Figure 2-6

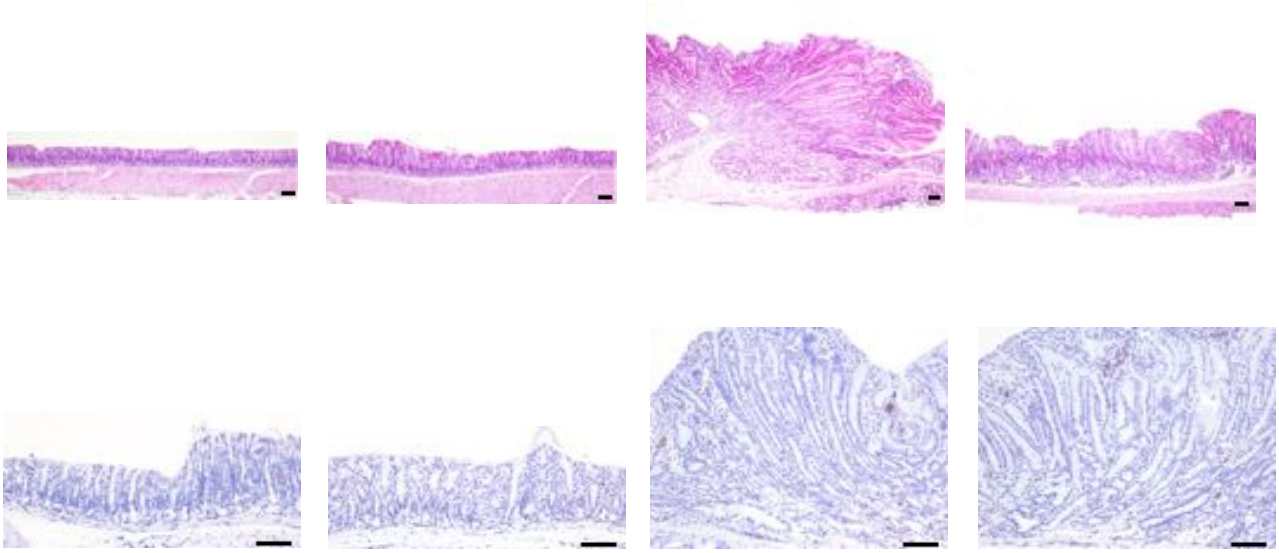

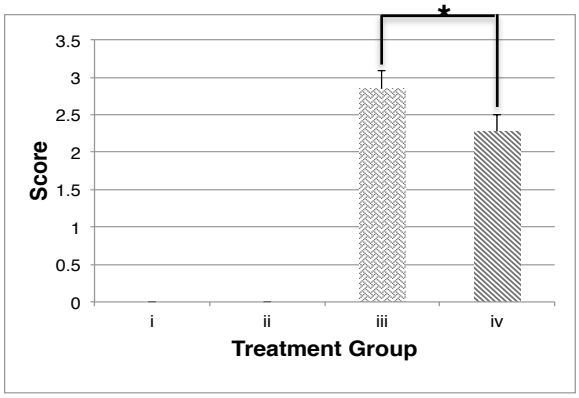
*
Score
3.5
3
2.5
2
1.5
1
0.5
0
i
ii
iii
iv
Treatment Group

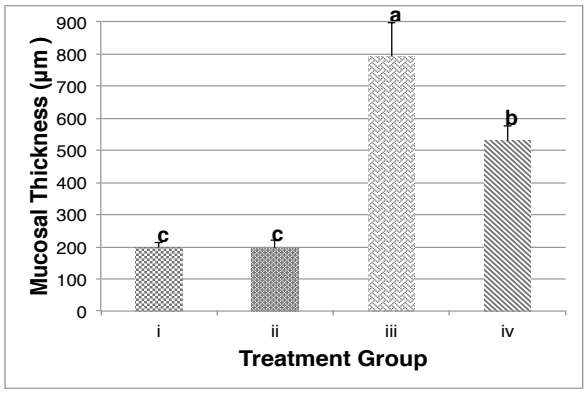
Mucosal Thickness (µm)
900
800
700
600
500
400
300
200
100
0
a
b
c
c
i
ii
iii
iv
Treatment Group

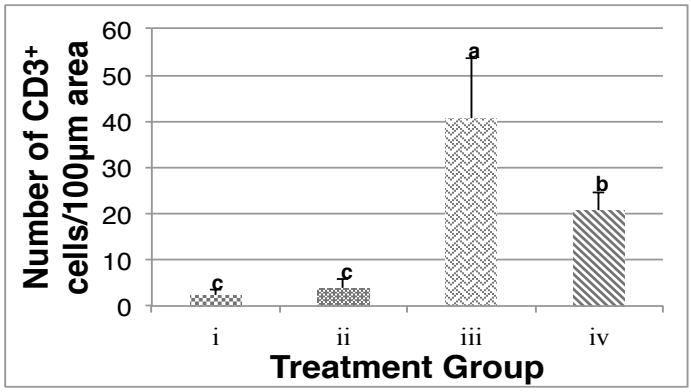
Number of CD3+ cells/100µm area
60
50
40
30
20
10
0
a
b
c
c
i
ii
iii
iv
Treatment Group

Figure 2-7

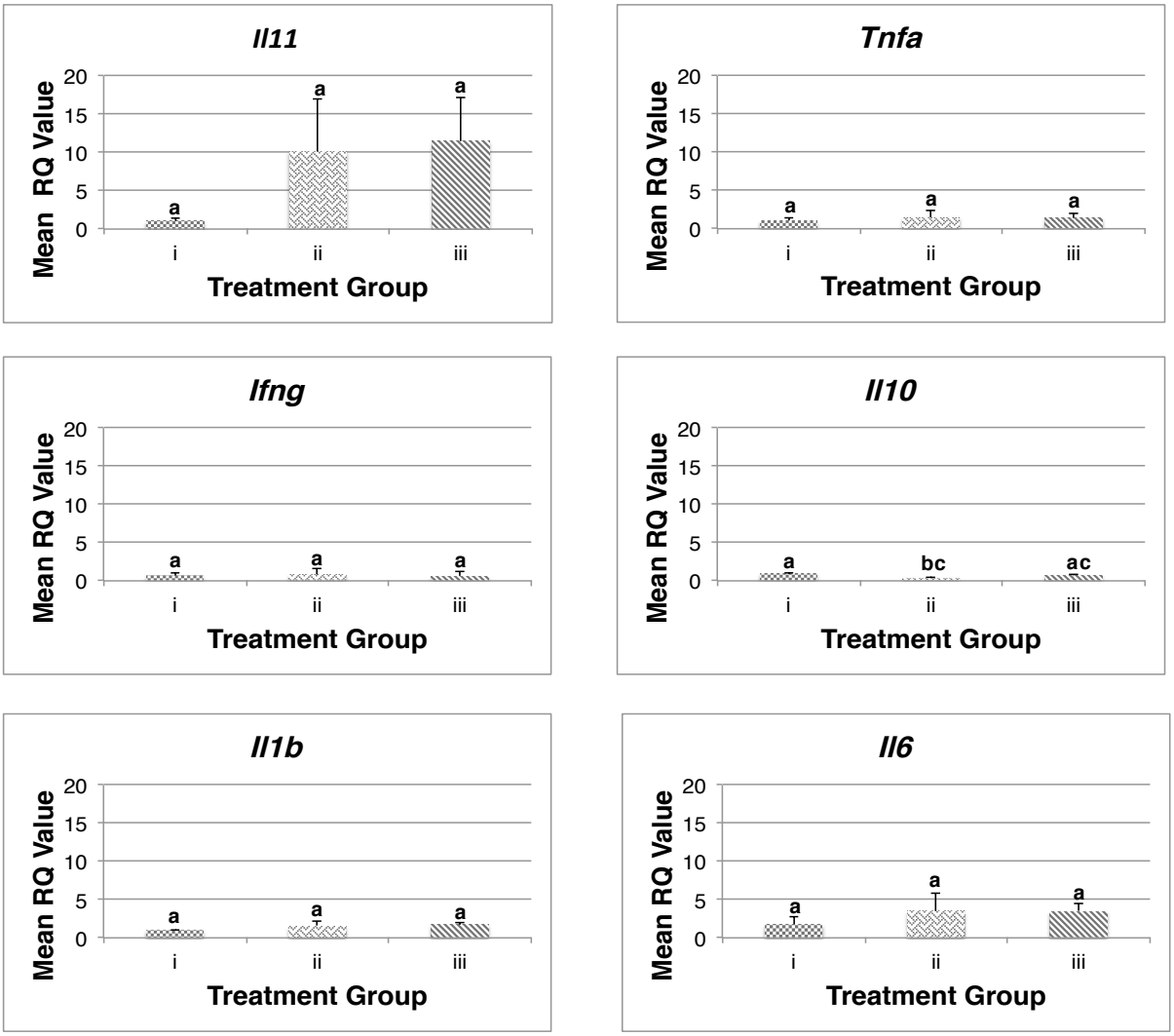
Il11
Mean RQ Value
20
15
10
5
0
a
a
a
i
ii
iii
Treatment Group
Tnfa
Mean RQ Value
a
a
a
Treatment Group
Ifng
Mean RQ Value
a
a
a
Treatment Group
Il10
Mean RQ Value
a
bc
ac
Treatment Group
Il1b
Mean RQ Value
a
a
a
Treatment Group
Il6
Mean RQ Value
a
a
a
Treatment Group

Figure 2-8

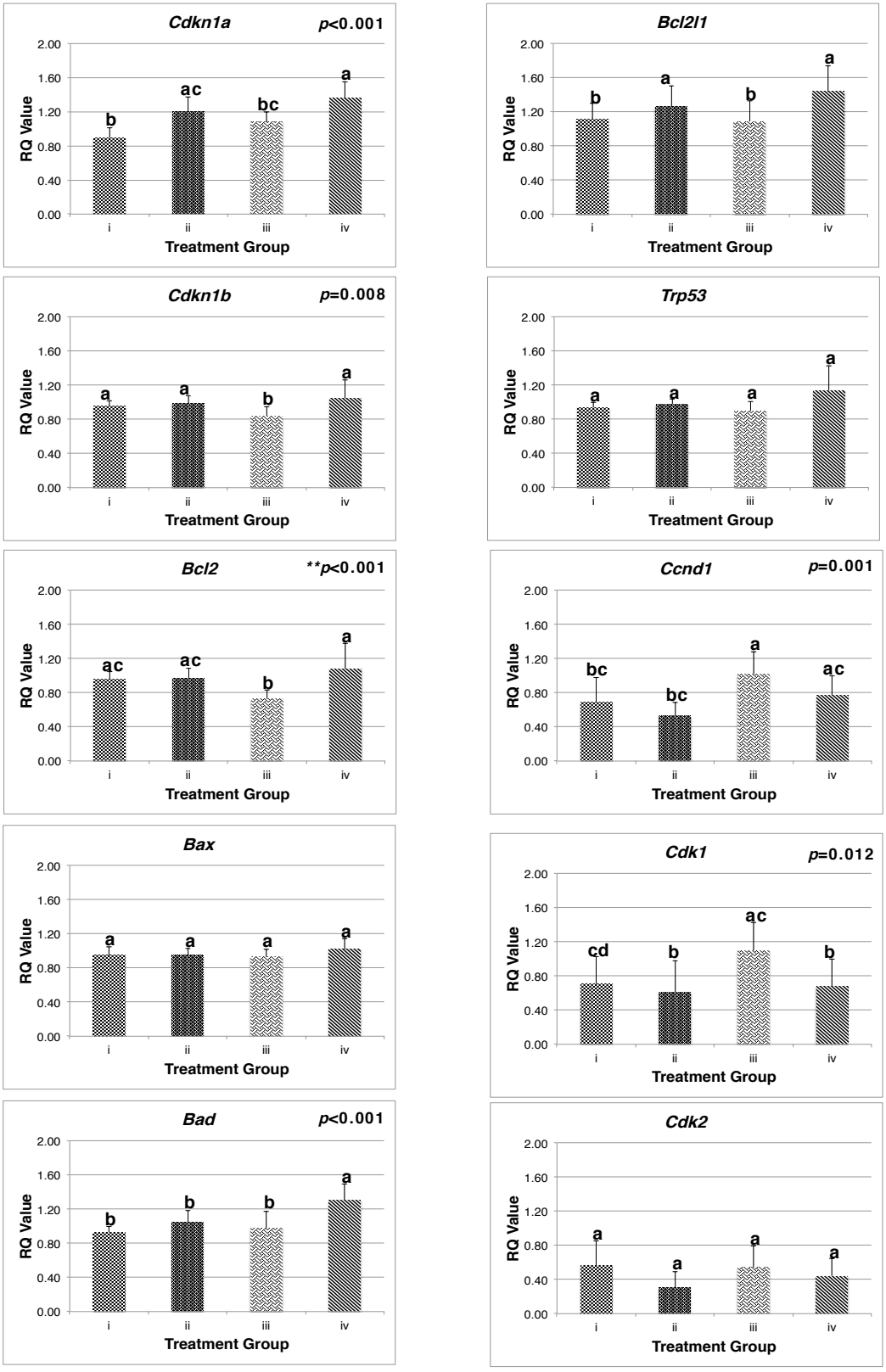
Cdkn1a
p<0.001
RQ Value
Treatment Group
Bcl2l1
Cdkn1b
p=0.008
Trp53
Bcl2
**p<0.001
Ccnd1
p=0.001
Bax
Cdk1
p=0.012
Bad
p<0.001
Cdk2

Figure 2-9

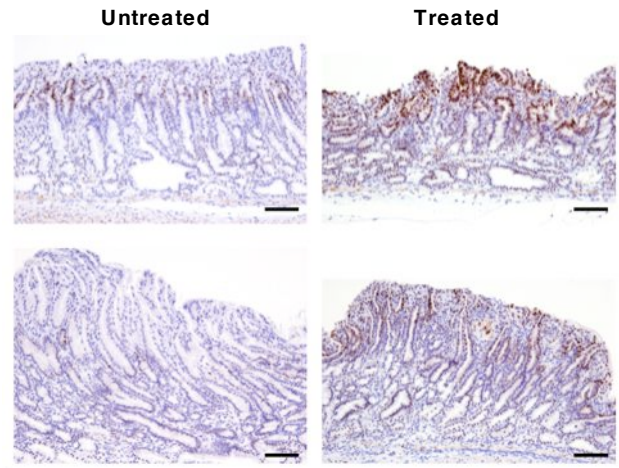
Untreated
Treated

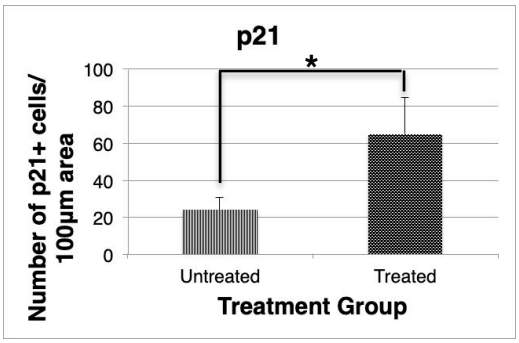
p21
*
Number of p21+ cells/ 100µm area
100
80
60
40
20
0
Untreated
Treated
Treatment Group

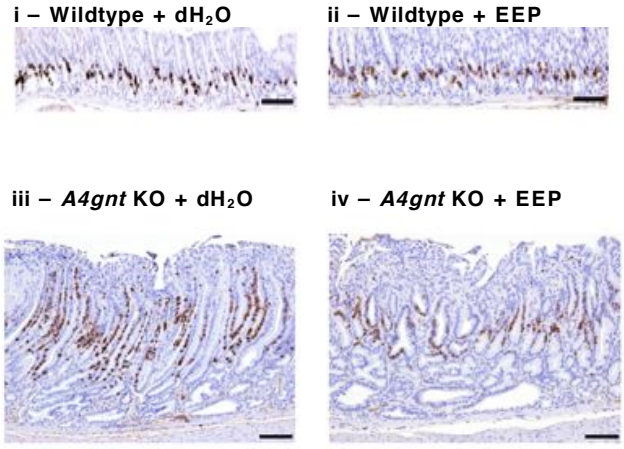
i – Wildtype + dH2O
ii – Wildtype + EEP
iii – A4gnt KO + dH2O
iv – A4gnt KO + EEP

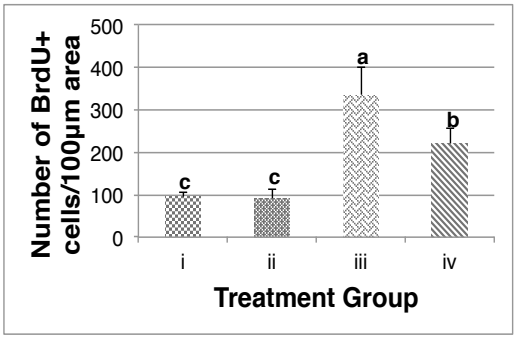
Number of BrdU+ cells/100µm area
500
400
300
200
100
0
a
b
c
c
i
ii
iii
iv
Treatment Group

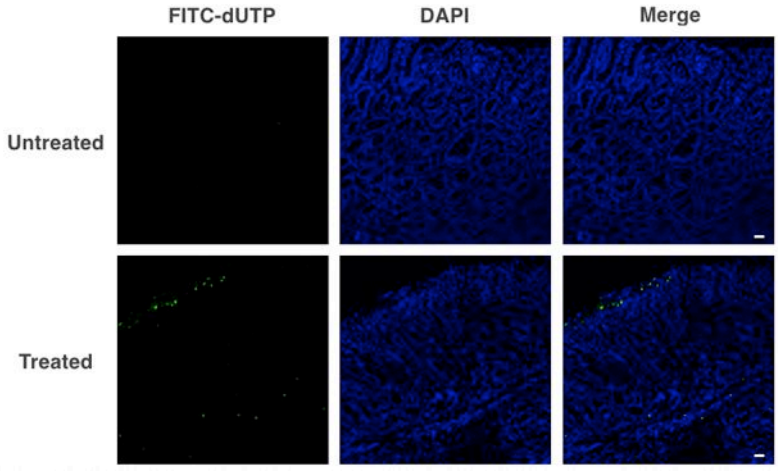
FITC-dUTP
DAPI
Merge
Untreated
Treated

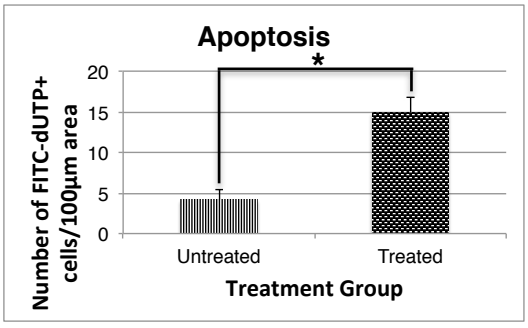
Apoptosis
*
Number of FITC-dUTP+ cells/100µm area
20
15
10
5
0
Untreated
Treated
Treatment Group

Table 2-1. Primer details of selected genes utilized in the present study.

	Genes	Forward	Reverse
Mouse	*Actb*	AAGTGTGACGTTGACATCCG	GATCCACATCTGCTGGAAGG
	Il10	GCTCTTACTGACTGGCATGAG	CGCAGCTCTAGGAGCATGTG
	Il11	TGTTCTCCTAACCCGATCCCT	CAGGAAGCTGCAAAGATCCCA
	Il1b	GCAACTGTTCCTGAACTCAACT	ATCTTTTGGGGTCCGTCAACT
	Tnfa	CCCTCACACTCAGATCATCTTCT	GCTACGACGTGGGCTACAG
	Ifng	ATGAACGCTACACACTGCATC	CCATCCTTTTGCCAGTTCCTC
	Il6	TAGTCCTTCCTACCCCAATTTCC	TTGGTCCTTAGCCACTCCTTC
	Bcl2	ATGCCTTTGTGGAACTATATGGC	GGTATGCACCCAGAGTGATGC
	Bcl2l1	GACAAGGAGATGCAGGTATTGG	TCCCGTAGAGATCCACAAAAGT
	Bax	TGAAGACAGGGGCCTTTTTG	AATTCGCCGGAGACACTCG
	Bad	AAGTCCGATCCCGGAATCC	GCTCACTCGGCTCAAACTCT
	Trp53	GCGTAAACGCTTCGAGATGTT	TTTTTATGGCGGGAAGTAGACTG
	Cdkn1a	CCTGGTGATGTCCGACCTG	CCATGAGCGCATCGCAATC
	Cdkn1b	TCAAACGTGAGAGTGTCTAACG	CCGGGCCGAAGAGATTTCTG
	Cdk1	AGAAGGTACTTACGGTGTGGT	GAGAGATTTCCCGAATTGCAGT
	Cdk2	CCTGCTTATCAATGCAGAGGG	GTGCTGGGTACACACTAGGTG
Human	*ACTB*	AAGTGTGACGTTGACATCCG	GATCCACATCTGCTGGAAGG
	BCL2	GGTGGGGTCATGTGTGTGG	CGGTTCAGGTACTCAGTCATCC
	BCL2L1	GACTGAATCGGAGATGGAGACC	GCAGTTCAAACTCGTCGCCT
	BAX	CCCGAGAGGTCTTTTTCCGAG	CCAGCCCATGATGGTTCTGAT
	BAD	CCCAGAGTTTGAGCCGAGTG	CCCATCCCTTCGTCGTCCT
	TP53	CAGCACATGACGGAGGTTGT	TCATCCAAATACTCCACACGC
	CDKN1A	TGTCCGTCAGAACCCATGC	AAAGTCGAAGTTCCATCGCTC
	CDKN1B	AACGTGCGAGTGTCTAACGG	CCCTCTAGGGGTTTGTGATTCT
	CCND1	GCTGCGAAGTGGAAACCATC	CCTCCTTCTGCACACATTTGAA
	CDK1	AAACTACAGGTCAAGTGGTAGCC	TCCTGCATAAGCACATCCTGA
	CDK2	CCAGGAGTTACTTCTATGCCTGA	TTCATCCAGGGGAGGTACAAC

Table 2-2. IC_{50} value of four human GC cell lines over time periods of 24 h, 48 h and 72 h.

	IC_{50} (μg/ml)			
	AGS	MKN45	NUGC4	MKN74
24 h	650	1156	580	1259
48 h	188	386	376	955
72 h	39	318	315	925
Cisplatin (48h)	~4	~3	~2	~12

Table 2-3. Summary data of the mean mRNA expression levels of selected cell cycle- and apoptosis-related genes in four human GC cell lines

	AGS			MKN-45			NUGC-4			MKN-74		
	Untreated	Treated	*p* value	Untreated	Treated	*p* value	Untreated	Treated	*p* value	Untreated	Treated	*p* value
CDKN1A	1.23±0.21	13.18±1.20	< 0.001	1.01±0.45	3.62±3.79	0.302	0.91±0.09	4.80±1.10	* 0.050	1.05±0.13	0.92±0.13	0.300
CDKN1B	1.15±0.16	2.38±0.17	0.001	0.81±0.22	0.43±0.11	0.057	1.16±0.15	0.98±0.18	0.248	1.07±0.06	0.55±0.11	*0.002
CDK1	0.90±0.09	0.11±0.01	* 0.050	1.06±0.06	0.19±0.01	< 0.001	1.05±0.13	0.16±0.04	< 0.001	1.05±0.10	0.57±0.02	** 0.050
CDK2	0.89±0.10	1.04±0.05	0.077	1.07±0.17	0.53±0.05	0.006	0.91±0.20	0.15±0.03	* 0.050	1.07±0.11	0.95±0.21	0.438
CCND1	1.08±0.08	1.89±0.06	< 0.001	1.42±0.66	0.46±0.01	* 0.050	1.05±0.11	0.39±0.12	0.002	0.99±0.03	0.54±0.02	*< 0.001
BCL2	1.11±0.26	0.66±0.17	0.068	0.74±0.30	0.27±0.21	0.084	0.97±0.03	0.07±0.03	< 0.001	1.16±0.17	1.53±0.40	0.210
BCL2L1	0.84±0.14	3.40±0.40	< 0.001	1.00±0.08	0.44±0.04	* 0.050	0.96±0.06	1.01±0.18	0.062	0.99±0.12	0.36±0.07	*0.002
TP53	0.99±0.04	1.35±0.10	0.005	0.98±0.12	0.71±0.06	0.241	1.02±0.05	0.78±0.11	0.027	0.93±0.06	0.51±0.10	*0.003
BAX	1.05±0.10	2.64±0.26	0.001	0.70±0.32	0.44±0.45	0.447	0.90±0.09	1.13±0.25	0.203	1.07±0.10	1.19±0.09	0.190
BAD	0.98±0.08	1.65±0.17	0.003	0.86±0.27	0.54±0.52	0.393	0.98±0.06	0.42±0.09	0.001	1.09±0.08	0.60±0.05	*0.001

Table 2-4. Summary data of the mean mRNA expression levels of selected inflammation-related genes in three different treatment groups.

		Genes					
		Il11	*Tnfa*	*Ifng*	*Il10*	*Il1b*	*Il6*
i	Wildtype + dH_20	1.03±0.48	1.08±0.29	0.69±0.41	0.92±0.21	1.00±0.07	1.72±1.00
ii	*A4gnt* KO + dH_20	10.15±6.88	1.49±0.94	0.81±0.86	0.38±0.14	1.55±0.73	3.53±2.26
iii	*A4gnt* KO + 30% EEP	11.49±5.64	1.40±0.62	0.60±0.61	0.74±0.17	1.71±0.36	3.46±1.01
	p value	**0.055	0.727	0.915	*0.02	**0.055	0.285

Table 2-5. Summary data of the mean mRNA expression levels of selected cell cycle- and apoptosis related genes in four different treatment groups.

	Treatment Groups				
	i	ii	iii	iv	
Genes	Wildtype + dH_20	Wildtype + 30% EEP	*A4gnt* KO + dH_20	*A4gnt* KO + 30% EEP	*p* value
Cdkn1a	0.90±0.11	1.20±0.18	1.08±0.12	1.36±0.19	*< 0.001
Cdkn1b	0.96±0.06	0.99±0.09	0.84±0.11	1.05±0.21	*0.008
Cdk1	0.71±0.32	0.61±0.37	1.10±0.33	0.68±0.32	*0.012
Cdk2	0.56±0.29	0.31±0.18	0.54±0.25	0.44±0.21	0.088
Ccnd1	0.69±0.29	0.53±0.16	1.02±0.26	0.77±0.23	*0.001
Bcl2	0.96±0.09	0.97±0.12	0.73±0.10	1.08±0.30	**< 0.001
Bcl2l1	1.12±0.18	1.26±0.25	1.09±0.24	1.44±0.30	*0.010
Trp53	0.94±0.06	0.98±0.06	0.90±0.11	1.14±0.29	0.076
Bax	0.95±0.10	0.95±0.08	0.93±0.09	1.02±0.13	0.225
Bad	0.93±0.07	1.05±0.13	0.98±0.19	1.31±0.19	*< 0.001

Table 2-6. Selected compounds obtained from the crude extract of Philippine stingless bee propolis

Pubchem CID	Compound	Molecular Formula	MW
227829	Guaiol	$C_{15}H_{26}O$	222
444008	Tibolone	$C_{21}H_{28}O_2$	312
5318517	Andrographolide	$C_{20}H_{30}O_5$	350
370	Gallic acid	$C_7H_6O_5$	170
91457	β-Eudesmol	$C_{15}H_{26}O$	222
2950	Danthron	$C_{14}H_8O_4$	240
6324617	Ginkgolide-B	$C_{20}H_{24}O_{10}$	424
444539	Cinnamic acid	$C_9H_8O_2$	148
6167	Colchicine	$C_{22}H_{25}NO_6$	399
528594	Protocatechuic acid	$C_{25}H_{48}O_4Si_3$	496
5281858	Ginkgolic acid	$C_{22}H_{34}O_3$	346
5281251	Rhodoxanthin	$C_{40}H_{50}O_2$	562
5281727	Pterostilbene	$C_{16}H_{16}O_3$	256
13966122	Rosmanol	$C_{20}H_{26}O_5$	346
31404	Butylated hydroxytoluene	$C_{15}H_{24}O$	220

Chapter 3

"As contents of this chapter are anticipated to be published in a scholarly journal, they cannot be published online. The paper is scheduled to be published within 5 years"

General Conclusion

“As contents of this chapter are anticipated to be published in a scholarly journal, they cannot be published online. The paper is scheduled to be published within 5 years”

Acknowledgement

I wish to extend my sincerest gratitude and heartfelt appreciation to the following people (as well as organization), who in one way or another have helped me through this long, arduous, yet meaning journey – chasing my doctorate degree:

To Professor Shigeru Kakuta, my adviser and mentor – I will forever be grateful and indebted for this golden opportunity. The sheer compassion, kindness, encouragement, and the unwavering confidence you have bestowed me have contributed a lot to the kind of person and researcher I am today.

To Professor Kyuwa, and the rest of the member of the Laboratory of Biomedical Sciences (both incumbent and alumni) – I am very much thankful for your utmost assistance and genuine support. I will always cherish all the wonderful memories we've shared. You have definitely made my stay in Japan truly rewarding.

To Professor Nakayama, Uchida, Chambers and the rest of the Pathology Laboratory members – I am profoundly grateful for your hospitality and generosity. Your warm accommodation has contributed a lot to the success of my work.

To Professor Iwakura and the members of the Research Institute for Biomedical Science – I am deeply appreciative of your invaluable assistance and thoughtful consideration.

To Professor Jun Nakayama – I am greatly indebted for your unfaltering support.

To Dr. Ma. Amelita Estacio – I have no words but pure gratitude. Thank you for being a constant source of confidence, inspiration, and support. You are indeed a blessing. I am truly humbled and honored to be part of your research team.

To Ate Letlet, Ate Gege, and Ate Shy – I always thank the Lord for having you in my life. Thank you for the much needed breather. You are a family.

To Ate Therese, Eeya and Min – I am lucky to have found a colleague, a friend, and most importantly a family in you. I always find comfort knowing that I would be working very closely with you again in the nearest future.

To Roj and Xenia – You are one of my ultimate support systems. Thank you for being a constant fixture in my life. I am truly blessed to have developed a strong and unbreakable bond with both of you.

To Cherry and Bev – Thank you for the genuine and strong friendship. I am honestly glad that our college friendship has bloomed into something that is worth keeping for life.

To Ate Zen, Ralph, Angel, Camille, Rogie, Edward, Jakie, Aizelle, Ate Jane, Mario – I am grateful for the true friendship. Thank you for making my stay in Japan extra special.

To Nezu Club and Komagome Badminton Club – I am happy to have been part of your wonderful group.

To the members of the Department of Basic Veterinary Sciences – I am thankful for all your hard work and sacrifices during the course of my PhD. I hope to be able to return back the favor in the future.

To Tojuro Iijima Foundation and Kobayashi Foundation – I am grateful for the financial support you have conferred me during my PhD.

To MEXT – I am profoundly grateful for the opportunity you have entrusted me. Without your financial assistance, the once far-fetched dream of acquiring a PhD degree wouldn't become a reality.

To my family – You have served my ultimate reason and inspiration to keep striving and believing amidst times of doubts and despair. Thank you for not giving up on me and for me keeping me sane all the time. I offer all of this to you.

To God Almighty – I am grateful for the gift of life and wisdom. Thank you for keeping my faith more intact during these trying times. I lift all the honor and glory to you.

And to all the Professors, Students and People who I have come across with – Allow me to thank you for your simple act of kindness, encouragement and support.

Abbreviations

α4gnt: α1, 4-*N*-acetylglucosaminyltransferase

αGlcNAc: α1, 4-linked *N*-acetylglucosamine residues

ACF: aberrant crypt foci

ACRG: Asian Cancer Research Group

ACS: adenoma-carcinoma sequence

ACTB: actin beta

AGC: advance gastric cancer

ANOVA: analysis of variance

BAD: BCL2 associated agonist of cell death

BAX: BCL2 associated X, apoptosis regulator

BCL2: B-cell lymphoma 2

BCL2L1: B-cell lymphoma 2-like 1

BRCA1: breast cancer gene 1

BRCA2: breast cancer gene 2

BrdU: 5-bromo-2-deoxyuridine

BRM: biological response modifier

CAPE: caffeic acid phenethyl ester

CCL2: C-C motif chemokine ligand 2

CCND1: cyclin D1

CDH17: cadherin 17

CDK: cyclin-dependent kinase

CDK1: cyclin-dependent kinase 1

CDK2: cyclin-dependent kinase 2

CDKN1A: cyclin-dependent kinase inhibitor 1A

CDKN1B: cyclin-dependent kinase inhibitor 1B

CD3: cluster of differentiation 3

CD31: cluster of differentiation 31

CIN: chromosomal instability

CKI: CDK inhibitor

CLEC7A: C-type lectin domain family 7 member A

CRD: carbohydrate recognition domain

CRF: commercial rodent pellet

CRISPR/Cas9: clustered regularly interspaced short palindromic repeats/

CRISPR associated protein 9

crRNA: CRISPR RNA

CXCL1: chemokine C-X-C motif ligand 1

DAB: 3,3'-diaminobenzidine tetrahydrochloride

DAPI: 4',6-diamidino-2-phenyl indole

DHA: docosahexanoic acid

DKO: double knockout

DMH: dimethylhydrazine

DNA: deoxyribonucleic acid

dNTP: deoxynucleoside triphosphate

EBV: Epstein-Barr virus

EEP: ethanolic extract of propolis

EGC: early gastric cancer

EGF: epidermal growth factor

EMT: epithelial to mesenchymal transition

EPA: eicosapentanoic acid

EphA2: Ephrin type A- receptor 2

EtBr: Ethidium bromide

FDGC: familial intestinal gastric cancer

FGC: familial gastric cancer

FGF7: fibroblast growth factor 7

FITC: flurorescein isothiocyanate

GAPPS: gastric adenocarcinoma and proximal polyposis of the stomach

GC: gastric cancer

GC-MS/MS: gas chromatography, triple quadruple mass-spectrometry

GS: genomic stable

G-DIF: genomic-diffuse

G-INT: genomic-intestinal

gp130: glycoprotein 130

HDGC: hereditary diffuse gastric cancer

HE: hematoxylin eosin

HGF: hepatocyte growth factor

HNPCC: hereditary nonpolyposis colon cancer

HRP: horseradish peroxidase

IARC: International Agency for Research on Cancer

IGF2: insulin-like growth factor 2

IHC: immunohistochemistry

IL1b: interleukin 1 beta

IL10: interleukin 10

IL11: interleukin 11

IFNg: interferon gamma

IVF: in vitro fertilization

JAK: Janus kinase

JNK: c-Jun N-terminal kinase

JRCB: Japanese Collection of Research Bioresource Cell Bank

Kbp: kilobase pair

kDa: kilodalton

KO: knockout

LGALS1: lectin, galactose binding, soluble 1

LGALS2: lectin, galactose binding, soluble 2

LGALS3: lectin, galactose binding, soluble 3

LGALS4: lectin, galactose binding, soluble 4

LGALS7: lectin, galactose binding, soluble 7

LGALS8: lectin, galactose binding, soluble 8

MNNG: *N*-methyl-*N*-nitro-*N*-nitrosoguanidine

MNU: *N*-methyl-*N*-nitrosourea

mRNA: messenger ribonucleic acid

MSI: microsomal instable

MSS: microsomal stable

MTT: 3-(4,5-dimethylthiazol-2-ly)-2,5-diphenyltetrazolium bromide

NF-κB: nuclear factor kappa-light-chain-enhancer of activated B cells

NIST: National Institute of Standards and Technology

PMNL: polymorphonuclear leukocytes

P-STAT3: phosphorylated STAT3

PTGS2: prostaglandin- endoperoxide synthase 2

qRT-PCR: quantitative reverse-transcriptase polymerase chain reaction

RB: retinoblastoma

RNA: ribonucleic acid

RPMI 1640: Roswell Park Memorial Institute 1640

RQ: relative quantification

RT-PCR: real time polymerase chain reaction

STAT3: signal transducers and activators of transcription 3

TCGA: The Cancer Genome Atlas

TKO: triple knockout

TMS: trimethylsilyl

TNFa: tumor necrosis factor alpha

TP53: tumor protein 53

tracrRNA: transactivating small RNA

TUNEL: terminal deoxynucleotidyl transferase dUTP nick-end labeling

WHO: World Health Organization

References

Abbas, T. & Dutta, A. p21 in cancer: Intricate networks and multiple activities. *Nat. Rev. Cancer* **9.** 400-414, doi: 10.1038/nrc2657 (2009).

Akama, Y., Yasui, W., Kuniyasu, H., Yokozaki, H., Akagi, M., Tahara, H., Ishikawa, T. & Tahara, E. Genetic status and expression of the cyclin-dependent kinase inhibitors in human gastric carcinoma cell lines. *Jpn. J. Cancer. Res.* **87.** 824-830 (1996).

Akao, Y., Maruyama, H., Matsumoto, K., Ohguchi, K., Nishizawa, K., Sakamoto, T., Araki, Y., Mishima, S. & Nozawa, N. Cell growth inhibitory effect of cinnamic acid derivatives from propolis on human tumor cell lines. *Biol. Pharm. Bull.* **26.** 1057-1059 (2003).

Alizadeh, A.M., Afrouzan, H., Dinparast-Djadid, N., Sawaya, A.C.H.F., Azizian, S., Hemmati, H.R., Mohagheghi, M.A. & Erfani, S. Chemoprotection of MNNG-initiated gastric cancer in rats using Iranian propolis. *Arach. Iran. Med.* **18.** 18-23 (2015).

Alvarez, P.L.J., Cruz, M.B., Micor, J.R.L., Fajardo Jr., A.C., Cervancia, C.R. & Hizon-Fradejas, A. Identification of flavonoids and phenolic compounds in propolis from stingless bees (*Tetragonula biroi* Friese) nests and extracts from five sources using tandem liquid chromatography-mass spectrometry. *Philipp Ent*. **27.** 91-99 (2013).

Amini-Sarteshnizi, N., Mobini-Dehkordi, M., Khosravi-Farsani, S. & Teimori, H. Anticancer activity of ethanolic extract of propolis on AGS cell line. *J. HerbMed Pharmacol*. **4.** 29-34 (2015).

Avital, I., Nissan, A., Golan, T., Lawrence, Y.R. & Stojadinovic. Cancer of the stomach. In: DeVita Jr. V.T., Lawrence, T.S. & Rosenberg, S.A. Cancer principles and practice of oncology. 11th edition. Philadelphia: Wolters Kluwer, 2019; 762-802.

Bang, Y-J., Cutsem, E.V., Feyereislova, A., Chung, H.C., Shen, L., Sawaki, A., Lordick, F., Ohtsu, A., Omuro, Y., Satoh, T., Aprile, G., Kulikov, E., Hill, J., Lehle, M., Ruschoff, J. & Kang, Y-K. Trastuzumab in combination with chemotherapy versus

chemotherapy alone for treatment of HER2-positive advanced gastric or gastro-oesophageal junction cancer (ToGA): A phase 3, open-label, randomised controlled trial. *Lancet* **317.** 687-697, doi: 10.1016/S0140-6736(10)61121-X (2010).

Bankova V. Chemical diversity of propolis and the problem of stardardization. *J. Ethnopharmacol*. **100.** 114-117, doi: 10.1016/j.jep.2005.05.004 (2005).

Baranoski, A., Oliveira, M.T., Semprebon, S.C., Niwa, A.M., Ribeiro, L.R. & Mantovani, M.S. Effects of sulfated and non-sulfated β-glucan extracted from *Agaricus brasiliensis* in breast adenocarcinoma cells- MCF7. *Toxicol. Mech. Methods.* **25.** 672-679 (2015).

Barsanti, L., Passarelli, V., Evangelista, V., Frassanito, A.M. & Gualtieri, P. Chemistry, physico-chemistry and applications linked to biological activities of β-glucans. *Nat. Prod. Rep.* **28.** 457-466 (2011).

Bartsch, H. & Nair, J. Chronic inflammation and oxidative stress in the genesis and perpetuation of cancer: role of lipid peroxidation, DNA damage, and repair. *Langenbecks Arch Surg.* **391.** 499-510 (2006).

Bayram, S., Bayram, N.E., Gercek, Y.C., Aydogan, M.N. & Oz, G.C. Chemical analysis and antimicrobial effect of propolis from Hakkari province of Turkey against some pathogenic microorganisms. *Eur. J. Biol.* **76.** 74-78, doi: 10.5152/EurJBiol.2017.1713 (2017).

Berg, D.J., Lynch, N.A., Lynch, R.G. & Lauricella, D.M. Rapid development of severe hyperplastic gastritis with gastric epithelial dedifferentiation in *Helicobacter felis*-infected IL-$10^{-/-}$ mice. *Am. J. Pathol.* **152.** 1377-1386 (1998).

Besson, A., Dowdy, S.F., & Roberts, J.M. CDK inhibitors: Cell cycle regulators and beyond. *Dev. Cell* **14.** 159-169, doi: 10.1016/j.devcel.2008.01.013 (2008).

Bijlsma, M.F., Sadanandam, A., Tan, P. & Vermeulen, L. Molecular subtypes in cancer of the gastrointestinal tract. *Nature Rev. Gastroenterol. Hepatol.* doi: 10.1038/nrgastro.2017.33 (2017).

Bonvehi, J.S. & Coll, F.V. Phenolic composition of propolis from China and from South America. *Z. Naturforsch*. **49c.** 712-718 (1994).

Borrmann, R. Geschwulste des magens and duodenums. In: Henke, F., Lubarsch, O. (eds.). Handbuch der speziellen pathologischen anatomie and histologie. Berlin: Springer-Verlag, 1926; 865.

Boussioutas, A., Li, H., Liu, J., Waring, P., Lade, S., Holloway, A.J., Taupin, D., Gorringe, K., Haviv, I., Desmond, P.V. & Bowtell, D.D.L. Distinctive patterns of gene expression in premalignant gastric mucosa and gastric cancer. *Cancer Res.* **63.** 2569-2577 (2003).

Bray, F., Ferlay, J. Soerjomataram, I., Siegel, R.L., Torre, L.A. & Jemal, A. Global cancer statistics: GLOBOCAN estimates of incidence and mortality worldwide for 36 cancers in 185 countries. *CA Cancer J. Clin*. **68.** 394-424, doi: 10.3322/caac.21492 (2018).

Brihoum, H., Maiza, M., Sahali, H., Boulmeltout, M., Barratt, G., Benguedouar, L. & Lahouel, M. Dual effect of Algerian propolis on lung cancer: Anti-tumor and chemoproventive effects involving antioxidant activity. *Braz. J. Pharm. Sci.* **54.** e17396, doi: http://dx.doi.org/10.1590/s2175-97902018000117396 (2018).

Brown, G.D. & Gordon, S. A new receptor for β-glucans. *Nature*. **413.** 36-37 (2001).

Cai, X., Carlson, J., Stoicov, C., Li, H., Wang, T.C., Houghton, J. *Helicobacter felis* eradication restores normal architecture and inhibits gastric cancer progression in C57BL/6J mice. *Gastroenterol.* **128.** 1937-1952 (2005).

Calhelha, R.C., Falcão, S., Queiroz, M.J.R.P., Vilas-Boas, M. & Ferreira, I.C.F.R. Cytotoxicity of Portuguese propolis: The proximity of the *in vitro* doses for tumor and

normal cell lines. *Biomed Res. Int.* Article ID 897361, 7 pages, doi: http://dx.doi.org/10.1155/2014/897361 (2014).

Cancer Genome Atlas Research Network: Comprehensive molecular characterization of gastric adenocarcinoma. *Nature.* **513.** 202-209, doi: 10.1038/nature13480 (2014).

Carneiro, F., Seixas, M., Sobrinho-Simoes M. New elements for an updated classification of the carcinomas of the stomach. *Pathol. Res. Pract.* **191.** 571-584, doi: 10.1016/s0344-0388(11)80878-2 (1995).

Carneiro, F. & Lauwers, G.Y. Epithelial tumours of the stomach. In: Shepherd, N.A., Warren, B.F., Williams, G.T., Greenson, J.K., Lauwers, G.Y. & Novelli, M.R. Morson and Dawson's Gastrointestinal Pathology. Fifth Edition. UK: Wiley-Blackwell, 2013;180-209.

Carrasco, V., Canfran, S., Rodriguez-Franco, F., Benito, A., Sainz, A. & Rodriguez-Bertos A. Canine gastric carcinoma: immunohistochemical expression of cell cycle proteins (p53, p21, and p16) and heat shock proteins(Hsp27 and Hsp70). *Vet. Pathol.* **48.** 322-329 (2011).

Catchpole, O., Mitchell, K., Bloor, S., Davis, P. & Suddes, A. Antiproliferative activity of New Zealand propolis and phenolic compounds vs human colorectal adenocarcinoma cells. *Fitoterapia* **106.** 167-174, doi: http://dx.doi.org/10/1016/j.fitote.2015.09.004 (2015).

Celińska-Janowicz, K., Zareba, I., Lazarek, U., Teul, J., Tomczyk, M., Palka, J. & Miltyk, W. Constituents of propolis: Chrysin, caffeic acid, p-coumaric acid, and ferulic acid induce PRODH/POX-dependent apoptosis in human tongue squamous cell carcinoma cell (CAL-27). *Front. Pharmacol.* **9.** 336, doi: 10.3389/fphar.2018.00336 (2018).

Cervancia, C.R., de Guzman, L.I., Polintan, E.A., Dupo, A.L.B. & Locsin, A.A. Current status of small hive beetle infestation in the Philippines. *J. Apic. Res.* doi: 10.1080/00218839.2016.1194053 (2016).

Chen, X., Leung, S.Y., Yuen, S.T., Chu, K- M., Ji, J., Li, R., Chan, A.S.Y., Law, S., Troyanskaya, O.G., Wong, J., So, S., Botstein, D. & Brown, P.O. Variation in gene expression patterns in human gastric cancers. *Mol. Biol. Cell.* **14.** 3208-3215, doi: 10.1091/mbc.E02-12-0833 (2003).

Chen, C-N., Wu, C-L. & Lin, J-K. Apoptosis of human melanoma cells induced by the novel compounds propolin A and propolin B from Taiwanese propolis. *Cancer Lett.* **245.** 218-231, doi: 10.1016/j.canlet.2006.01.016 (2007).

Collins, K.J., Fitzgerald, G.F., Stanton, C. & Ross, R.P. Looking beyond the terrestrial: the potential of seaweed derived bioactive to treat non-communicable diseases. *Mar. Drugs.* **14.** 60, doi: 10.3390/md14030060 (2016).

Cooper, J.P., & Youle, R.J. Balancing cell growth and death. *Curr. Opin. Cell Biol.* **24.** 802-803 (2012).

Correa, P. & Piazuelo, M.B. The gastric precancerous cascade. *J. Dig. Dis.* **13.** 2-9 (2012).

Coussens, L.M. & Werb, Z. Inflammation and cancer. *Nature.* **420.** 860-867 (2002).

Cristescu, R., Lee, J., Nebozhyn, M., Kim, K-M., Ting, J.C., Wong, S.S., Liu, J., Yue, Y.G., Wang, J., Yu, K., Ye, X.S., Do, I-G., Liu, S., Gong, L., Fu, J., Jin, J.G., Choi, M.G., Sohn, T.S., Jung, S-H., Tan, P., Chen, R., Hardwick, J., Kang, W.K., Ayers, M., Hongyue, D., Reinhard, C., Loboda, A., Kim, S. & Aggarwal, A. Molecular analysis of gastric cancer identifies subtypes associated with distinct clinical outcomes. *Nat Med.* **21.** 449-456, doi: 10.1038/nm.3850 (2015).

Cunningham, D., Allum, W.H., Stenning, S.P., Thompson, J.N., Van de Velde, C.J.H., Nicolson, M., Scarffe, H., Lofts, F.J., Falk, S.J., Iveson, T.J., Smith, D.B., Langley, R.E., Verma, M., Weeden, S & Chua, W.J. Perioperative chemotherapy versus surgery alone for resectable gastroesophageal cancer. *N. Engl. J. Med.* **355.** 11-20 (2006).

Da Cunha, M.G. *et al*. Antimicrobial and antiproliferative activities of stingless bee *Melipona scutellaris* geopropolis. *BMC Complem. Altern. M.* **13.** 23, doi: http://www.biomedcentral.com/1472-6882/13/23 (2013).

Desamero, M.J.M., Villablanca, M.A., Bariuan, J.V., Collantes, T.M.A., Ang Gobonseng, D.T., Ang, M.J.C., Fajardo, A.C., Cervancia, C.R., Estacio, M.A.C. Honey and propolis abrogate neurologic deficit and neuronal damage in the hippocampus and cerebral cortex of ischemic stroke rats. *IJARNP*. **10.** 7-15 (2017).

Desamero, M.J.M., Kakuta, S., Chambers, J.K., Uchida, K., Hachimura, S., Takamoto, M., Nakayama, J., Nakayama, H & Kyuwa, S. Orally administered brown seaweed-derived β-glucan effectively restrained development of gastric dysplasia in *A4gnt* KO mice that spontaneously develop gastric adenocarcinoma. *Int. Immunopharm*. **60**. 211-220, doi: https://doi.org/10.1016/j.intimp.2018.05.002 (2018).

Driscoll, M., Hansen, R., Ding, C., Cramer, D.E. & Yan, J. Therapeutic potential of various β-glucan sources in conjunction with anti-tumor monoclonal antibody in cancer therapy. *Cancer Biol. Ther.* **8.** 218-225 (2009).

El-Khawaga, O-A., Salem, T.A. & Elshal, M.F. Protective role of Egyptian propolis against tumor in mice. *Clin. Chim. Acta.* **338.** 11-16, doi: 10.1016/S0009-8981(03)00323-1 (2003).

Ermakova, S., Men'shova, R., Vishchuk, O., Kim, S.M., Um, B.H., Isakov, V. & Zvyagintseva, T. Water-soluble polysaccharide from the brown alga, *Eisenia bicyclis*: structural characteristics and antitumor activity. *Algal Res.* **2.** 51-58 (2013).

Ernst, M., Najdovska, M., Grail, D., Lundgren-May, T., Buchert, M., Tye, H., Matthews, V.B., Armes, J., Bhathal, P.S., Hughes, N.R., Marcusson, E.G., Karras, J.G., Na, S., Sedgwick, J.D., Hertzog, P.J. & Jenkins, B.J. STAT3 and STAT1 mediate IL-11-

dependent and inflammation-associated gastric tumorigenesis in gp130 receptor mutant mice. *J. Clin. Invest.* **118.** 1727-1738 (2008).

Evan, G.I. & Vousden, K. H. Proliferation, cell cycle and apoptosis in cancer. *Nature* **411.** 342-438 (2001).

Ferlay, J., Shin, H-R., Bray, F., Forman, D., Mathers, C. & Parkin, D.M. Estimates of worldwide burden of cancer in 2008: GLOBOCAN 2008. *Int. J. Cancer.* **127.** 2893-2917, doi: 10.1002/ijc.25516 (2010).

Fox, J.G., Beck, P., Dangler, C.A., Whary, M.T., Wang, T.C., Shi, H.N. & Nagler-Anderson, C. Concurrent enteric helminth infection modulates inflammation and gastric immune responses and reduces helicobacter-induced gastric atrophy. *Nat. Med.* **6.** 536-542 (2000).

Franklin, D. S., Godfrey, V.L., O'Brien, D.A., Deng, C. & Xiong, Y. Functional collaboration between different cyclin-dependent kinase inhibitors suppresses tumor growth with distinct tissue specificity. *Mol. Cell Biol.* **20.** 6147-6158 (2000).

Frioń-Herrera, Y., Díaz-Garcia, A., Ruiz-Fuentes, J., Rodríguez-Sánchez, H. & Sforcin, J.M. Mechanism underlying the cytotoxic effect of propolis on human laryngeal epidermoid carcinoma cells. *Nat. Prod. Res.* **32.** 2085-2091, doi: http://doi.org/10.1080/14786419.2017.1363749 (2018).

Goodridge, H.S., Reyes, C.N., Becker, C.A., Katsumoto, T.R., Ma, J., Wolf, A.J., Bose, N., Chan, A.S.H., Magee, A.S., Danielson, M.E., Weiss, A., Vasilakos, J.P. & Underhill, D.M. Activation of the innate immune receptor Dectin-1 upon formation of a "phagocytic synapse". *Nature.* **472.** 471-475 (2011).

Goseki, N., Takizawa, T., Koike M. Differences in the mode of the extension of the gastric cancer classified by histological type: new histological classification of gastric carcinoma. *Gut.* **33.** 606-612 (1992).

Grivennikov, S.I., Greten, F.R. & Karin, M. Immunity, inflammation, and cancer. *Cell* **140.** 883-899 (2010).

Gulmen, S., Kiris, I., Kocyigit, A., Dogus, D.K. & Ceylan, B.G. Meteoglu, β-glucan protects against lung injury induced by abdominal aortic ischemia-reperfusion in rats. *J. Surg. Res.* **164.** e325-e332 (2010).

Harvey, A.L., Edrada-Ebel, R. & Quinn, R.J. The re-emergence of natural products for drug discovery in the genomics era. *Nat. Rev. Drug Discov.* **14.** 111-129, doi: 10.1038/nrd4510 (2015).

Hasler, C.M. Functional foods: benefits, concerns and challenges – a position paper from the American council of science and health. *J. Nutr.* **132.** 3772-3781 (2002).

Hayakawa, Y., Fox, J.G., Gonda, T., Worthley, D.L., Muthupalani, S. & Wang, T.C. Mouse models of gastric cancer. *Cancers*. **5.** 92-130, doi: 10.3390/cancers5010092 (2002).

Hazama, S., Watanabe, S., Ohashi, M., Yagi, M., Suzuki, M., Matsuda, K., Yamamoto, T., Suga, Y., Suga, T., Nakazawa, S. & Oka, M. Efficacy of orally administered superfine dispersed lentinan (β-1, 3-Glucan) for the treatment of advanced colorectal cancer. *Anticancer Res.* **29.** 2611-2618 (2009).

He, G., Siddik, Z.H., Huang, Z., Wang, R., Koomen, J., Kobayashi, . Induction of p21 by p53 following DNA damage inhibits Cdk4 and Cdk2 activities. *Oncogene* **24,** 2929-2943 (2005).

Helicobacter and cancer collaborative group. Gastric cancer and *Helicobacter pylori*: a combined analysis of 12 case control studies nested within prospective cohorts. *Gut.* **49.** 347-353 (2001).

Herre, J., Marshall, A.S.J., Caron, E., Edwards, A.D., Williams, D.L., Schweighoffer, E., Tybulewicz, V., Sousa, C.R., Gordon, S. & Brown, G.D. Dectin-1 uses novel mechanisms for yeast phagocytosis in macrophages. *Blood.* **104.** 4038-4045 (2004).

Hoffman, R., Paper, D.H., Donaldson, J. & Vogl, H. Inhibition of angiogenesis in murine tumour growth by Laminaran sulphate. *Br. J. Cancer.* **73.** 1183-1186 (1996).

Hong, F., Yan, J., Baran, J.T., Allendorf, D.J., Hansen, R.D., Ostroff, G.R., Xing, P.X., Cheung, N.-K.V. & Ross, G.D. Mechanism by which orally administered of β-1,3-glucans enhance the tumoricidal activity of antitumor monoclonal antibodies in murine tumor models. *J. Immunol.* **173.** 797-806 (2004).

Hong, H., Kim, C.J., Kim, J.D. & Seo, J.H. β-glucan reduces exercise-induced stress through downregulation of c-Fos and c-Jun expression in the brains of exhausted rats. *Mol. Med. Rep.* **9.** 1660-1666 (2014).

Hu, B., El Hajj, N., Sittler, S., Lammert, N., Barnes, R. & Meloni-Ehrig, A. Gastric cancer: classification, histology and application of molecular pathology. *J. Gastrointest. Oncol.* **3.** 251-261, doi: 10.3978/j.issn.2078-6891.2012.021, (2012).

Hugen, S., Thomas, R.E., German, A.J., Burgener, I.A. & Mandiger, P.J.J. Gastric carcinoma in canines and humans, a review. *Vet. Comp. Oncol.* **15.** 692-705, doi: 10.1111/vco. 12249 (2017).

Hunter, T. & Pines, J. Cyclins and cancer ii: Cyclin D and CDK inhibitors come of age. *Cell.* **79.** 573-582 (1994).

IARC Working Group on the Evaluation of Carcinogenic Risks to Humans. Lyon, 7-14 June 1994. Schistosomes, liver flukes and *Helicobacter pylori*. *IARC Monogr. Eval. Carcinog. Risks Hum.* **61.** 1-241 (1994).

Ida, K., Yamanoi, K., Asaka, S., Takeuchi, H., Miyamoto, T., Shiozawa, T. & Nakayama, J. αGlcNAc and its catalyst α4GnT are diagnostic and prognostic markers in uterine cervical tumor, gastric type. *Sci. Rep.* **9.** 13043, doi: https://doi.org/10.1038/s41598-019-49376-7.

ILSI. Safety assessment and potential health benefits of food components based on selected scientific criteria. *Crit. Rev. Food Sci. Nutr.* **39.** 203-206 (1999).

Ina, K., Kataoka, T. & Ando, T. The use of Lentinan for treating gastric cancer. *Anticancer Agents Med. Chem.* **13.** 681-688 (2013).

Ishihara, M., Naoi, K., Hashita, M. & Suzui, M. Growth inhibitory activity of ethanolic extracts of Chinese and Brazilian propolis in four human colon carcinoma cell lines. *Oncol. Rep.* **22.** 349-354, doi: 10.3892/or_00000444 (2009).

Iwaya, Y., Hasebe, O., Koide, N., Kitahara, K., Suga, T., Shinji, A., Muraki, T., Yokosawa, S., Yamada, S., Arakura, N., Tanaka, E. & Nakayama, J. Reduced expression of αGlcNAc in Barrett's oesophagus adjacent to Barrett's adenocarcinoma- a possible biomarker to predict the malignant potential of Barrett's esophagus. *Histopathol.* **64.** 536-546 (2014).

Jafaar, Z.M.T., Litchfield, L.M., Ivanova, M.M., Radde, B.N., Al-Rayyan, N. & Klinge, C.M. β-D-glucan inhibits endocrine-resistant breast cancer cell proliferation and alters gene expression. *Int. J. Oncol.* **44.** 1365-1375 (2014).

Jang, B-G. & Kim, W.H. Molecular pathology of gastric carcinoma. *Pathobiology*. **78.** 302-310, doi: 10.1159/000321703 (2011).

Japanese Gastric Cancer Association. Japanese classification of gastric carcinoma: 3rd English edition. *Gastric Cancer.* **14.** 101-112, doi: 10.1007/s10120-011-0041-5 (2011).

Jemal, A., Center, M.M., DeSantis, C. & Ward, E.M. Global patterns of cancer incidence and mortality rates and trends. *Cancer Epidemiol. Biomarkers Prev.* **19.** 1893-1907, doi: 10.1158/1055-9965.EPI-10-0437 (2010).

Jerkovic, I., Marijanovic, Z., Kus, P.M. & Tuberoso, C.I.G. Comprehensive study of Mediterranean (Crotian) propolis peculiarity: Headspace volatiles, anti-*Varroa*-treatment

residue, phenolics and antioxidant properties. *Chem. Biodivers.* **13.** 210-218, doi: 10.1002/cbdv.201500053 (2016).

Jiang, Y. &Yu, Y. Transgenic and gene knockout mice in gastric cancer research. *Oncotarget.* **8.** 3696-3710 (2017).

Kalogeropoulos, N., Konteles, S.J., Troullidou, E., Mourtzinos, I. & Karathanos, V.T. Chemical composition, antioxidant activity and antimicrobial properties of propolis extracts from Greece and Cyprus. *Food Chem*. **116.** 452-461, doi: 10.1016. /j.foodchem.2009.02.060 (2009).

Karasawa, F., Shiota, A., Goso, Y., Kobayashi, M., Sato, Y., Masumoto, J., Fujiwara, M., Yokosawa, S., Muraki, T., Miyagawa, S., Ueda, M., Fukuda, M.N., Fukuda, M., Ishihara, K., & Nakayama, J. Essential role of gastric gland mucin in preventing gastric cancer in mice. *J. Clin. Invest.* **122.** 923-934, doi: 10.1172/JCI59087 (2012).

Karin, M. Nuclear factor-κB in cancer development and progression. *Nature.* **441.** 431-436 (2006).

Kaškonienė, V., Kaškonas, P., Maruška, A. & Kubilienė, L. Chemometric analysis of volatiles of propolis from different regions using static headspace GC-MS. *Cent. Eur. J. Chem.* **12.** 736-746, doi: 10.2478/s11532-014-0521-7 (2014).

Kawakubo, M., Ito, Y., Okimura, Y., Kobayashi, M., Sakura, K., Kasama, S., Fukuda, M.N., Katsuyama, T. & Nakayama, J. Natural antibiotic function of human gastric mucin against *Helicobacter pylori* infection. *Science*. **305.** 1003-1006 (2004).

Kim, J.W., Cho, H.R. & Ku, S.K. Efficacy of Polycan, a beta-glucan originated from *Aureobasidium pullulans* SM-2001, on anterior cruciate ligament transection and partial medial meniscectomy-induced-osteoarthritis rats. *J. Microbiol. Biotechnol.* **22.** 274-282 (2012).

Kotawong, K., Chaijaroenkul, W., Muhamad, P. & Na-Bangchang K. Cytotoxic activities and effects of atractylodin and β-eudesmol on the cell cycle arrest and apoptosis on cholangiocarcinoma cell line. *J. Pharmacol. Sci.* **136.** 51-56, doi: https://doi.org/10/1016/j.jphs.2017.09.033 (2018).

Kustiawan, P.M., Puthong, S., Arung, E.T. & Chanchao, C. *In vitro* cytotoxicity of Indonesian stingless bee products against human cancer cell lines. *Asian Pac. J. Trop. Biomed.* **4.** 549-556, doi: 10.12980/APJTB.4.2014APJTB-2013-0039 (2014).

Kustiawan, P.M., Phuwapraisirisan, P., Puthong, S., Palaga, T., Arung, E.T. & Chanchao, C. Propolis from the stingless bee *Trigona encisa* from East Kalimantan, Indonesia, induces *in vitro* cytotoxicity and apoptosis in cancer. *Asian Pac. J. Cancer P.* **16.** 6581-6589, doi: http://dx.doi.org/10.7314/APJCP.2015.16.15.6581 (2015).

Lamberte, L.E., Cabrera, E.C. & Rivera, W.L. Activity of ethanolic extract of propolis (EEP) as a potential inhibitor of quorum sensing-mediated pigment production in *Chromobacterium violaceum* and virulence factor production in *Pseudomonas aeruginosa*. *Philipp. Agric. Scientist* **94.** 14-22 (2011).

Lauren, P. The two histological main types of gastric carcinoma: diffuse and so-called intestinal-type carcinoma: an attempt at a histo-clinical classification. *Acta. Path. et. Microbiol. Scandinav.* **64,** 31-49 (1965).

Lauwers, G.Y., Carneiro F., Graham, D.Y. Gastric carcinoma. In: Bowman, F.T., Carneiro F., Hruban, R.H. & Theise, N.D. (eds). Classification of Tumours of the Digestive System. Lyon: IARC Press, 2010: 48.

Lee, C., Lee, H., Hwang, S.Y., Moon, C.M. & Hong, S.N. IL-10 plays a pivotal role in Tamoxifen-induced spasmolytic polypeptide-expressing metaplasia in gastric mucosa. *Gut Liver* **11.** 789-797 (2017).

Lei, Z., Tan, I.B., Das, K., Deng, E., Zouridis, H., Pattison, S., Chua, C., Feng, Z., Guan, Y.K., Ooi, C.H., Ivanova, T., Zhang, S., Lee, M., Wu, J., Ngo, A., Manesh, S., Tan, E., Teh, B.T., So, J.B.Y., Goh, L.K., Boussioutas, A., Lim, T.K.H., Flotow, H., Tan, P & Rozen, S.G. Identification of molecular subtypes of gastric cancer with different responses to PI3-kinase inhibitors and 5-fluorouracil. *Gastroenterology*. **145.** 554-565, doi: http://dx.doi.org/10.1053/j.gastro.2013.05.010 (2013).

Lee, H-L., Lin, C-S., Kao, S-H. & Chou, M-C. Gallic acid induces G1 phase arrest and apoptosis of triple-negative breast cancer cell MDA-MB-231 via p38 mitogen-activated protein kinase/p21/p27 axis. *Anti-Cancer Drugs*. **28.** 1150-1156, doi: 10.1097/CAD.0000000000000565 (2017).

Lee, Y.K., Bae, K., Yoo, H-S. & Cho, S-H. Benefit of adjuvant traditional herbal medicine with chemotherapy for resectable gastric cancer. *Integr. Cancer Ther.* **17.** 619-627, doi: 10.1177/1534735417753542 (2018).

Lordick, F. & Janjigian, Y.Y. Clinical impact of tumor biology in the management of gastroesophageal cancer. *Nature Rev. Clin. Oncol.* **13.** 348-360, doi: 10.1038/nrclinonc.2016.15 (2016).

Lu, H., Ouyang, W. & Huang, C. Inflammation, a key event in cancer development. *Mol. Cancer Res.* **4.** 221-233 (2006).

Malfertheirner, P., Sipponen, P., Naumann, M., Moayyedi, P., Mégraud, F., Xiao, S-D., Sugano, K. & Nyrén, O. *Helicobacter pylori* infection has the potential to prevent gastric cancer: a state-of-the-art critique. *Am. J. Gastroenterol.* **100.** 2100-2115, doi: 10.1111/j.1572-0241-2005.41688.x (2005).

Mannino, M.H., Zhu, Z., Xiao, H., Bai, Q., Wakefield, M.R. & Fang, Y. The paradoxical role of IL-10 in immunity and cancer. *Cancer Lett.* **367.** 103-107 (2015).

Massaro, F.C., Brooks, P.R., Wallace, H.M. & Russell, F.D. Cerumen of Australian stingless bees (*Tetragonula carbonaria*): gas chromatography- mass spectrometry fingerprints and potential anti-inflammatory properties. *Naturwissenschaften* **98.** 329-337, doi: 10.1007/s00114-011-0770-7 (2011).

Masuda, Y., Inoue, M., Miyata, A., Mizuno, S. & Nanba, H. Maitake β-glucan enhances therapeutic effect and reduces myelosupression and nephrotoxicity of cisplatin in mice. *Int. J. Immunopharmacol.* **9.** 620-626 (2009).

Masuda, Y., Inoue, H., Ohta, H., Miyake, A., Konishi, M. & Nanba, H. Oral administration of soluble β-glucans extracted from *Grifola frondosa* induces systemic antitumor immune response and decreases immunosuppression in tumor-bearing mice. *Int. J. Cancer* **133.** 108-120 (2013).

Mcdonald, J.S., Smalley, S.R., Benedetti, J., Hundahl, S., Estes, N.C., Stemmermann, G.N., Haller, D.G., Ajani, J.A., Gunderson, L.L., Jessup, J.M. & Martenson, J.A. Chemoradiotherapy after surgery compared with surgery alone for adenocarcinoma of the stomach or gastroesophageal junction. *N. Engl. J. Med.* **345.** 725-730 (2001).

Mclean, M.H. & El-Omar, E.M. Genetics of gastric cancer. *Nature Rev. Gastroenterol. Hepatol.* **11.** 664-674, doi: 10.1038/nrgastro.2014.143 (2014).

Melliou, E., Stratis, E. & Chinou, I. Volatile constituents of propolis from various regions of Greece. *Food Chem.* **103.** 375-380, doi: 10.1016/j.foodchem.2006.07.033 (2006).

Menaker, R.J., Sharaf, A.A. & Jones, N.L. Helicobacter pylori infection and gastric cancer: host, bug, environment, or all three?. *Current Gastroenterol. Rep.* **6.** 429-435 (2004).

Men'shova, R.V., Ermakova, S.P., Um, B.H. & Zvyagintseva, T.N. The composition and structural characteristics of the brown alga *Eisenia bicyclis*. *Russ. J. Mar. Biol.* **39.** 208-213 (2013).

Ming, S.C. Gastric carcinoma: a pathological classification. *Cancer*. **39.** 2475-2384 (1977).

Miyahara, R., Niwa, Y., Matsuura, T., Maeda, O., Ando, T., Ohmiya, N., Itoh, A, Hirooka, Y. & Goto, H. Prevalence and prognosis of gastric cancer detected by screening in a large Japanese population: Data from a single institute over 30 years. *J. Gastroenterol. Hepatol.* **22.** 1435-1442, doi: 10.1111/j.1440-1746.2007.04991.x (2007).

Mosser, D.M. & Zhang, X. Interleukin-10: new perspective on an old cytokine. *Immunol. Rev.* **226.** 205-218 (2008).

Motomura, M., Kwon, K.M., Suh, S-J., Lee, Y-C., Kim, Y-K., Lee, I-S., Kim, M-S., Kwon, D.Y., Suzuki, I. & Kim, C.H. Propolis induces cell cycle arrest and apoptosis in human leukemic U937 cells through Bcl-2/Bax regulation. *Environ. Toxicol. Pharmacol*. **26.** 61-67, doi: 10.1016/j.etap.2008.01.008 (2008).

Mulligan, R.M. Histogenesis and biological behavior of gastric carcinoma. In: Pathology Annual. Volume 7. New York: Appleton Century Crofts, 1972: 349.

Nakashima, A., Yamada, K., Iwata, O., Sugimoto, R., Atsuji, K., Ogawa, T., Ishibashi-Ohgo, N. & Suzuki, K. β-glucans in foods and its physiological functions. *J. Nutr. Sci. Vitaminol.* **64.** 8-17 (2018).

Nakayama J., Yeh J-C., Misra, A.K. Ito, S., Katsuyama, T. & Fukuda, M. Expression cloning of a human α-1,4-*N*-acetylglucosaminyltransferase that forms GlcNAcα1→4Galβ→R, a glycan specifically expressed in gastric gland mucous cell-type mucin. *Proc. Nat. Acad. Sci. U. S. A*. **96.** 8991-8996 (1999).

Noureddine, H., Hage-Sleiman, R., Wehbi, B., Fayyad-Kazan, H., Hayar, S., Traboulssi, M., Alyamani, O.A., Faour, W.H. & ElMakhour, Y. Chemical characterization and cytotoxic activity evaluation of Lebanese propolis. *Biomed. Pharmacother*. **95.** 298-307, doi: http://dx.doi.org/10.1016/j.biopha.2017.08.067 (2017).

Novak, M. & Vetvicka, V. β-glucans, history, and the present: immunomodulatory aspects and mechanisms of action. *J. Immunotoxicol.* **5.** 47-57 (2008).

Oršolić, N., Terzić, S., Mihaljević, Ž., Šver, L. & Bašić, I. Effects of local administration of propolis and its polyphenolic compounds on tumor formation and growth. *Biol. Pharm. Bull.* **28.** 1928-1933 (2005).

Pan, M-H., Chang, Y-H., Badmaev, V., Nagabhushanam, K. & Ho, C-T. Pterostilbene induces apoptosis and cell cycle arrest in human gastric cancer cell lines. *J. Agric. Food Chem.* **55.** 7777-7785 (2007).

Park, C.H., Lee, J.G., Lee, A-R., Eun, C.S. & Han, D.S. Network construction of gastric microbiome and organization of microbiome modules associated with gastric carcinogenesis. *Sci. Rep.* **9.** 12444, doi: https://doi.org/10.1038/s41598-019-48925-4 (2019).

Pereira-Filho, R.N., Batista, F.S., Ribeiro, D.R., de Melo, G.C., Reis, F.R., de Melo, A.U.C., Gomes, M.Z., Cardoso, J.C. & Albuquerque Junior, R.L.C. Chemopreventive effect of Brazilian green propolis on experimental dermal carcinogenesis in murine model. *Int. J. Morphol.* **32.** 522-530 (2014).

Pitulescu, M.E., & Adams, R.H. Eph/ephrin molecules—a hub for signaling and endocytosis. *Genes Dev.* **24.** 2480-2492 (2010).

Poh, A.R., O'Donoghue, R.J.J., Ernst, M. & Putoczki, T.L. Mouse models of gastric cancer: matching models to biological questions. *Gastroenterol Hepatol.* **31.** 1257-1272, doi: 10.1111/jgh.13297 (2016).

Ohya, A., Yamanoi, K., Shimojo, H., Fujii, C. & Nakayama, J. Gastric gland mucin-specific *O*-glycan expression decreases with tumor progression from precursor lesions to pancreatic cancer. *Cancer Sci.* **108.** 1897-1902 (2017).

Qiu, M-Z., Cai, M-Y., Zhang, D-S., Wang, Z-Q., Wang, D-S., Li, Y-H. & Xu, R-H. Clinicopathological characteristics and prognostic analysis of lauren classification in gastric adenocarcinoma in China. *J. Transl. Med.* **11.** 58, doi: 10.1186/1479-5876-11-58 (2013).

Ragasa, C.Y., Galian, R.A.F., Ebajo Jr., V.D., Aguda, R.M., Cervancia, C.R. & Shen, C.C. Propolins and glyasperin A from stingless bee nests. *Rev. Bras. Farmacogn.* **25.** 177-179, doi: http://dx.doi.org/10.1016/j.bjp.2015.03.006 (2015).

Ribeiro-Junior, J.A. *et al*. Gastroprotective effect of geopropolis from *Melipona* scutellaris is dependent on production of nitric oxide and prostaglandin. *J. Evid. Based Complementary Altern. Med.* Article ID459846, 5 pages, doi: http://dx.doi.org/10.1155/2015/459846 (2015).

Rice, P.J., Adams, E.L., Ozment-Skelton, T., Gonzalez, A.J., Goldman, M.P., Lockhart, B.E., Barker, L.A., Breuel, K.F., DePonti, W.K., Kalbfleisch, J.H., Ensley, H.E., Brown, G.D., Gordon, S. & Williams, D.L. Oral delivery and gastrointestinal absorption of soluble glucans stimulate increased resistance to infectious challenge. *J. Pharmacol. Exp. Ther.* **314.** 1079-1086 (2005).

Ruthes, A.C., Carbonero, E.R., Córdova, M.M., Baggio, C.H., Santos, A.R.S., Sassaki, G.L., Cipriani, T.R., Gorin, P.A.J. & Iacomini, M. *Lactarius rufus* (1→3), (1→6)-β-D-glucans: structure, antinociceptive and anti-inflammatory effects. *Carbohydr. Polym.* **94.** 129-136 (2013).

Sakuramoto, S., Sasako, M., Yamaguchi, T., Kinoshita, T., Fujii, M., Nashimoto, A., Furukawa, H., Nakajima, T., Ohashi, Y., Imamura, H., Higashino, M., Yamamura, Y., Kurita, A. & Arai, K. Adjuvant chemotherapy for gastric cancer with S-1, an oral fluoropyrimidine. *N. Engl. J. Med.* **357.** 1810-1820 (2007).

Samuelsen, A.B.C., Schrezenmeir, J. & Knutsen, S.V. Effects of orally administered yeast-derived beta-glucans: a review. *Mol. Nutr. Food Res.* **58.** 183-193 (2014).

Sanches, M.A., Pereira, A.M.S. & Serrão, J.E. Pharmacological actions of extracts of propolis of stingless bees (meliponini). *J. Apic. Res.* **56,** 50-57, doi: https//doi.org/10.108/00218839.2016.1260856 (2017).

Sandvik, A., Wang, Y.Y., Morton, H.C., Aasen, A.O., Wang, J.E. & Johansen, F.E. Oral and systemic administration of β-glucan protects against lipopolysaccharide-induced shock and organ injury in rats. *Clin. Exp. Immunol.* **148.** 168-177 (2007).

Sawaya, A.C.H.F. Composition and antioxidant activity of propolis from three species of *Scaptotrigona* stingless bees. *Food Chem. Toxicol.* **1.** 37-42, doi: 10.3896/IBRA.4.01.2.03 (2009).

Seim-Wikse, T., Kolbjornsen, O., Jorundsson, E., Benestad, S.L., Bjornvad, C.R., Grotmol, T., Kristensen, A.T & Skancke, E. Tumour gastrin expression and serum gastrin concentration in dogs with gastric carcinoma are poor diagnostic indicators. *J. Comp. Path.* **151.** 207-211 (2014).

Sforcin, J.M. & Bankova, V. Propolis: Is there a potential for the development of new drugs? *J. Ethnopharmacol*. **133.** 253-260, doi: 10.1016/ j.jep.2010.10.032 (2010).

Shen, R.L., Wang, Z., Dong, J.L., Xiang, Q.S. & Liu, Y.Q. Effects of oat soluble and insoluble β-glucan on 1,2-dimethylhydrazine-induced early colon carcinogenesis in mice. *Food Agric. Immunol.* **27.** 657-666 (2016).

Shimizu, K., Das, S.K., Hashimoto, T., Sowa, Y., Yoshida, T., Sakai, T., Matsuura, Y. & Kanazawa, K. Arterpillin C in Brazilian propolis induces G0/G1 arrest via stimulation of Cip1/p21 expression in human colon cancer cells. *Mol. Carcinog*. **44.** 93-299, doi: 10.1002/mc.20148 (2014).

Shiratsu, K., Higuchi, K. & Nakayama, J. Loss of gastric gland mucin-specific *O*-glycans is associated with progression of differentiated-type adenocarcinoma of the stomach, *Cancer Sci.* **105.** 126-133 (2014).

Silva-Carvalho, R., Baltazar, F. & Almeida-Aguiar, C. Propolis: A complex natural product with plethora of biological activities that can be explored for drug development. *J. Evid. Based Complementary Altern. Med.* Article ID 206439, 29 pages, doi: http//dx.doi.org/10.1115/2015/20649 (2015).

Sitarz, R., Skierucha, M., Mielko, J., Offerhaus, G.J.A., Maciejewski, R. & Polkowski, W.P. Gastric Cancer: epidemiology, prevention, classification, and treatment. *Cancer Manag. Res.* **10.** 239-248 (2018).

Smiderle, F.R., Olsen, L.M., Carbonero, E.R., Baggio, C.H., Freitas, C.S., Marcon, R., Santos, A.R.S., Gorin, P.A.J. & Iacomini, M. Anti-inflammatory and analgesic properties in a rodent model of a (1→3), (1→6)-linked β-glucan isolated from *Pleurotus pulmonarius*. *Eur. J. Pharmacol.* **597.** 86-91 (2008).

Staton, C.A., Chetwood, A.S.A., Cameron, L.C., Cross, S.S., Brown, N.J. & Reed, M.W.R. The angiogenic switch occurs at the adenoma stage of the adenoma-carcinoma sequence in colorectal cancer. *Gut.* **56.** 1426-1432 (2007).

Sulaiman, G.M., Ad'hiah, A.H., Al-Sammarrae, K.W., Bagnati, R., Frapolli, R., Bello, E., Uboldi, S., Romano, M., Panini, N., Scanziani, E., Pezzolato, M., Erba, E. & D'Incalci, M. Assessing the anti-tumour properties of Iraqi propolis *in vitro* and *in vivo*. *Food Chem. Toxicol.* **50.** 1632-1641, doi: 10.1016/j.fct.2012.01.022 (2012).

Swidergall, M., Solis, N.V., Lionakis, M.S. & Filler, S.G. EphA2 is an epithelial cells pattern recognition receptor for fungal β-glucans. *Nat. Microbiol.* **3.** 53-61 (2018).

Takasu, S., Tsukamoto, T., Cao, X.Y., Toyoda, T., Hirata, A., Ban, H., Yamamoto, M., Sakai, H., Yanai, T., Masegi, T., Oshima, M. & Tatematsu, M. Roles of cyclooxygenase-2 and microsomal prostaglandin E synthase-1 expression and beta-catenin activation in gastric carcinogenesisin N-methyl-N-nitrosourea-treated K19-C2mE transgenic mice. *Cancer Sci.* **99.** 2356-2364 (2008).

Tan, I.B., Ivanova, T., Lim, K.H., Ong, C.W., Deng, N., Lee, J., Tan, S.H., Wu, J., Lee, M.H., Ooi, C.H., Rha, S.Y., Wong, W.K., Boussioutas, A., Yeoh, K.G., So, J., Wong, W.P., Tsuburaya, A., Grabsch, H., Toh, H.C., Rozen, S., Cheong, J.H., Noh, S.H., Wat, W.K., Ajani, A.J., Lee, J-S., Tellez, M.S. & Tan, P. Intrinsic subtypes of gastric cancer, based on gene expression pattern, predict survival and respond differently to chemotherapy. *Gastroenterology* **141.** 476-485, doi: 10.1053/j.gastro.2011.04.042 (2011).

Tan, P. & Yeoh, K-G. Genetics and molecular pathogenesis of gastric adenocarcinoma. *Gastroenterology*. **149.** 1153-1162, doi: http://dx.doi.org/10.1053/j.gastro.2015.05.059 (2015).

Tanaka, K.I., Tanaka, Y., Suzuki, T. & Mizushima, T. Protective effects of β-(1,3→1,6)-D-glucan against irritant-induced gastric lesions. *Br. J. Nutr.* **106.** 475-485 (2011).

Tang, C., Kamiya, T., Liu, Y., Kadoki, M., Kakuta, S., Oshima, K., Hattori, M., Takeshita, K., Kanai, T., Saijo, S., Ohno, N. & Iwakura, Y. Inhibition of dectin-1 signaling ameliorates colitis by inducing *Lactobacillus*-mediated regulatory T cell expansion in the intestine. *Cell Host Microbe* **18.** 183-197 (2015).

Tang, H., Yao, X., Yao, C., Zhao, X., Zuo, H. & Li, Z. Anti-colon cancer effect of caffeic acid p-nitro-phenethyl ester in vitro and in vivo and detection of its metabolites. *Sci. Rep.* **7.** 7599, doi: 10.1038/s41598-017-07953-8 (2017).

Tanikawa, T., Wilke, C.M., Kryczek, I., Chen, G.Y., Kao, J., Núñes, G. & Zou, W. Interleukin-10 ablation promotes tumor development, growth, and metastasis. *Cancer Res.* **72.** 420-429 (2012).

Tay, S.T., Leong, S.H., Yu, K., Aggarwal, A., Tan, S.Y., Lee, C.H., Wong, K., Visvanathan, J., Lim, D., Wong, W.K., Soo, K.C., Kon, O.L. & Tan, P. A combined comparative genomic hybridization and expression microarray analysis of gastric cancer reveals novel molecular subtypes. *Cancer Res.* **63.** 3309-3316 (2003).

Teerasripreecha, D., Phuwapraisirisan, P., Puthong, S., Kimura, K., Okuyama, M., Mori, H., Kimura, A. & Chanchao, C. In vitro antiproliferative/cytotoxic activity on cancer cell lines of a cardanol and a cardol enriched from Thai *Apis mellifera* propolis. *BMC Complem. Altern. M.* **12.** 27, doi: http://www.biomedcentral.com/1472-6882/12/27 (2012).

Thrumurthy, S.G., Chaudry, M.A., Chau, I. & Allum, W. Does surgery have a role in managing incurable gastric cancer? *Nat. Rev.Clin. Oncol.* **12.** 676-682 (2015).

Tsukada, C., Yokoyama, H., Miyaji, C., Ishimoto, Y., Kawamura, H. & Abo, T. Immunopotentiation of intraepithelial lymphocytes in the intestine by oral administrations of β-glucan. *Cell. Immunol.* **221.** 1-5 (2003).

Tsukamoto, T., Tsutomu, M. & Tatematsu, M. Animal models of gastric carcinogenesis. *Toxicol. Pathol.* **35.** 636-648, doi: 10.1080/01926230701420632 (2007).

Umthong, S., Phuwapraisirisan, P., Puthong, S. & Chanchao, C. In vitro antiproliferative activity of partially purified *Trigona laeviceps* propolis from Thailand on human cancer cell lines. *BMC Complem. Altern. M.* **11.** 37, doi: http://www.biomedcentral.com/1472-6882/11/37 (2011).

Wang, X., Sankarapandian, K., Cheng, Y., Woo, S.O., Kwon, H.W. Perumalsamy, H. & Ahn, Y-J. Relationship between total phenolic contents and biological properties of propolis from 20 different regions in South Korea. *BMC Complem. Altern. M.* **16.** 65, doi: 10.1186/s12906-016-1043-y (2016).

Watabe, M., Hishikawa, K., Takayanagi, A., Shimizu, N. & Nakaki, T. Caffeic acid phenethyl ester induces apoptosis by inhibition of NFκB and activation of Fas in human breast cancer MCF-7 cells. *J. Biol. Chem.* **279.** 6017-6026, doi: 10.1074/jbc.M306040200 (2004).

Weng, M-S., Liao, C-H., Chen, C-N., Wu, C-L. & Lin, J-K. Propolin H from Taiwanese propolis induces G1 arrest in human lung carcinoma cells. *J. Agric. Food Chem.* **55.** 5289-5298, doi: 10.1021/jf070201n (2007).

Wroblewski, L.E., Peek, Jr. R.M., & Wilson, K.T. *Helicobacter pylori* and gastric cancer: factors that modulate disease risk. *Clin. Microbiol. Rev.* **23.** 713-739, doi: 10.1128/CMR.00011-10 (2010).

Xu, H., Zou, W., Xu, X. & Zhang, L. Anti-tumor effect of β-glucan from *Lentinus edodes* and the underlying mechanism. *Sci. Rep.* **6.** 28802 (2016).

Xuan, H., Li, Z., Yan, H., Sang, Q., Wang, K., He, Q., Wang, Y. & Hu, F. Antitumor activity of Chinese propolis in human breast cancer MCF-7 and MDA-MB-231 cells. *J. Evid. Based Complementary Altern. Med.* Article ID 280120, 11 pages, doi: http/dx.doi.org/10.1155/2014/280120 (2014).

Yamamoto, M., Tsukamoto, T., Sakai, H., Shirai, N., Ohgaki, H., Furihata, C., Donehower, L.A., Yoshida, K. & Tatematsu, M. p53 knockout mice (-/-) are more susceptible than (+/-) and (+/+) mice to N-methyl-N-nitrosourea stomach carcinogenesis. *Carcinogenesis.* **21.** 1891-1897 (2000).

Yamamoto, M., Furihata, C., Ogiu, T., Tsukamoto, T., Inada, K., Hirano, K. & Tatematsu, M. Independent variation in susceptibilities of six different mouse strains to induction of pepsinogen-altered pyloric glands and gastric tumor intestinalization by *N*-methyl-*N*-nitrosourea. *Cancer Lett.* **179.** 121-132 (2002).

Yamamoto, Y., Kimura, T., Sugitachi, A. & Matsuura, N. Anti-angiogenic and anti-metastatic effects of β-1,3-D-glucan purified from Hanabiratake, *Sparassis crispa. Biol, Pharm. Bull.* **32.** 259-263 (2009).

Yamanoi, K., Sekine, S., Higuchi, K., Kushima, R. & Nakayama, J. Decreased expression of gastric gland mucin-specific glycan α1,4-linked *N*-acetylglucosamine on its

scaffold mucin 6 is associated with malignant potential of pyloric gland adenoma of the stomach. *Histopathol.* **67.** 898-904 (2015).

Yamanoi, K. & Nakayama, J. Reduced αGlcNAc glycosylation on gastric gland mucin is a biomarker of malignant potential for gastric cancer, Barrett's adenocarcinoma and pancreatic cancer. *Histochem. Cell Biol.* **149.** 569-575, doi: https://doi.org/10.1007/s00418-018-1667-8 (2018).

Yan, H., Kakuta, S., Nishihara, M., Sugi, M., Adachi, Y., Ohno, N., Iwakura, Y. & Tsuji, N.M. *Kjellmaniella crassifolia* Miyabe (gagome) extract modulate intestinal and systemic immune responses. *Biosci. Biotechnol. Biochem.* **75.** 2178-2183 (2011).

Yang, H., Huang, Z., Huang, Y., Dong, W., Pan, Z. & Wang, L. Characterization of Chinese crude propolis by pyrolysis-gas chromatography/mass spectrometry. *J. Anal. Appl. Pyrol.* **113.** 158-164, doi: http://dx.doi.org/10.1016/j.jaap.2014.12.006 (2014).

Yang, X., Zhu, J., Wu, J., Huang, N., Cui, Z., Luo, Y., Sun, F., Pan, Q., Li, Y. & Yang, Q. (-)-Guaiol regulates autophagic cell death depending on mTOR signaling in NSCLC. *Cancer Biol. Ther.* **19.** 706-714, doi: https://doi.org10.1080/15384047.2018.1451277 (2018).

Ye, W., Nyren, O & Adami, H-L. In: Adami, H-O., Hunter, D.J., Lagiou, P. & Mucci, L. (eds). Textbook of Cancer Epidemiology. Third edition. New York: Oxford University Press, 2018: 213-242.

Yu, S., Yang, M. & Nam, K.T. Mouse models of gastric carcinogenesis. *J. Gastric Cancer.* **14.** 67-86, doi: http://dx.doi.org/10.5230/jgc.2014.12.2.67 (2014).

Yuasa, Y. Control of gut differentiation and intestinal-type gastric carcinogenesis. *Nat. Rev. Cancer*. **3.** 592-600, doi: 10.1038/nrc1141 (2003).

Zacchetti, A., Garderen, E.V., Teske, E., Nederbragt, H., Dierendonck, J.H. & Rutteman, D.R. Validation on the use of proliferation markers in canine neoplastic and non-

neoplastic tissues: comparison of KI-67 and proliferating nuclear cell antigen (PCNA) expression versus bromodeoxyuridine labeling by immunohistochemistry. *APMIS.* **111.** 430-438 (2003).

Zheng, H., Takahashi, H., Murai, Y., Cui, Z., Nomoto, K., Miwa, S., Tsuneyama, K. & Takano, Y. Pathobiological characteristics of intestinal and diffuse-type gastric carcinoma in Japan: An immunostaining study on the tissue microarray. *J. Clin. Path.* **60.** 273-277, doi: 10.1136/jcp.2006.038778 (2007).